



Gernot Metnitzer, BSc.

Hydrothermal conversion of carbon-rich process streams from the pulp and paper industry to carboxylic acids

MASTER´S THESIS

to achieve the university degree of

Diplom-Ingenieur

in

Process Engineering

submitted to

University of Technology Graz

Supervisor:

Dipl.-Ing. Dr.techn. Marlene Kienberger

Institute of Chemical Engineering and Environmental Technology

Graz, March 2019

AFFIDAVIT

I declare that I have authored this thesis independently, that I have not used other than the declared sources/resources, and that I have explicitly indicated all material which has been quoted either literally or by content from the sources used. The text document uploaded to TUGRAZonline is identical to the present doctoral thesis.

Graz,
date

.....
(signature)

Abstract

The trend of industry to down cycle raw material utilization is already practiced and developed in the pulp and paper industry. That means that the denomination “waste stream” changed to “side” or “side product stream” which increases the overall yield from input materials and brings new economic benefits. The carbon rich, renewable and abundant basic material of the pulp and paper industry is lignocellulose. Besides the products pulp and paper, carbon rich process streams like fines and black liquor occur in the course of Kraft chemical pulping.

The present thesis provides a theoretical observation as well as batch experiments of hydrothermal conversion to carboxylic acids of the above-mentioned process streams. The major goal was to investigate the conversions under variation of reaction conditions regarding acids yield, lignin concentration and pH-value. The formation of lactic, formic and acetic acid was analyzed by high performance liquid chromatography. In addition, the concentration of lignin phenolic hydroxy groups was evaluated by UV-spectroscopy.

With 38% the highest yield of lactic acid was achieved by bleached pulp in a 0.4 M solution of calcium hydroxide at the highest temperature of 230°C. At lower temperatures the initial substrates were not totally converted after 2880 minutes which consequently resulted in lower yields. By the kinetic evaluation according to 1st order reactions that was represented numerically. The formation of acetic acid and formic acid was much lower than that of lactic acid in almost all cases. Fines had similar yields as pulp but the reactivity seemed to be higher at lower temperatures. Both sodium hydroxide and calcium hydroxide acted as effective catalysts for the conversion of cellulosic material. Nevertheless, slightly higher yields were reached by using calcium hydroxide. The switch of the pH-value into the acidic regime during the duration of experiments led to lower yields and char formation caused by different reaction pathways. Throughout heat treatment of the lignin-based materials, isolated lignin and black liquor, they showed an increase of acids to similar amounts but a significantly lower yield than cellulosic material.

The results showed the potential of hydrothermal conversion of the observed carbon rich resources. Further investigations regarding an increase of yield and selectivity as well as in effective separation technologies should be done.

Kurzfassung

Der Trend, Rohstoffe kaskadisch zu nutzen ist insbesondere in der biobasierten Industrie zu beobachten bzw. wird dort bereits in hohem Maße praktiziert. Die Bezeichnung "Abfallstrom" verschwindet somit und wird zu "Nebenstrom" oder "Nebenproduktstrom". Dies erhöht die Gesamtanlagenausbeute und bringt durch die höhere Wertschöpfung neue wirtschaftliche Vorteile. Das kohlenstoffreiche und erneuerbare Grundmaterial der Zellstoff- und Papierindustrie ist Lignozellulose. Neben den Produkten Zellstoff und Papier treten im Zuge des Kraft-Zellstoffaufschlusses kohlenstoffreiche Prozessströme wie Feinstoffe und Schwarzlauge auf.

Die vorliegende Arbeit liefert eine theoretische Betrachtung sowie Batch-Experimente der hydrothermischen Umwandlung dieser Stoffströme zu Carbonsäuren. Das Hauptziel bestand darin, die Ausbeuten unter verschiedenen Reaktionsbedingungen hinsichtlich Säureausbeute, Ligninkonzentration und pH-Wert zu untersuchen. Die Bildung von Milchsäure, Ameisensäure und Essigsäure wurde mittels Hochleistungsflüssigkeitschromatographie analysiert. Darüber hinaus wurde die Konzentration von phenolischen Lignin-Hydroxygruppen mit UV-Spektroskopie bestimmt.

Mit 38% wurde die höchste Ausbeute an Milchsäure mit gebleichtem Zellstoff in einer 0,4 M Calciumhydroxid-Lösung bei der höchsten Temperatur von 230°C erzielt. Bei niedrigeren Temperaturen wurden die Ausgangsstoffe nach 2880 min nicht vollständig umgewandelt, was zu niedrigeren Ausbeuten führte. Durch die reaktionskinetische Auswertung nach 1. Ordnung wurde dies in Zahlen belegt. Die Bildung von Essigsäure und Ameisensäure war in fast allen Fällen viel geringer als die von Milchsäure. Die hydrothermale Behandlung von Feinstoffen führte im Vergleich zu ähnlichen Ausbeuten wie Zellstoff. Sowohl Calciumhydroxid als auch Natriumhydroxid fungierten als wirksame Katalysatoren für die Umwandlung von Zellulosematerial, wobei mit Calciumhydroxid etwas höhere Ausbeuten erzielt wurden. Die Wärmebehandlung der auf Lignin basierenden Materialien, isoliertes Lignin und Schwarzlauge, ergab einen Anstieg der Säuren in ähnlichen Mengen, jedoch deutlich geringere Ausbeuten als bei Zellulosematerial.

Die Ergebnisse zeigten das Potenzial der hydrothermalen Umwandlung. Weitere Untersuchungen bezüglich der Steigerung von Selektivität und Ausbeuten sowie von effektiven Trenntechnologien sollten durchgeführt werden.

Content

1	Introduction and motivation	1
2	Theoretical background.....	3
2.1	Biomass source	3
2.2	Chemical pulping process.....	6
2.2.1	Pulp and paper.....	8
2.2.2	Fines	8
2.2.3	Black liquor.....	9
2.3	Carboxylic acids.....	10
2.3.1	Lactic acid	10
2.3.2	Formic acid.....	11
2.3.3	Acetic acid.....	11
2.4	Basic reactions of biomass conversion	12
2.5	Hydrothermal conversion of cellulose and its derivatives to monosaccharides	15
2.6	Hydrothermal conversion of monosaccharides to platform chemicals	17
2.6.1	Conversion to lactic acid	19
2.6.2	Conversion to formic acid.....	21
2.6.3	Conversion to acetic acid	23
2.6.4	Conversion to other substances.....	24
2.7	Hydrothermal conversion of lignin.....	26
2.8	Reaction kinetics.....	27
3	Experimental setup	31
3.1	Equipment.....	31
3.2	Process.....	34
3.3	Safety and limits	37
4	Experimental procedure	39
4.1	Overview.....	39
4.2	Substrates and chemicals.....	40
4.3	Procedure	42
5	Analysis.....	43
5.1	High-performance liquid chromatography	43
5.1.1	General	43
5.1.2	Sample preparation.....	45
5.2	UV-VIS spectroscopy analysis.....	47
5.2.1	General	47
5.2.2	Sample preparation.....	48

5.3	pH-measurement.....	48
5.4	Dry solids content measurement	49
6	Results and discussion.....	50
6.1	Conversion of pulp.....	52
6.1.1	Temperature dependency	52
6.1.2	Substrate dependency	57
6.1.3	Influence of different catalysts.....	59
6.1.4	Influence of catalysts concentration	61
6.2	Conversion of paper	64
6.3	Conversion of fines	65
6.4	Conversion of lignin	67
6.5	Conversion of black liquor.....	69
7	Conclusion and outlook.....	72
8	Appendix	75
8.1	Bibliography	75
8.2	List of abbreviations.....	82
8.3	List of figures	83
8.4	List of tables.....	86
8.5	Supplementary data.....	87
8.5.1	Experimental setup	87
8.5.2	Analysis.....	91
8.5.3	Procedure.....	91
8.5.4	Results	92

1 Introduction and motivation

By moving away from fossil resources towards renewable materials, the topic of biorefinery is becoming more and more the focus of attention. The advantages of biomass, especially lignocellulosic material with its abundance, renewability and worldwide distribution are obvious. The extensive amount of carbon compounds forms the base for potential conversion into energy, fuels or chemical substances. Bulk acids like lactic, formic and acetic acid can be formed in a relatively simple way by hydrothermal conversion directly from biomass. Their demand is increasing annually because of their widespread use in different industry sectors like food-, chemical-, pharmaceutical- and production industries to name a few. Lactic acid, for example, forms the monomer of polylactic acid (PLA) which is the main constituent of biodegradable plastics. [1,2]

Many studies were done by scientists to find the best conditions to cleave and arrange the C-C as well as C-O bonds in the right way to form desired compounds. [3] Roughly put, the conversion of cellulose and its derivatives goes the way from polysaccharides to monosaccharides which are subsequently degraded to acids to a certain degree. The reaction conditions as well as the catalysts are playing an important role in this and are directing the reaction path to a specific product. As shown in Figure 1-1, many parameters like temperature, pressure, reaction atmosphere, as well as the type of catalyst and its concentrations are influencing the reaction pathways and the selectivity of conversions.

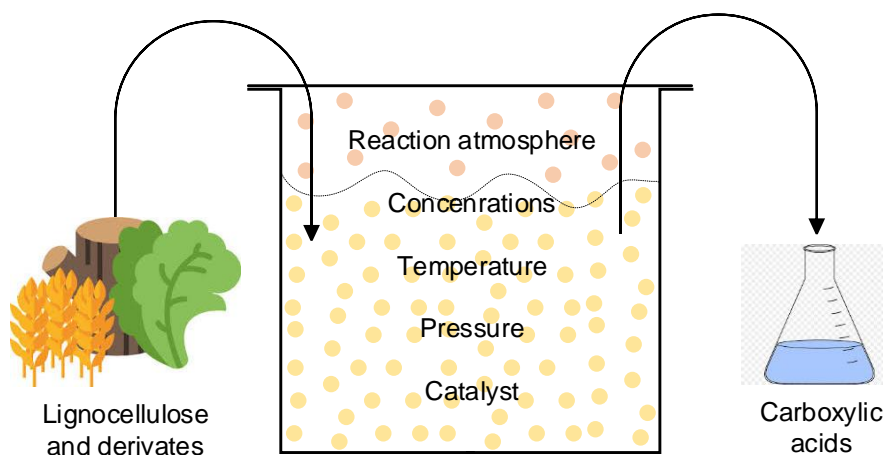


Figure 1-1: Simplified scheme of hydrothermal conversion of biomass to carboxylic acids, including the reaction parameters

The pulp and paper industry, whose usual feedstock is wood, is paying growing attention to the conversion of internal side or waste flow streams to valuable products. Besides combustion, the flow streams can be converted to value-added products and bulk chemicals. The degradation of lignocellulose happens already during wood digestion and generates carboxylic acids in different amounts, depending on the process conditions. [4,5]

The present diploma thesis investigates the hydrothermal conversion of lignocellulose rich or more precisely carbon rich streams from the Kraft process to carboxylic acids, like lactic, formic or acetic acid. The conversion of different forms of cellulose, hemicellulose and lignin in the presence of a catalyst or a mixture of chemicals at defined conditions is analyzed. In order to build up a model, side process streams like fines and black liquor as well as the products pulp, paper and lignin are used as feed substrate for the experiments. As process parameter, the catalyst and the catalyst concentration, the temperature and hence the resulting pressure are varied.

The experiments were done by using a temperature-controlled batch reactor, which allowed sampling at defined time intervals. Analysis performed include the pH-value, the concentrations of acids and phenolic hydroxide groups and the dry substance content to perform mass balances, reaction mechanisms and kinetics.

To give an overview of this diploma thesis, in the following chapter the theoretical background of the pulp and paper process and its products and flow streams as well as information of the researched acids and the supposed reaction pathways and kinetics are given. Subsequently, the experimental setup and procedures are described. Finally, the results, measured with the analytical methods described in the chapter before, are discussed and the most significant are summarized in the last chapter including a short outlook.

2 Theoretical background

2.1 Biomass source

Biomass, which means a non-fossilized and biodegradable material, includes substances which originate from plants, animals and microorganisms. Thus, it is generally recognized as renewable resource. [6] Hereinafter the focus is on plant biomass, or more precisely wood that has the same basic components as other plants but with differing compositions.

The major component of plant biomass is lignocellulose which consists of the three polymers cellulose, hemicellulose and lignin. Depending on the species of plant the proportion of these primary constituents varies. However, together they form the main framework of the plant, in which cellulose (35-50%), followed by hemicellulose (20-40%) and lignin (10-35%), represents the major component. [7-9]

Cellulose

As principal component of plant cell walls, cellulose is the quantitatively most important substance of living organisms all over the world. As pictured in Figure 2-1, cellulose is a linear polymer that consists of D-glucose monosaccharide units linked by β -1,4-glycosidic bonds. Thousands of these molecules form long chains, crosslinked by hydrogen bonds and van der Waals forces, called fibrils. This structure gives the cellulose its high tensile and flexural strength. [4,7] The degree of polymerization (DP) defines the number of repeated glucose units which varies from about 100 to 15,000 units depending on the origin and pretreatment of pulp. [2]

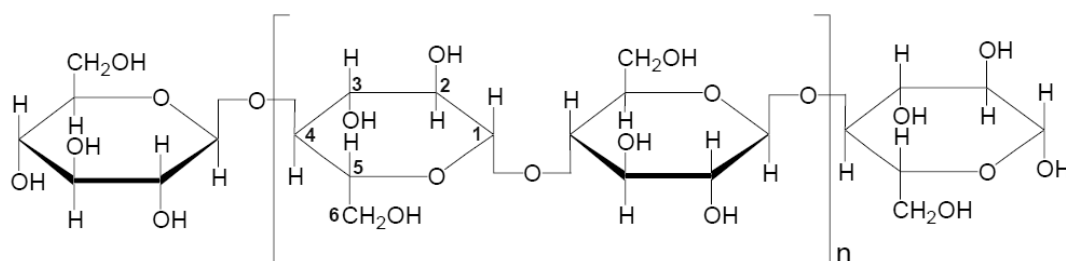


Figure 2-1: Chemical structure of cellulose [10]

Hemicellulose

In contrast to cellulose, hemicellulose is an amorphous heteropolysaccharide; that means it is formed by different monomer units. Furthermore, the degree of polymerization is with approximately 100-200 sugar units per molecule much lower. It mainly consists of pentoses, hexoses and sugar acids. Therefore, it is more unstable and consequently degrades easier than cellulose. The composition of hemicellulose depends strongly on the origin. For example, hemicellulose in softwood consists to a large extent of mannoses and galactoses, whereas a higher amount of xyloses can be found in hardwood. At cell walls hemicellulose is located in the matrix between the cellulose fibrils to keep a constant distance among them. [4,8,11] Furthermore it acts as a stabilizer between cellulose and lignin in the plant structure. [12]

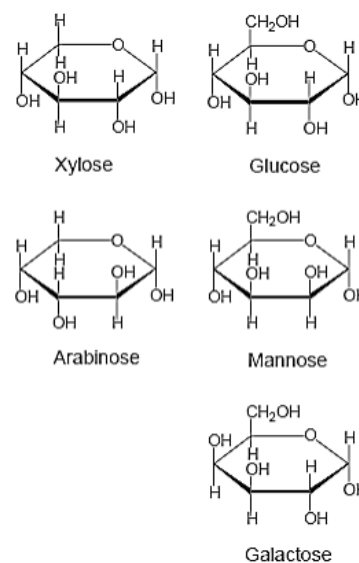


Figure 2-2: Pentoses and hexoses that mainly occur in hemicellulose [10]

Lignin

Lignin is a complex mixture that consists of a large group of aromatic polymers. [13] The basic structure is formed by linked phenylpropane units that can be separated, depending on the number of methoxy groups, into the three main types p-coumaryl alcohol, coniferyl alcohol and sinapyl alcohol shown in Figure 2-3. The most important chemical groups of lignin are methoxy- (-OCH₃), carbonyl- (-CO) and hydroxy- (-OH) groups. It is amorphous, hydrophobic, has a very low solubility in water and is responsible for the brown coloring of wood. In nature, it is the hardener of plants that makes the structure rigid and firm, mostly in combination with hemicellulose as randomly oriented microfibrils. [4,7,10]

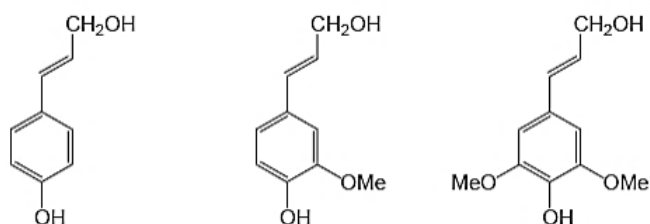


Figure 2-3: Basic building blocks of lignin (from left to right): p-coumaryl alcohol, coniferyl alcohol, sinapyl alcohol [10]

It has to be taken into consideration, that native lignin differs from lignin that is isolated with a harsh chemical process like the Kraft process. Because of lignin fragmentation the solubility and hydrophilic properties thereof are increased. [14]

Biomass wood

Wood, which is the main feedstock of the pulp and paper industry, also has different compositions regarding the above described lignocellulose components. It can be divided into two groups that are on the one hand softwood and on the other hand hardwood. Softwoods are evergreen plants or conifers and hardwoods are flowering plants or broadleaf. [9]

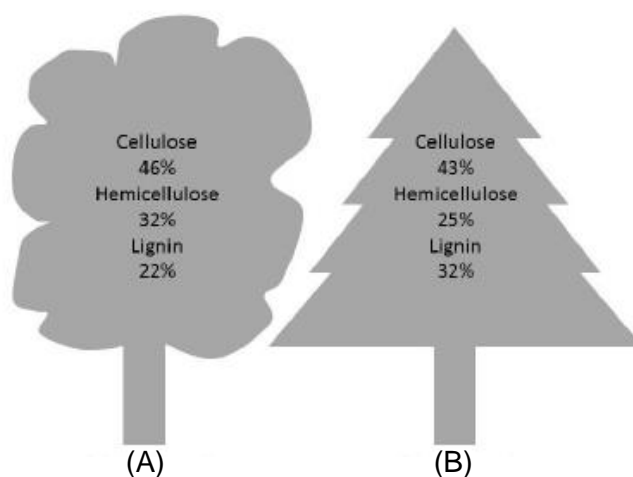


Figure 2-4: Average lignocellulosic composition of (A) hardwood and (B) softwood [9]

Beside the differences in lignocellulosic composition, shown in Figure 2-4 there are some other differences between the two types of wood. For example, one of them is the fiber size; softwood fibers are basically longer and thicker than hardwood fibers. Another one is the different composition of the lignin. [9] These and some other varying characteristics lead to more or less distinct differences during the treatment of these materials.

2.2 Chemical pulping process

In chemical pulping, wood fibers and extractives are chemically separated from each other to make them suitable for further treatment. There are two different processes that are mainly applied for this procedure, called delignification. The predominating sulfate or Kraft process and the sulfite process which accounts for a much smaller part of global pulp production. In contrast to the Kraft process the sulfite process often deals with acidic digestion which makes the process more variable but more sensitive to inhomogeneous feed material and the produced paper has a lower stability. [15]

Hereinafter, only the Kraft process is explained more in detail.

Pulp and paper process - Kraft process

To get pulp or paper from its origin material wood, many process steps are necessary. As shown in Figure 2-5, after the preparation and crushing of the raw wood material the digestion step follows. For the Kraft process the wood chips are cooked in a pressure-digester in the presence of white liquor at a temperature of about 140°C to 170°C for 3 to 4 hours. [16] The white liquor, which is distinguishing the Kraft process, is a solution of NaOH and Na₂S. Combined with the harsh cooking conditions it is responsible for the delignification of lignocellulose. The advantages of the alkaline Kraft process compared to others are the ability to use almost any raw material, the possibility to bleach to full brightness, the high strength characteristics of pulp and paper as well as the efficient and simple recovery of the used chemicals. The chemicals are collected after the digestion step by washing the pulp and extracting a mixture of inorganic cooking chemicals and combustible material called black liquor. [15]

The recovery cycle of black liquor is an integral part of the Kraft process. This cycle treats the black liquor by thickening, combusting and causticizing steps to regenerate the former used white liquor. In this cycle the chemical recovery as well as the energy generation by the combustion of the organic components from black liquor are significant for the whole process. [15]

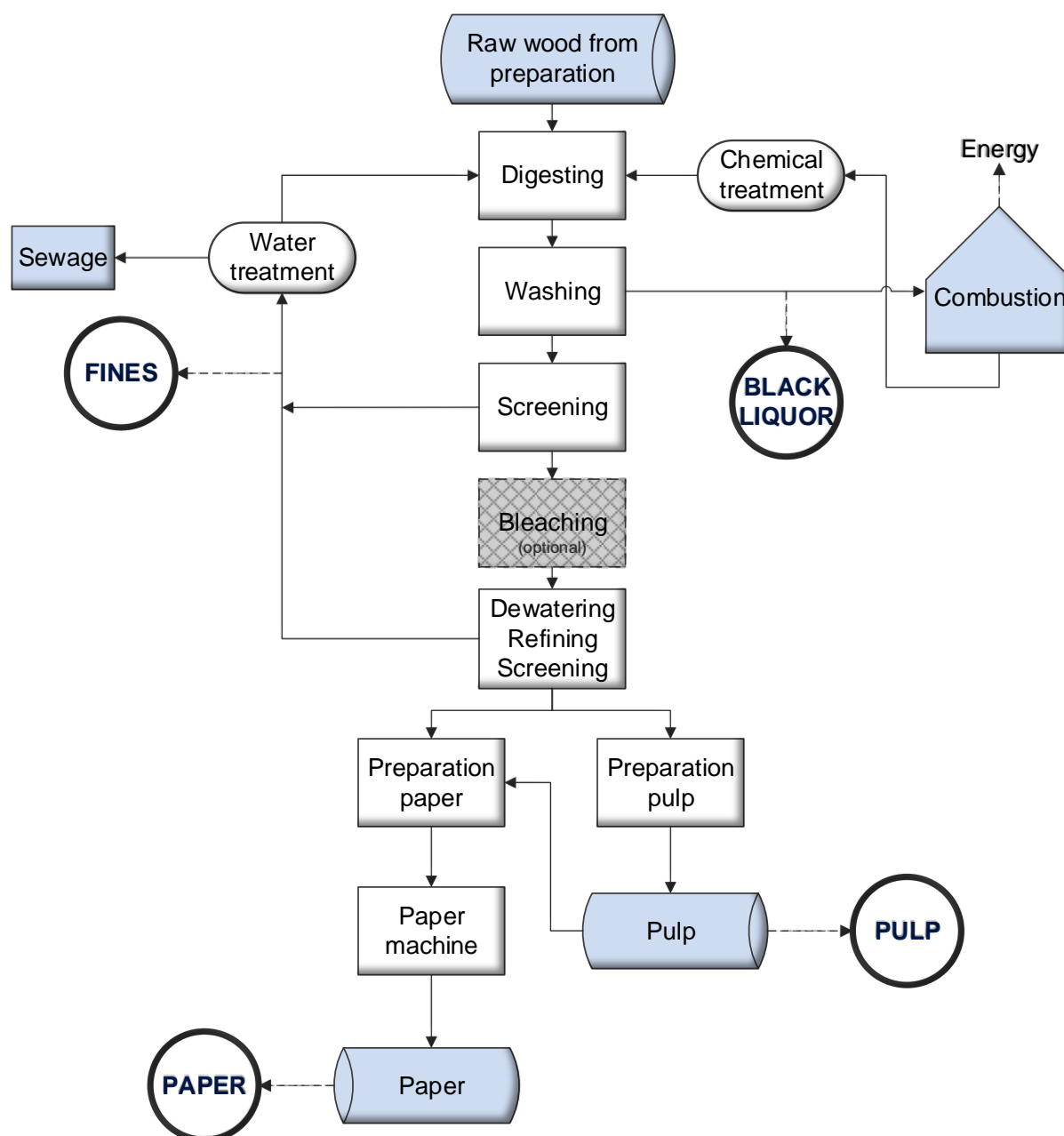


Figure 2-5: Simplified flow sheet of a pulp and paper making procedure using the Kraft process; circles are representing the taken experimental feed substrates

After separation and washing of the cellulosic mass from black liquor, the next step is the screening process. There the pulp is separated from solid contaminants like sand, bark, shives or speck. Furthermore, a fractionation by fiber size is carried out. Short chain fibers go to the recycling stream.

Depending on the requirements the pulp can be bleached. In this process step the remaining lignin is removed chemically. It can be said that this is the second delignifi-

cation after the digesting process. At the following dewatering step, the fibers are purified and sieved. Many short chain carbohydrates, called fines, generated over the entire process as well as chemicals are separated here and sent to the digester as recycle stream. [5,16–19]

At this point of the process, the paper and the pulp production processes are different. To get the finished pulp, the fibers are dried and ripped depending on the requirements. The paper making process continues by addition of additives to give the paper its desired properties and subsequent preparation by the paper machine. [15]

In the following points the nature, properties and use of the products and side streams are elaborated.

2.2.1 Pulp and paper

Pulp mainly consists of cellulose and is basically produced from wood. In its bleached or unbleached form, it can be used as sanitary article, composite material or as basic material for the paper production. To produce paper the pulp has to pretreated in several steps. Depending on the type of paper, preparations like cleaning, blending with other pulps, dilution and addition of chemicals have to be done. The prepared feed for the paper machine is called furnish and consists of about 99.5% water. It is pumped into the paper machine where it is dewatered, compacted, dried and finally flattened. [15,17]

2.2.2 Fines

Fines are known as the smallest components of fibers as well as other wooden components accruing from the pulp- and papermaking process. They are defined as the fine particles that are capable to pass through holes with a diameter of 76 μm . [20] Depending on the progress of the production steps of chemical pulp, it can be differentiated between two types of fines. The primary fines that accrue from the chemically intensive and harsh pulping and bleaching steps and the secondary fines generated during the mechanical refining of pulp. Figure 2-6 shows the origin of the two types and their main components. [21,22]

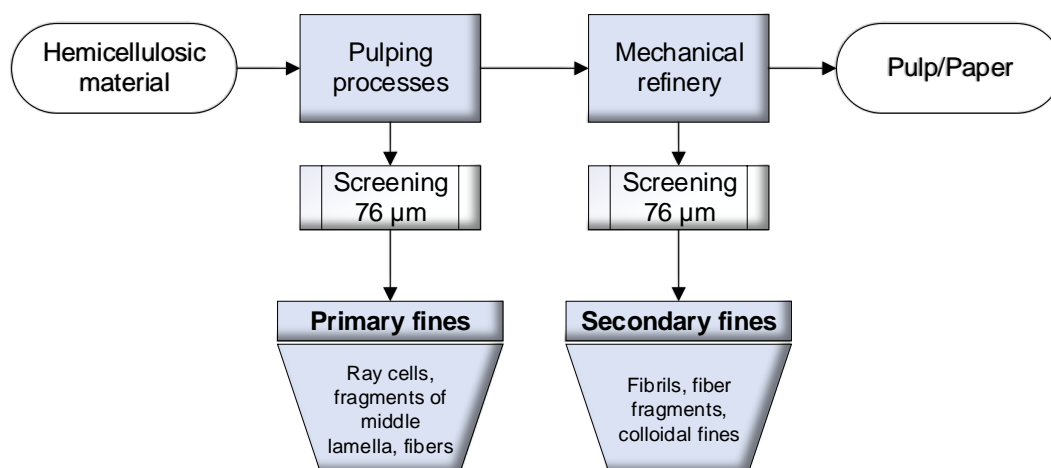


Figure 2-6: Types of fines including their main components, adapted [20]

The properties of fines are considerably different in comparison to the cellulosic fibers, also primary and secondary fines already differ to a certain extent. Nevertheless, the main characteristics are low dewatering ability and high specific surface combined with a high swelling ability. Both types are ultimately contained in the final products of pulp and paper industry to a certain degree. On the one hand they ensure positive characteristics e.g. higher paper strength, but on the other hand they promote negative aspects especially for the production performance e.g. high consumption of chemicals, hindered dewatering or impaired bleachability. Furthermore, it is hard to control the fines content which makes it challenging to keep the paper quality constant. Therefore, there are several attempts to remove fines systematically from the pulp and paper processes, for example by filtration. [21–26]

2.2.3 Black liquor

The separated brown to black colored mixture of lignin, chemicals, parts of hemicellulose and other organic concomitant substances after delignification of lignocellulosic biomass in the Kraft process is called black liquor. The composition and properties vary among the different pulp mills depending on the process conditions as well as the feed material. Roughly, the dry residue consists of 30-40% inorganics, resulting from the used pulping chemicals, and 60-70% organic matter. [18]

With about one third of total inorganics, sodium is the dominating compound, however, sulfur compounds, which make handling of the liquid much more difficult, cannot be neglected. The organic part consists of 30-35% lignin and the rest is made up of extractives and degradation products like acetic acid, lactic acid, formic acid. Depending

on the stage of vaporization, black liquor has a dry solids content from 10% to 80% and a pH-value of about 13.5. [16,18]

2.3 Carboxylic acids

The present theses focus on the conversion of lignocellulosic biomass to carboxylic acids. Lactic acid, formic acid and acetic acid are chosen as example acids, also other carboxylic acids may be formed, but are not considered in the present work. The properties, use and current production methods are described in the following points.

2.3.1 Lactic acid

Lactic acid, also known as 2-hydroxypropanoic acid, is an organic compound with the molecular formula $C_3H_6O_3$. With its hydroxyl (-OH) and carboxyl (-COOH) group it belongs to the group of hydroxycarboxylic acids. The two functional groups entail a bifunctional reactivity that gives the possible reactions high versatility. [27] The racemate consists of a 1:1-mixture of

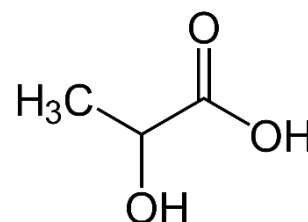


Figure 2-7: Structural formula of lactic acid

the enantiomers D-lactic acid and L-lactic acid. The melting point of the racemate is 17°C and the boiling point is 122°C . The acid is colorless, almost odorless and has an oily flow behavior. [28,29]

The acid is mainly used in the food industry, as preservative or as flavor enhancer but also in the chemical and pharmaceutical industry. As versatile raw material lactic acid can act as a basis substance for the transformation to different value-added chemicals. One of them is poly-lactic acid which can be used as biodegradable plastic to replace polyethylene and polystyrene. Therefore mainly as pure as possible L-lactic acid is used to form a homogeneous polymer structure. [30,31]

Currently, over 90% of industrial production of lactic acid are done by fermentation, the remaining share is produced chemically. However, production by fermentation has some drawbacks like high enzyme costs, complex purification, low space time yield and undesirable salt waste effluents. A further drawback is that raw biomass cannot be converted directly and has to undergo costly pretreatment. Nevertheless, by fermentation with specific bacteria, high yields of only L-lactic acid can be reached. [30,32]

2.3.2 Formic acid

Formic acid, also known as methanoic acid, has the molecular formula CH_2O_2 and forms the simplest carboxylic acid. Its carboxylic group ($-\text{COOH}$) determines the properties to a high degree. The melting point is 8°C and the boiling point is 101°C . It is colorless and at room temperature a pungent-smelling liquid. [28,33]

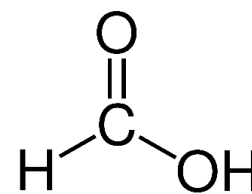


Figure 2-8: Structural formula of formic acid

The acid is used in a wide range of industrial fields especially because of its acidity and reducing properties. It is used for biomass preservation, in the leather industry as tanning agent, for the production of textiles as pH-regulator, as feed and food additive, as synthetic intermediate for pharmaceuticals as well as active ingredient of cleaning agents, to name just some of them. [33]

The main production method of formic acid is the hydrolysis of methyl formate. It accounts for approximately 90% of the world-wide production. Another production method deals with the formation of the acid from its salts. Therefore, sodium formate and calcium formate, produced by thermal reaction of the sodium hydroxide and calcium hydroxide with carbon monoxide, are generally used. [33,34]

2.3.3 Acetic acid

Acetic acid is the second simplest carboxylic acid, has the molecular formula $\text{C}_2\text{H}_4\text{O}_2$ and is also known as ethanoic acid. It is formed by a methyl ($-\text{CH}_3$) and a carboxyl ($-\text{COOH}$) group. At standard conditions it melts at 17°C and boils at 118°C . It is a colorless liquid with a pungent odor. [28,35]

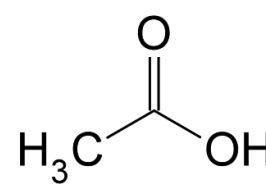


Figure 2-9: Structural formula of acetic acid

About 40% of worldwide production are used to form vinyl acetate which is an important industrial polymer used for coatings, paints and plastics. Also, the ester cellulose acetate is produced from acetic acid and used for cellulose plastics, cigarette filters as well as for textile fibers. Furthermore, the acid is often used as solvent for different applications. [35]

A high amount of acetic acid is produced by the carbonylation of methanol at high temperature and high pressure. Another method mainly used in the past is the direct

oxidation of saturated hydrogens like n-butane and light naphtha. Further used methods are the oxidation of acetaldehyde as well as the microbial production from ethanol and sugar. [35]

2.4 Basic reactions of biomass conversion

The following points describe the most common basic reactions that occur during hydrothermal conversion of biomass. It has to be considered that there is a huge amount of different reaction mechanisms in organic chemistry. Depending on substances and conditions most of them occur in parallel or/and in series.

Substitution reaction

A substitution reaction is, like shown in Equation 2-1, an exchange reaction where one fragment is replaced by another. The reactive fragment can be a nucleophile, electrophile or a radical. The reverse reaction is again a substitution reaction with the same mechanism. This reaction mostly occurs at saturated hydrocarbons like alkanes but also at aromatic molecules like benzene or phenol. [36]



One example is the alkaline substitution of bromoethane to ethanol by the reaction with potassium hydroxide. There, as shown in Figure 2-10, the hydroxide ion of potassium hydroxide is exchanged with the bromine atom of bromoethane, forming ethanol and potassiumbromine. [37]

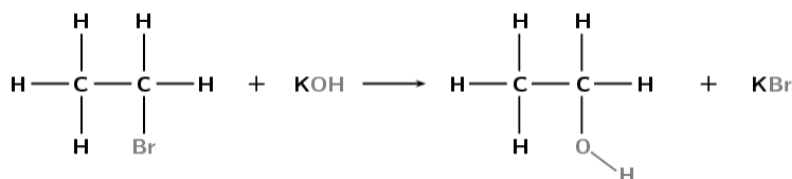


Figure 2-10: Alkaline substitution of bromoethane to ethanol [37]

Addition reaction

During addition reactions one molecule or atom is added to a molecule by the breakage of a double or triple bond. The simplified reaction is shown in Equation 2-2. [36]



Depending on the nature of the involved substances, in chemistry it is differentiated between electrophile-, radical-, nucleophile- and cyclo-addition reactions. [38] The aldol addition reaction is a common reaction in organic chemistry. As shown in Figure 2-11, aldehyde and ketone form an aldol (aldehyde with hydroxy group) by C-C bond formation. The reverse reaction often happens in the course of hydrothermal degradation of biomass and would be a form of elimination reaction. [39]

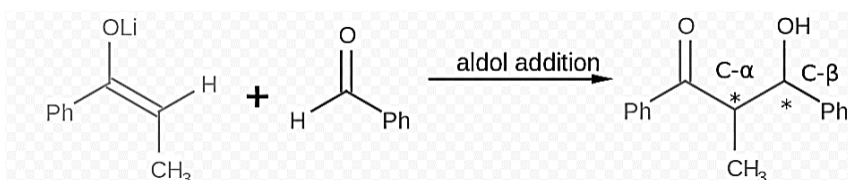


Figure 2-11: Addition reaction of ketone and aldehyde to an aldol, adapted [39]

Elimination reaction

Elimination reactions occur if there is one molecule of starting compound and afterwards two molecules or molecule groups are split off. In most cases it is the backlash of an addition reaction. [40] The simplified equation is shown in Equation 2-3.



Special cases of elimination reaction are e. g. the dehydrogenation, where two hydrogen atoms are abstracted and the dehydration where a water molecule is abstracted. [40] Figure 2-12 shows the dehydration of ethanol to ethylene under acidic conditions.

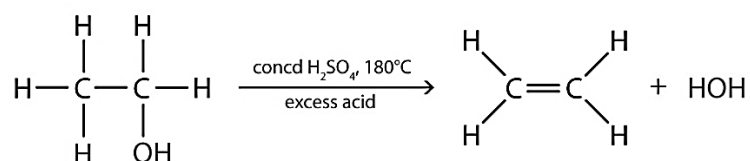


Figure 2-12: Dehydration of ethanol to ethylene, adapted [41]

Rearrangement reaction

A rearrangement is a reaction where a group or an atom is changing its position inter- or intramolecularly. Equation 2-4 shows the simplified principle.



Rearrangement reactions are usually called isomerization if the reaction occurs intramolecularly. In general isomerization names the mechanism where a molecule is transformed into another form with exactly the same atoms but different arrangement. Consequently, the molecules have the same molecular mass but mostly different chemical and physical properties. Figure 2-13 shows the isomerization from one tautomer into another, also called tautomerization. [42]

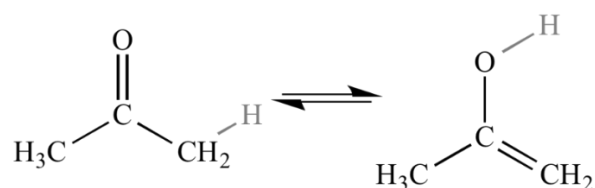
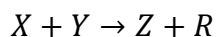


Figure 2-13: Isomerization of one tautomer into another [43]

To mention one more example, the 1,2-shift reaction is an organic reaction that involves two adjacent atoms of a chemical compound where the two atoms are substituted for one another. In this case the reactant and the product are structural isomers. If the rearrangement involves a hydrogen atom, the reaction is called 1,2-hydride shift. [44]

Condensation and solvolysis reaction

A condensation reaction is a fusion of two fragments to form one bigger complex, including the abstraction of a small molecule like water, ammonia or alcohol. Equation 2-5 shows the basic mechanism of this reaction. [45] It is similar to the substitution reaction, but in contrast the two fragments associate with each other and do not stay separate. Nevertheless, it can be seen as part of it.



Equation 2-5

The reversion of a condensation reactions including addition of water is called hydrolysis, like shown in

Figure 2-14. In general, these reversals are called solvolysis. There are numerous examples for these reactions like the hydrolysis of fats or esters with water to form alcohols and fatty acids. Also, the degradation of biomass to produce glucose follows this reaction pathway. [46]

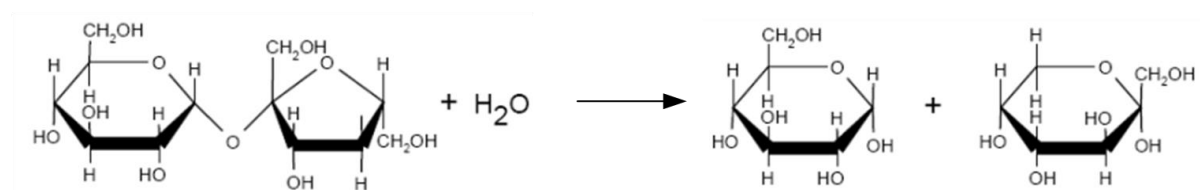


Figure 2-14: Hydrolysis of saccharose to glucose and fructose, adapted [47]

2.5 Hydrothermal conversion of cellulose and its derivatives to monosaccharides

In the following just the conversion of cellulose will be discussed, but because of the similar structure of hemicellulose, it is assumed that they have a related behavior. At any case, it is known that hemicellulose is faster hydrolyzed than cellulose. [48] Because of the totally different structure of lignin, its hydrothermal conversion is considered separately in chapter 2.7.

The hydrothermal and catalyzed transformation of cellulose to valuable chemicals can be done under many different conditions. Mostly many reaction steps and intermediates are necessary respectively appear on the conversion route to the desired product. To get the highest yield and selectivity a multifunctional system at optimal conditions must be found. To be able to optimize the conversion it is helpful to know something about the possible pathways to the desired products.

As shown in Figure 2-15, the first step of the conversion to chemicals is the degradation of the long-chained cellulose polymers to monomers or strictly speaking to convert the polysaccharides into monosaccharides. Based on the monosaccharides, chemicals can be formed by different pathways. It requires multiple reactions to form intermediates that finally generate the desired acids.

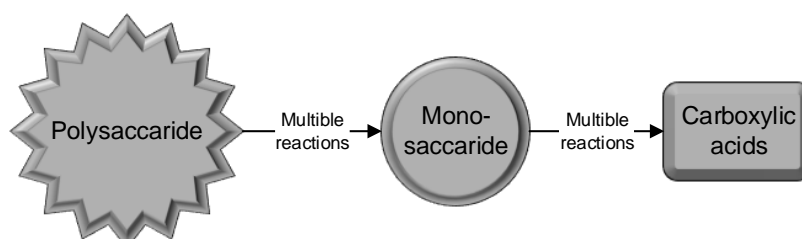


Figure 2-15: Simplified way from polysaccharides to carboxylic acids

Figure 2-16 shows the overall pathways in more detail. The monosaccharides glucose and fructose are the initial intermediates for the conversion to carboxylic acids. The chemical transformation from cellulose is described below in this chapter.

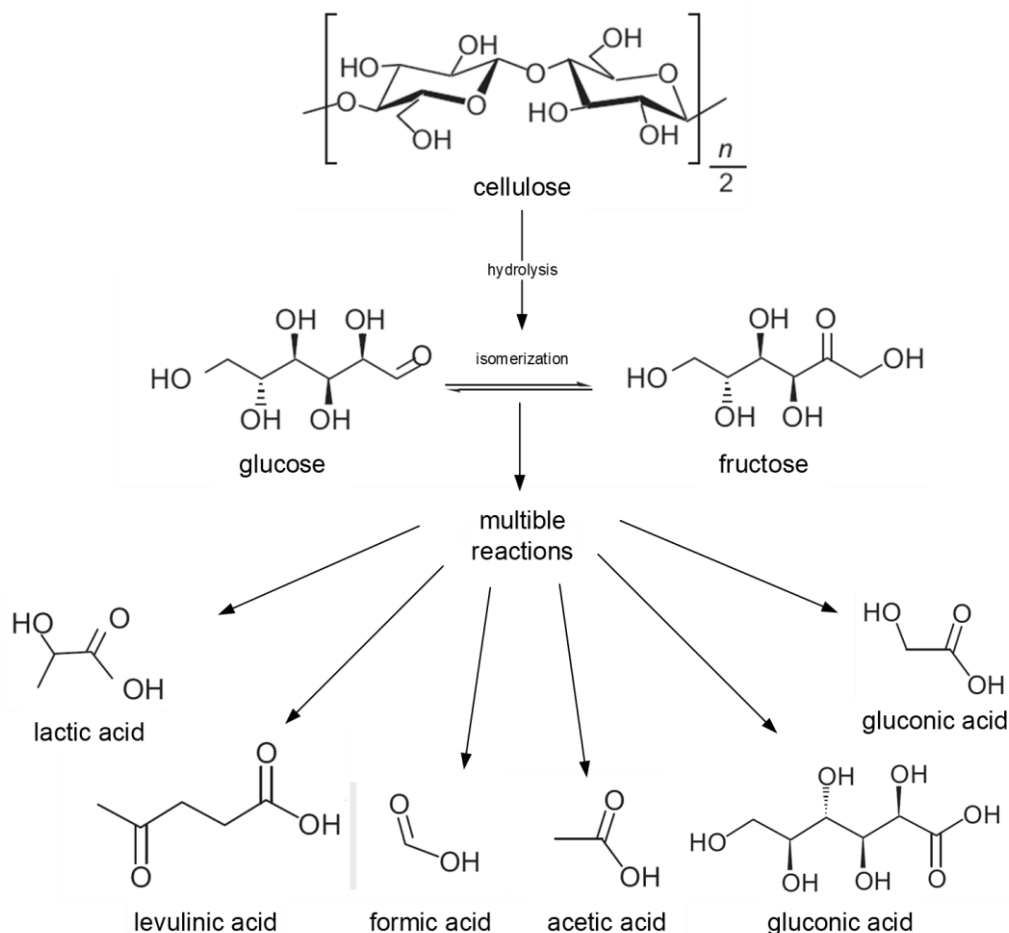


Figure 2-16: Some possible acids formed by the conversion of cellulose; adapted [2]

Hydrolysis to glucose

During cellulose degradation, hydrolysis to monosaccharides is usually the initial reaction. More precisely, the β -1,4-glycosidic bonds are cleaved upon reaction with water and simple sugars like the monomer glucose as well as partly hydrolyzed oligomers are formed. The solubility of the glucose oligomers (oligosaccharides) in water depends strongly on the temperature. At ambient temperature they still dissolve in water until DP 6 and lower. Because of the intra- and intermolecular bonding network of cellulosic polymers, caused by hydroxyl groups, it is difficult to activate cellulose under mild conditions. [2]

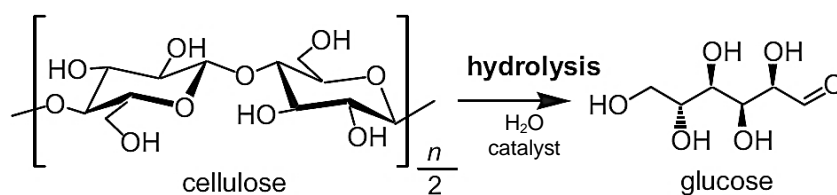


Figure 2-17: Hydrolysis of cellulose to glucose; adapted [2]

well as on the environmental conditions. To form the desired substance there are some needed intermediates, but there appear also some unwanted side products in the multireaction pathways. Therefore, multifunctional catalysts are necessary to reach high yields and high selectivity. The key mechanism for the formation of organic acids with less than six carbon atoms is the retro-aldol reaction that cleaves the C-C bonds of C₆-compounds to smaller molecules. In this case, a decisive factor for the reaction to a specific compound is where this cleavage takes place. In turn, the catalysts and process conditions are responsible for this. But not only cleavage of C-C bonds plays an important role to form the desired chemical, also rearrangements of oxygen and hydrogen-groups are indispensable. [3]

Beside the catalyst, the reaction atmosphere has a key function on the conversion. For this reason it is known that the type of reaction products as well as the yield can be significantly influenced under superimposed nitrogen, hydrogen or oxygen atmosphere. [3]

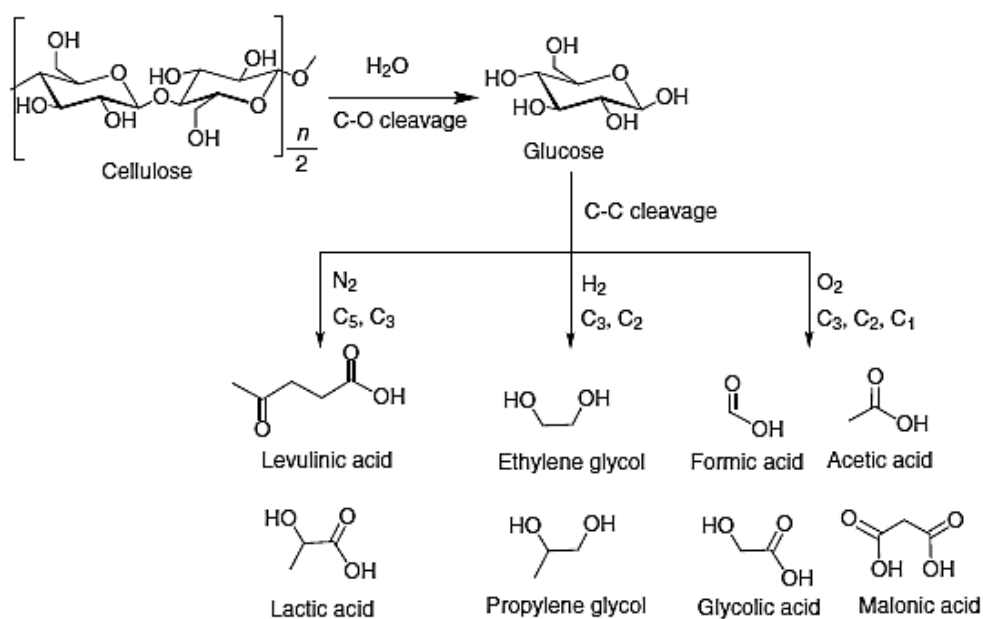


Figure 2-19: Scheme of preferred product formation of cellulose at hydrothermal conditions under nitrogen, hydrogen or oxygen superimposed reaction atmospheres [3]

As shown in Figure 2-19 it is expected that levulinic acid and lactic acid are formed under inert conditions, caused by a superposition of nitrogen or helium in the reactors atmosphere. The shown polyols are formed by reductive cleavage of C-C bonds under

hydrogen atmosphere and the low-carbon acids formic acid and acetic acid by oxidative cleavage under oxygen atmosphere. [3] Also different concentrations of the converted substrate as well as the use of an acidic or alkaline reaction environment lead to different products and yields and must not be neglected. [50]

In the following the supposed conversion pathways as well as some methods to form the three targeted acids and other important substances are discussed.

2.6.1 Conversion to lactic acid

The conversion of cellulose to the C₃-molecule lactic acid is a multi-reaction with several intermediates. As shown in Figure 2-20, it is supposed that the transformation happens in two further reaction steps following the hydrolysis of cellulose and isomerization of glucose to fructose. The first one is a retro-aldol fragmentation to the two trioses dihydroxyacetone and glyceraldehyde. For that, the C₃-C₄ bond of fructose is cleaved. By further isomerization of those C₃-compounds lactic acid is formed under appropriate conditions. [30,51]

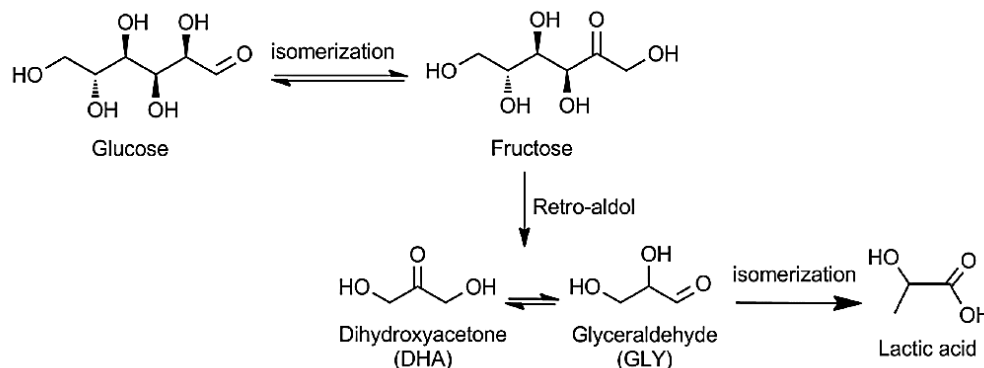


Figure 2-20: Supposed pathway to lactic acid [30]

A possible method for the conversion of cellulose or glucose to lactic acid is the treatment with subcritical or supercritical water. No additional catalyst is needed for this conversion but the selectivity is very low. [49] In general it is known that lactic acid is formed under base catalyzed hydrothermal treatment of cellulose. In further consequence many studies of base catalyzed conversions of lignocellulosic materials were done. The conversion of glucose in a NaOH-solution at 300°C yielded 27% lactic acid. The same experiment was done with a Ca(OH)₂-catalyst and led to a yield of 20%. [52]

A further study was done at 300°C in a NaOH-solution and by adding Zn and Ni ions as well as activated carbon. Cellulose was converted to 42% to lactic acid. [53]

The conversion of glucose and fructose from cellulose hydrolysate to lactic acid at 300°C with a ZnSO₄-catalyst in aqueous solution was investigated. The lactic acid yield was 42% and 48% respectively, leading to the conclusion that fructose has a higher selectivity for the conversion to lactic acid than glucose. [49] At lower temperatures of 190°C tungstated alumina (AlW) was used as catalyst for the conversion of cellulose under inert atmosphere. This experiment resulted in a yield of 28% lactic acid at a total conversion of 47%. [54] Further investigations were done at the same conditions but with ball-milled cellulose and diluted Pb(II) ions as catalyst. The yield was with 62% significantly higher, but the different form of cellulose must be taken into account. [55] Nevertheless it is a high yield and selective system for lactic acid conversion but the high toxicity of lead may hampers a large-scale application.

A less toxic catalyst was found in the vanadium salt VOSO₄. Depending on the reaction atmosphere, cellulose can be converted to formic or lactic acid where lactic acid is formed under inert atmosphere. With the described catalyst 54% of lactic acid was formed from ball-milled cellulose at 180°C. [56] A further promising group of catalysts is the group of lanthanide triflates (Ln(OTf)₃). They are clean and easy to recover and thus known as environmentally friendly catalysts. Especially the triflate group with erbium (Er(OTf)₃) is very effective for the conversion of cellulose to lactic acid. The experiment was done at 240°C under inert atmosphere (N₂) and with microcrystalline cellulose and yielded 63% lactic acid. [57] However, it has to be highlighted that the group of lanthanides, including erbium, are rare earth elements and hence they are limited resources which complicates practical application.

Beside the above described experiments with H₂O as solvent, also methanol (CH₃OH) was used for the conversion of cellulosic biomass. In contrast to H₂O, the alcohol forms methyl lactate instead of lactic acid. [30]

Bases as well as metals and ions, in homogeneous or heterogenous form, are catalysts leading to a high yield and selective conversion of cellulose and its derivatives to lactic acid. Table 2-1 summarizes the above described experiments.

Table 2-1: Experiments for hydrothermal conversions of different raw materials to lactic acid in H₂O

Substrate	Catalyst	T [°C]	t [h]	Yield [%]	Atmosphere	Ref
Cellulose	NaOH + Zn, Ni and activated carbon	300	0.08	42	-	[53]
Cellulose (ball-milled)	Pb ^{II}	190	15	62	Superimposed N ₂	[55]
Cellulose	AlW oxides	190	24	28	Superimposed He	[54]
Microcrystalline cellulose	Er(OTf) ₃	240	0.5	63	Superimposed N ₂	[57]
Corn cobs	Ca(OH) ₂	300	0.5	45	-	[58]
Glucose	NaOH	300	0.02	27	-	[51]
Glucose	VOSO ₄	180	2	54	Superimposed N ₂	[56]
Glucose	Ca(OH) ₂	300	0.02	20	-	[51]
Glucose	ZnSO ₄	300	0.02	42	-	[49]
Fructose	ZnSO ₄	300	0.02	48	-	[49]

2.6.2 Conversion to formic acid

The transformation of glucose to formic acid might go the route over the formation of aldehydes by C-C bond cleavage. As shown in Figure 2-21, it is supposed that glyceraldehyde, glyoxal and glycerolaldehyde are formed as main intermediates. In further consequence, formic acid is generated by the formation of the by-product CO₂. [50]

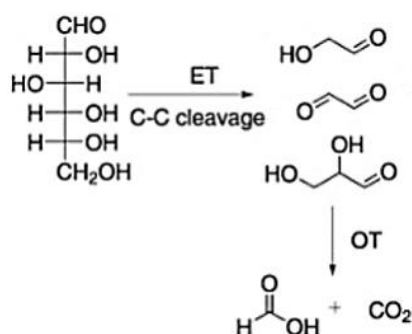


Figure 2-21: Scheme of the transformation of glucose to formic acid under O₂ reaction atmosphere [50]

This pathway was developed by using a phosphovanadomolybdate polyoxometalate (H₅PV₂Mo₁₀O₄₀) as catalyst under O₂-atmosphere. The highest yield of glucose conversion to formic acid was 55% by using this catalyst under oxygen atmosphere at

100°C. At higher temperatures the yield decreased under otherwise similar conditions. Also, cellulose was converted by using the $H_5PV_2Mo_{10}O_{40}$ -catalyst in an acidic solution of H_2O and HCl . A maximum yield of 34% was achieved. [50]

Another pathway, shown in Figure 2-22, describes the transformation of cellulose and glucose catalyzed by VO^{2+} -cations using a $VOSO_4$ -catalyst. The main intermediate fructose is formed by isomerization of glucose. In a further reaction step fructose is transformed to the C_3 -intermediates glyceraldehyde and 1,3-dihydroxyacetone by retro-aldol fragmentation. Depending on the reaction atmosphere formic acid and CO_2 as well as lactic acid can be formed by superposition of oxygen or nitrogen. For the formation of lactic acid the main by-product is hydroxymethylfurfural (HMF), but to a much lesser extent than CO_2 for the formation of formic acid. [56]

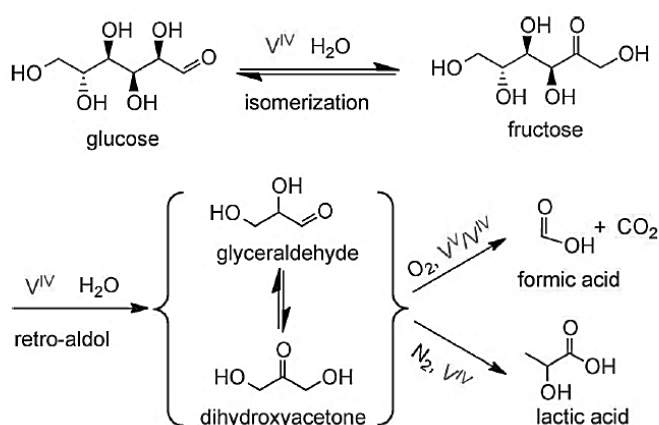


Figure 2-22: Scheme of the transformation of glucose in water catalyzed by $VOSO_4$ under N_2 and O_2 reaction atmosphere [56]

By using the $VOSO_4$ -catalyst the conversion of glucose in water under nitrogen atmosphere at 180°C yielded 53% formic acid. A significantly higher yield of 73% was obtained by adding ethanol under the same conditions but at 140°C. The formation of the by-product CO_2 was much lower by using this solution. The same experiment was done with ball-milled cellulose at 160°C and yielded 70% formic acid. That shows that the catalyst also promotes the hydrolyzation of cellulose to glucose. [56]

Further experiments were done with hydrogen peroxide solution as oxidant for the conversion of glucose to formic acid, at 250°C the yield was 24%. The same experiment was carried upon addition of $NaOH$, resulting in a yield of 70%. [59] Table 2-2 shows

a selection of experiments, most of them described above, that were done to investigate the transformation of cellulose and its derivatives to formic acid.

Table 2-2: Experiments for hydrothermal conversions of different raw materials to formic acid

Substrate	Solution	Catalyst	T [°C]	t [h]	Yield [%]	Atmosphere	Ref
Cellulose	H ₂ O + H ₂ SO ₄	H ₅ PV ₂ Mo ₁₀ O ₄₀	170	9	28	Superimposed O ₂	[50]
Cellulose	H ₂ O + HCl	H ₅ PV ₂ Mo ₁₀ O ₄₀	170	9	34	Superimposed O ₂	[50]
Cellulose ball-milled	H ₂ O + C ₃ H ₅ OH	VO ₂ SO ₄	160	5	70	Superimposed O ₂	[56]
Glucose	H ₂ O	VO ₂ SO ₄	180	2	53	Superimposed O ₂	[56]
Glucose	H ₂ O + C ₃ H ₅ OH	VO ₂ SO ₄	140	3	73	Superimposed O ₂	[56]
Glucose	H ₂ O	H ₂ SO ₄	150	3	9	Superimposed O ₂	[50]
Glucose	H ₂ O	H ₅ PV ₂ Mo ₁₀ O ₄₀	100	3	55	Superimposed O ₂	[50]
Glucose	H ₂ O	H ₅ PV ₂ Mo ₁₀ O ₄₀	150	3	29	Superimposed O ₂	[50]
Glucose	H ₂ O ₂	-	250	0.02	24	-	[59]
Glucose	H ₂ O ₂	NaOH	250	0.02	70	-	[59]

2.6.3 Conversion to acetic acid

Experiments were performed to convert cellulose in an H₂O₂-solution at 400°C in a batch reactor. An acetic acid yield of 11% was obtained. At the same temperature the transformation of glucose in a NaOH-solution yielded 36% of acetic acid. Furthermore, glucose was converted at 250°C in a mixture of H₂O₂ and NaOH. The result was a yield of 17% acetic acid but a higher yield of formic acid (38%) and glycolic acid (22%). [60]

To enhance the yield and selectivity of acetic acid generation a two-step process was developed. As depicted in Figure 2-23, the first step was a hydrothermal degradation of the polysaccharides to form mainly HMF, 2-furaldehyde and lactic acid. In contrast to step two this step is without oxygen supply. In the second step, the formed furans as well as lactic acid were oxidized to acetic acid by oxygen supply. Experiments were done with cellulose at 300°C without adding a catalyst. One of them was done with

permanent oxygen supply (one-step) and obtained a yield of 9%. In the same experiment, carried out with the two-step procedure, the yield of acetic acid increased to 16%. Furthermore, it was determined that about 40% and 20% of total acetic acid yield were from the furans and lactic acid, respectively. So the origin of the remaining 40% was from other derivatives of cellulose. [3,61]

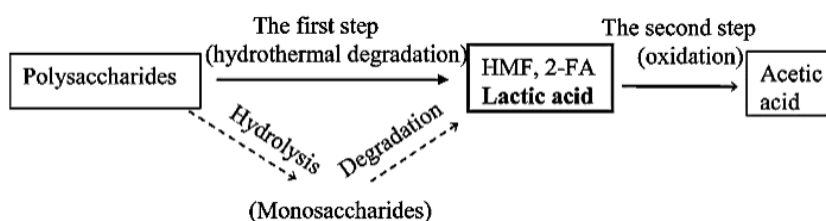


Figure 2-23: Conversion of polysaccharides to acetic acid by a two-step process [61]

An alkaline two-step process was performed to convert glucose at 300°C to acetic acid. For that, calcium hydroxide was used as catalyst. [53] It is known that lactic acid is preferably formed under these conditions and in further consequence the yield for the oxidation to acetic acid is about twice as high as from furans. [61] The result was a yield of 27% by adding hydrogen peroxide in the second step. [53] Table 2-3 summarizes the selection of experiment discussed above.

Table 2-3: Experiments for hydrothermal conversions of different raw materials to acetic acid

Substrate	Solution	Catalyst	T [°C]	t [h]	Yield [%]	Atmosphere	Ref
Cellulose	H ₂ O + H ₂ O ₂	-	400	0.8	11	-	[60]
Cellulose	H ₂ O + H ₂ O ₂	-	300	0.2	9	-	[61]
Cellulose (two-step)	H ₂ O	H ₂ O ₂ added @ 2 nd step	300	0.2-0.3	16	-	[61]
Glucose	H ₂ O	NaOH	400	0.8	36	-	[60]
Glucose	H ₂ O ₂	NaOH	250	0.8	17	-	[60]
Glucose	H ₂ O	Ca(OH) ₂ + H ₂ O ₂ added @ 2 nd step	300	0.2-0.3	27	-	[53]

2.6.4 Conversion to other substances

Beside the acids described above, many other products can be formed by the conversion of monosaccharides and cellulose, respectively. Some important substances are briefly presented in this chapter.

Hydroxymethylfurfural (HMF)

HMF has to be taken into consideration as an important intermediate product for the production of a variety of chemicals and fuels. It consists of an aldehyde- and furan-association and represents a C₆-substance. [62] In contrast to lactic acid, it is well known that HMF is efficiently formed under acidic conditions. Similar to lactic acid both are formed without the presence of hydrogen or oxygen. As shown in Figure 2-24, after the hydrolysis of cellulose, HMF is finally formed by the dehydration of fructose. [30]

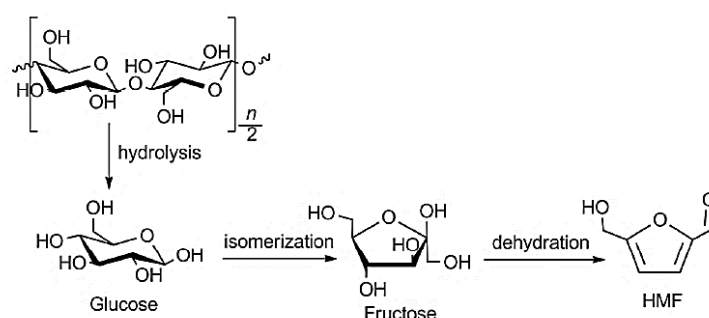


Figure 2-24: Reaction pathway of cellulose to HMF [30]

A very selective system for the conversion of HMF was possible by the use of the ionic liquid 1-Ethyl-3-methylimidazolium chloride ([EMIM]Cl). Together with the catalysts chrome chloride and ruthenium chloride a maximum yield of 60% was achieved at 120°C. [63]

Levulinic acid

Levulinic acid contains a carboxylic keto-group and a carboxylic group and is soluble in water. The C₅-compound is a considerable platform chemical that can be used as basis for many chemical applications because of its high chemical reactivity. It can be used for the production of transportation fuels, to name one. [64]

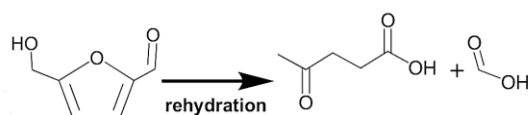


Figure 2-25: Conversion step from HMF to levulinic acid and formic acid as by-product [2]

It is supposed that levulinic acid is mainly formed under acidic conditions by the rehydration of HMF. As depicted in Figure 2-25, in this conversion step also formic acid can be formed to a certain extent. [2] For example, the conversion of cellulose at 240°C using zirconium oxide as catalyst in water under nitrogen atmosphere results in 52%

yield of levulinic acid. [65] In another experiment the yield from cellulose was 60% at 180°C with hydrochloric acid as catalyst. [66]

2.7 Hydrothermal conversion of lignin

The basic structure of lignin consists of the three units sinapyl alcohol, coniferyl alcohol, and p-coumaryl alcohol which are connected by C-C and ether bonds. It accounts for approximately 40% of the energy content in lignocellulosic biomass. Thus, its conversion to chemicals and fuels has high potential. Because of the fact that lignin is a highly complex and crosslinked macromolecule, the knowledge of reaction pathways is still very limited. [1,14] It has to be taken into account that isolated lignin mainly occurs as by-product in the pulp and paper industry and undergoes in the course of these processes chemical structural modifications. Therefore, it has similar but not the same properties as native lignin. [1] This chapter gives a short overview of the hydrothermal conversion of lignin to acids.

It is supposed that the depolymerization at temperatures up to 320°C leads to aromatic aldehydes like vanillin, syringaldehyde and p-hydroxy-benzaldehyde. As shown in Figure 2-26, the aldehydes can act as intermediates to form acids, in the course of a complex parallel and series multireaction network. To increase the yields, noble metals as well as transition metals are used as effective catalysts. Because of the much lower activation energy, the degradation of lignin is considered to be the faster reaction step in comparison to the oxidation of the intermediates into organic acids like formic, vanillic, lactic and p-hydroxybenzoic acids. [14]

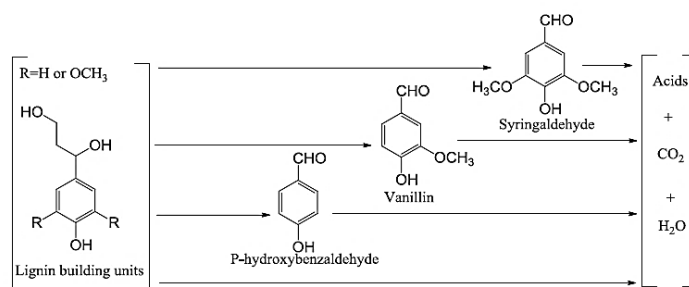


Figure 2-26: Overall reaction scheme of hydrothermal conversion of lignin at up to 320°C [14]

An experiment was done to produce vanillin from Kraft lignin in a batch reactor. The lignin was diluted in a NaOH-solution and heated up to 123°C under oxygen atmosphere. It resulted in a yield of 7.6% from low-molecular weight lignin (softwood) and

3.5% for high-molecular weight lignin (hardwood). [67] However, vanillin from lignosulfonates is sold already.

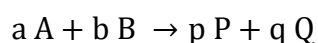
To reduce the complexity, researchers use some model compounds like phenol, guaiacol or syringol instead of lignin. By using these model compounds the formation of formic acid and acetic acid was examined. It is supposed that the addition of alkali changes the main reaction pathways and therefore influences the yields. In general, it is assumed that the reaction pathway to the low molecular weight acids can be separated into two reaction parts. The first one is the ring-opening reaction where the aromatic ring is cleaved and the second one is the reaction to the products like acetic acid and formic acid. Both parts include a lot of reactions and intermediates. At 300°C and in a H₂O₂-water mixture the above-named model substrates yielded up to about 9% of acetic acid. [68]

Alkaline lignin was converted in a H₂O₂-water mixture and had the highest yield of acetic acid (12.3%) and formic acid (4.5%) at 300°C. To improve the yield, NaOH was added and it resulted in 23.3% of acetic acid and 10.3% of formic acid. These experiments showed that the yield of these acids increases significantly by adding alkali and under oxygen supply. [1]

2.8 Reaction kinetics

Upon consideration of reaction kinetics, it is possible to describe the formation of reaction-products over time. For that, the reaction rate (r) is the central value. The main factors influencing the reaction rate are beside the structure and nature of reactants and solvents, the temperature, the pressure and the used catalysts or other additives. For heterogenous systems additional factors like diffusion and adsorption have to be considered. [69,70] However, only homogeneous reactions will be discussed in this chapter.

Equation 2-6, shows the stoichiometric equation of an irreversible reaction from two reactants to two products. The lowercase letters stand for the stoichiometric coefficients of the substances that are in capital letters.



Equation 2-6

Considering that the system is closed and there are constant conditions the reaction rate equivalent for each substance can be calculated by Equation 2-7. In Equation 2-8 the reaction rate by each substance, which means the change of concentration during a time interval, is depicted.

$$r = -\frac{1}{a} * \frac{d[A]}{dt} = -\frac{1}{b} * \frac{d[B]}{dt} = \frac{1}{p} * \frac{d[P]}{dt} = \frac{1}{q} * \frac{d[Q]}{dt} \quad \text{Equation 2-7}$$

$$-r_A = -\frac{d[A]}{dt}; -r_B = -\frac{d[B]}{dt}; r_P = \frac{d[P]}{dt}; r_Q = \frac{d[Q]}{dt} \quad \text{Equation 2-8}$$

In general, it is not possible to solve Equation 2-7 from the stoichiometric coefficients. The generally used formula for the equivalent reaction rate of the reaction from Equation 2-6 is shown in Equation 2-9. k represents the reaction rate constant, its dimension depends on the order of the reaction. It is a function of time and temperature and is independent of the concentration. [70]

$$-r = k * [A]^\alpha * [B]^\beta = k * c_A^\alpha * c_B^\beta \quad \text{Equation 2-9}$$

The overall order of the reaction is described by the sum of exponents of the concentration of reactants or products, in Equation 2-9 α and β . These values can be determined experimentally. Table 2-4 shows the different forms of kinetic laws from zero to second order. Because of the fact that in experiments mostly the concentration at defined times is determined, the integral form is generally used for the evaluation of the kinetic behavior. [70]

Table 2-4: Overview of the different forms of rate laws, reaction orders and the associated dimension of the reaction rate constant, adapted [70]

Order	Differential form	Integral form	Dimension of k
0	$-r = -\frac{1}{a} \frac{dc_A}{dt} = k$	$c_{A,0} - c_A = a * k * t$	$\text{mol} * (\text{l} * \text{s})^{-1}$
1	$-r = -\frac{1}{a} \frac{dc_A}{dt} = k * c_A$	$\ln\left(\frac{c_{A,0}}{c_A}\right) = a * k * t$	s^{-1}
2	$-r = -\frac{1}{a} \frac{dc_A}{dt} = k * c_A^2$	$\frac{1}{c_A} - \frac{1}{c_{A,0}} = a * k * t$	$\text{l} * (\text{mol} * \text{s})^{-1}$

Most reactions are bimolecular reactions, that means two molecules react to products. Reactions up to third order are relatively common but trimolecular ones, where three different molecules react similar, are rare. [70]

Reaction process

Many chemical reactions do not proceed in a single step. Depending on the reaction process it is differentiated between simple, reversible, parallel and consecutive reactions. Figure 2-27 shows the concentration gradients over time for these reactions to the product "C". The simple reaction designates the formation of one product by two reactants. The reversible reaction is characterized by a forward reaction to the product and a backward reaction to the reactants. The reaction rate constant of both reactions is mostly different and can be influenced by the reaction conditions. Parallel reactions form more than one product simultaneously from the reactant in contrast to consecutive reactions, where the product only can arise after an intermediate is formed. For these reactions the reaction to the intermediate can be the limiting reaction. [71]

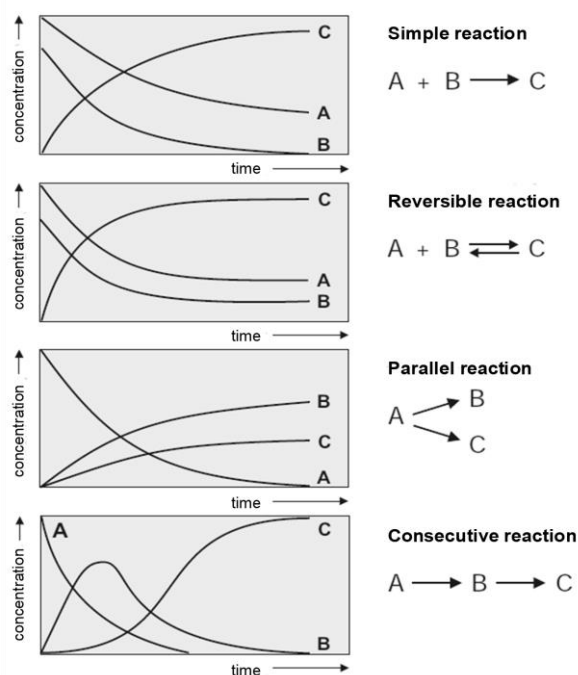


Figure 2-27: Different reaction processes, modified [71]

In many cases the described reactions occur in sequence or simultaneously before a desired product is yielded.

Determination of reaction order

The determination of the reaction order is based on experimental data. For that, the reaction rate is measured at different educt concentrations. Many methods like integral, difference quotient, graphical, numerical differentiation, half-life, nonlinear regression and polynomial fit are developed. Depending on the measurement data some methods are more suitable than others.

Temperature dependency

Especially by increasing the temperature, chemical reactions can be sped up significantly. With the Arrhenius equation, shown in Equation 2-10, the influence of temperature can be described quantitatively by the change of the reaction rate constant k . It is determined at a defined temperature T with the universal gas constant R and the two

empirical constants A and E_a . E_a is the needed activation energy which decreases the reaction rate constant k at high values. A is called pre-exponential factor and has the same dimension as k , depending on the reaction order. It considers the frequency of collisions under the respective reaction conditions. [72]

$$k = A * e^{-\frac{E_a}{R*T}} \quad \text{Equation 2-10}$$

The activation energy can be calculated by the measurement of the reaction rate constant at different temperatures. In Equation 2-11 the activation energy is then the only unknown factor and can be calculated. [72]

$$\ln \frac{k_1}{k_2} = \frac{E_a}{R} * \left(\frac{1}{T_2} - \frac{1}{T_1} \right) \quad \text{Equation 2-11}$$

3 Experimental setup

Figure 3-1 shows the experimental setup, commissioned for the present master thesis. It was built up especially for this diploma thesis, but with the precondition to be able to use it also for further tasks. The setup provides a heatable pressure-vessel which can be mixed by a magnetic stirrer as well as two sampling lines, one for the liquid phase and one for the gas phase.



Figure 3-1: Picture of the experimental setup; cycles show the valves for the liquid (green) and gas (blue) sample lines

3.1 Equipment

Reactors and sealing

Two similar reactors were used, each consisting of a vessel, a cover and eight screws (M10) with washers. The vessel and the cover are made from stainless steel. Figure 3-2 shows the dimensions of the vessel. The overall volume of the vessels is 1 L. To seal the reactor, a groove is provided for an O-ring gasket. The gasket is made of

polyfluorelastomers (FFKM) which is a highly resistant material mainly used for chemical applications at high temperature. The datasheet (Figure 8-1) as well as the material properties (Figure 8-2) of the gasket are available in the appendix.

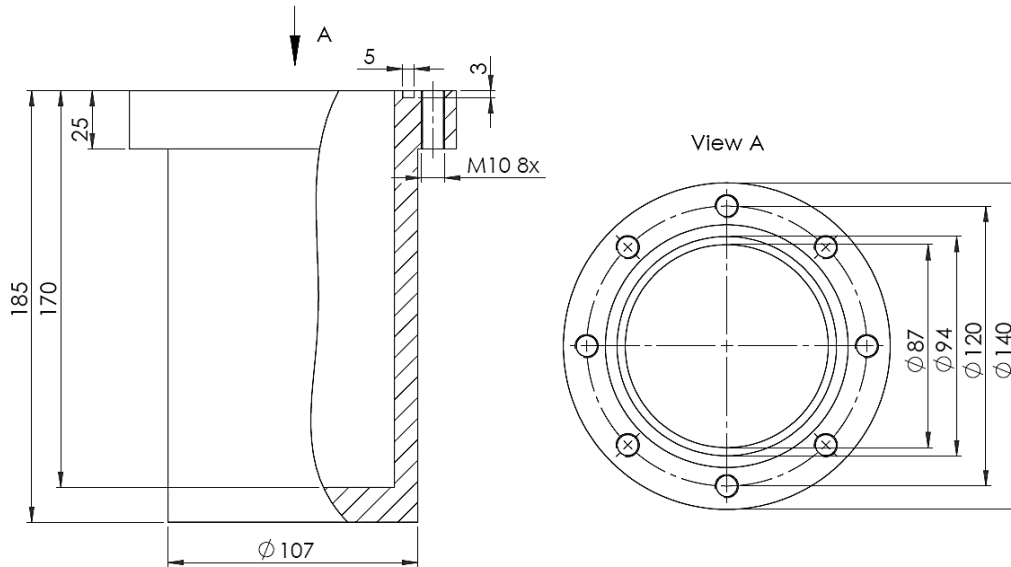


Figure 3-2: Drawing of the vessels – dimensions in mm

As shown in Figure 3-3, four compression fittings (3x 1/4", 1x 1/8") are welded onto the cover. These fittings are the connection points for sampling as well as for measuring devices.

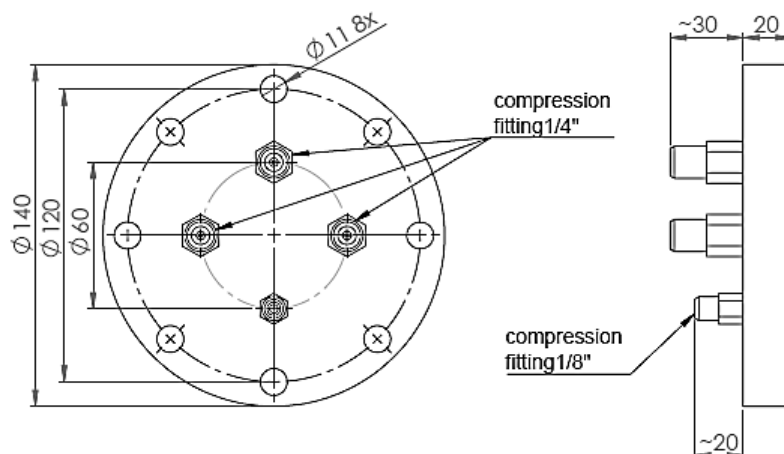


Figure 3-3: Drawing of covers – dimensions in mm

Reactor internals

As shown in Figure 3-4, two of the 1/4" connections are used for the temperature measurement. For that, two PT100 temperature sensors were provided with a clamp ring and a nut to allow them to extend beyond the openings into the reactor. The other two

connections were used for the sampling line of gas and liquid whereas the liquid sampling extends over a pipe to the vessel's bottom. To avoid blockage of the valve and pipe a filter was installed. The filter consists of a connection part which is wrapped at one end with a close-meshed stainless-steel grid and filled with stainless-steel wool.

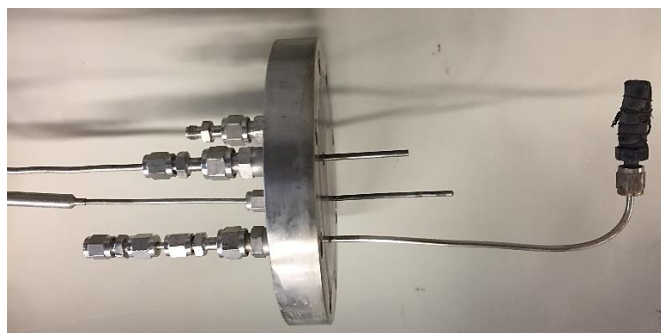


Figure 3-4: Cover of the reactor with fittings

Heat plate and temperature control

The energy for heating is provided by the heat plate of a magnetic stirrer. There, the maximum plate temperature and the rotation speed of the stirring bar which is placed inside the reactor is controlled.

For temperature control, one of the temperature sensors is used for the digital display (R40/2 - Fa. LAUDA) of the temperature and the other one is used for the safety switch off (Unicontrol R325 - Fa. LAUDA), in case the temperature control of the heat plate not fulfills this function. For that a maximum vessel temperature can be set on the control device. If the temperature is exceeded the entire current for the heating plate is switched off. Thus the temperature can be kept constant.

The setup is shown in Figure 3-5, where the magnetic stirrer is placed on the left side and the safety control as well as the temperature display are on the right side.

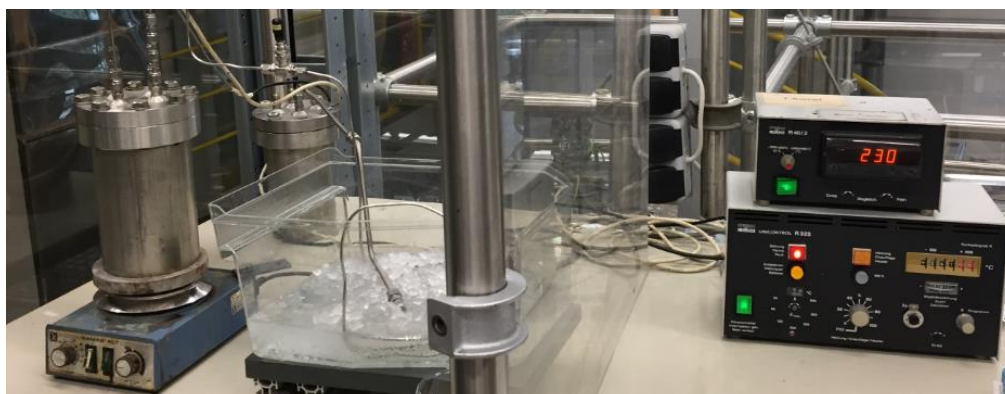


Figure 3-5: Experimental setup

Valves, Fittings and piping

Valves, fittings and pipes were ordered at Burde Co Präzisionsarmaturen GesmbH. For the liquid sampling line, a HOKE 1/8" dosing valve (1315G2Y) was purchased. For the gas line a HOKE 1/4" dosing valve (1315G4Y) was reused from the institute. The datasheet (Figure 8-3) as well as the flow curves (Figure 8-4) of the valves are available in the appendix.

The fittings and pipes are made of stainless steel and are resistant to temperature, pressure and chemicals. They were adapted at the institute's workshop according to the requirements.

Miscellaneous

To monitor the pressure of the system a bourdon gauge (Fa. WIKA 0-60 bar) was installed in the gas line before the valve. Due to high temperature values at venting or sampling as well as the contact with abrasive media and pressure impulses, a syphon (O-shape) was constructed and filled with deionized water to protect the bourdon gauge.

In order to reduce heat emissions, the reactor was placed in a stainless-steel tube that acts like an isolation as the hot air between the pipe and container wall accumulates.

Due to the high temperatures, the liquid samples would evaporate upon sampling due to the pressure drop after the valve and exit in gaseous form. At the gas line the sample is gaseous anyway. To obtain liquid samples, both sampling lines went through a plastic cooling bowl filled with crashed ice.

3.2 Process

The scheme of the experimental setup is shown in Figure 3-6. With this setup it is possible to heat mixtures up to 230°C and take samples of the gaseous or liquid phase during a running experiment. Furthermore, the gaseous phase can be flashed.

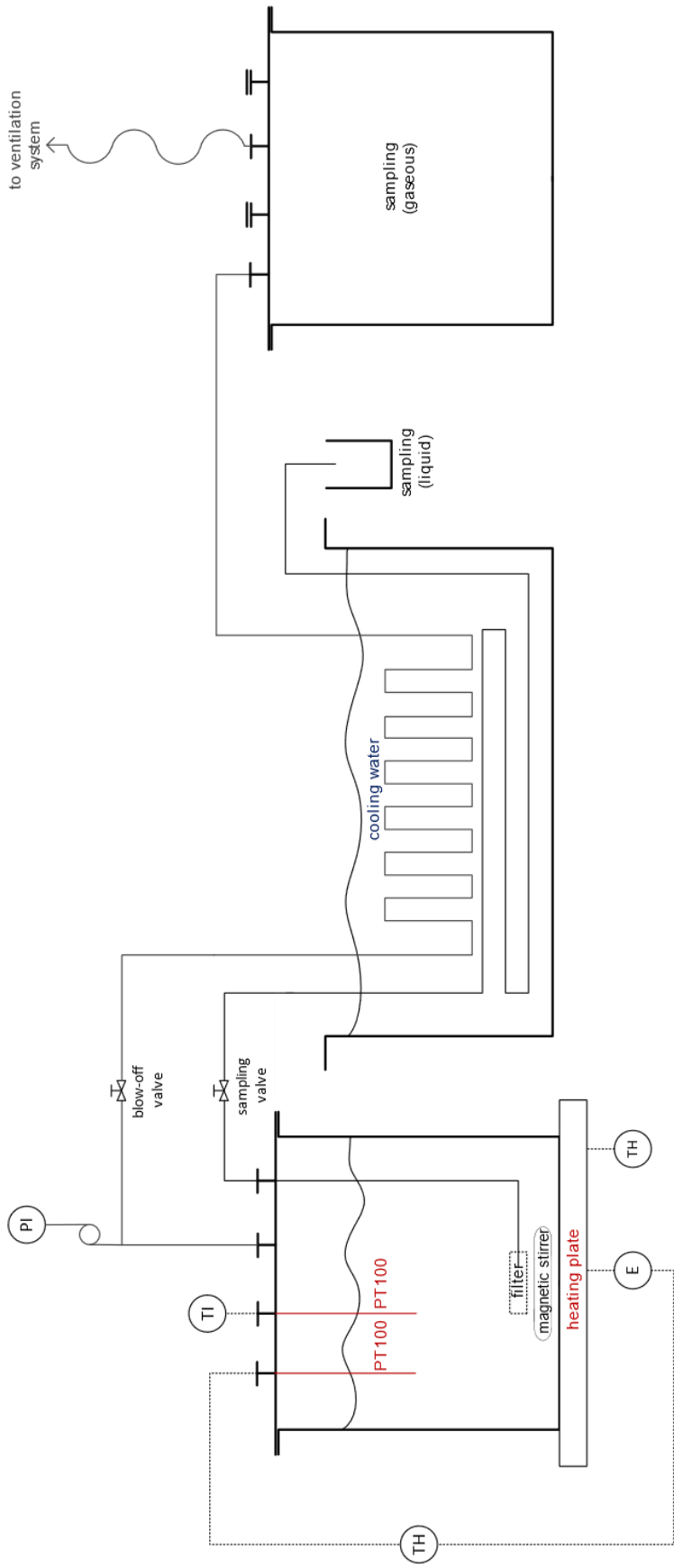


Figure 3-6: Scheme of the experimental setup

Heat up, temperature setting and cool down

After the reactor was filled and the cover and the connection points were fastened, the magnetic stirrer was started and the heat plate was set to maximum temperature (~320°C for the used heat plate). Therefore, the quickest heat up was possible. The heat up time to reach 170°C was about 40 min, for 200°C about 55 min and for 230°C about 80 min at a liquid (H₂O) volume of 600 ml.

After the desired temperature has been reached, the heat plate was regulated down to hold the respective temperature. The hold-temperature of the heat plate is about 200°C to set 170°C, about 250°C to set 200°C and about 300°C to set 230°C. To get the final position of the temperature adjusting wheel, it is recommendable to check the temperature repeatedly until it is stable. As a second temperature control a Unicontrol device was used especially for overnight experiments. At this device the maximum temperature was set 5°C higher than the desired temperature so that the heat plate is automatically switched off if this value is exceeded.

To end the experiment the heat plate was switched off, but stirring continued, and the reactor wall was cooled with crashed ice or water. At the end the vent valve was opened to release the pressure inside the reactor. For a faster cool down the valve can also be opened after the last sampling, but mass losses over the gas phase have to be expected. After cool down, the reactor was disconnected from the sampling/venting lines and opened under the fume hood.

Sampling, flashing and venting

To ensure that a sample exits the pipe in liquid form, crashed ice has to be in the cooling bowl. With the two sample lines, samples can be taken during a running experiment.

Liquid phase line: The liquid phase can be sampled by opening the 1/8"-valve. It has to be considered that some liquid stays in the pipe after sampling, before collecting a new sample the corresponding volume has to be discarded to avoid sample contaminations. The volume to discard was calculated to be at least 10 mL.

Gas phase line: This line can be used for sampling, flashing or venting by opening the 1/4"-valve. For flashing or venting the line ends in the second reactor which is additionally connected to the ventilation system by a hose so that volatile components do not poison the ambient air. For sampling the pipe can be disconnected from the second reactor. The volume to discard was calculated to be at least 20 mL.

3.3 Safety and limits

Because the experimental setup deals with high temperatures, high pressures and hazardous substances, safety installations had to be considered. In order to prevent a break-down of the setup, the limits of the components are pointed out in further consequence.

First of all, it is important that the personal protective equipment, consisting of a lab coat, LaTeX gloves and protection goggles, is worn. The setup is placed in a big walkable box which is closed with plexiglass panes and equipped with a ventilation system. If the air is contaminated with hazardous gases the box can be evacuated. To protect the persons working inside the box from possible leakages and consequently spouting of hot substances, the setup itself is surrounded by plexiglass panes.

For the different parts of the equipment several limits regarding temperature, pressure and chemical stability exists. These limits are summarized in Table 3-1.

Table 3-1: Equipment limits of the experimental setup

Equipment	Material	Temperature range	Pressure range	Note
O-ring gasket	FFKM	-25°C to 270°C (short time 300°C)	min. 50 bar	High chemical resistance, see Figure 8-2
Valves	Stainless steel	-54°C to 232°C	345 bar @21°C	Teflon gaskets - high chemical and temperature resistance
Pressure gauge	Copper alloy	-20°C to 60°C	0 bar to 60 bar	Temperature and chemical protection by siphon
Pipes and fittings	Stainless steel	-200°C to 426°C	min. 200 bar	
Reactor	Stainless steel	min. 250°C	max. 185 bar @250°C	Calculation see Figure 8-5

The reactor limits were roughly calculated with regard to the limit of the screws and the limit of the vessel wall, see Figure 8-5 in appendix. The comparably weakest parts are the valves and the gasket. Especially the gasket should be renewed if traces of use are visible. The positive aspect for the valves as well as for the pressure gauge is that they are not permanently loaded with the high temperature because they are located outside away from the reactor.

Because of the formation of partly toxic gases, the reactor cover was removed under a high-performance laboratory fume hood. During work with black liquor, a gas warning device was worn on the body that could detect the liberation of hazardous hydrogen sulfide.

4 Experimental procedure

4.1 Overview

Several different experiments were done for this diploma thesis. The first ones are not included in the results because they were only performed to get a feeling for what happens with the substrates and the setup, hints about the reaction kinetics, which duration is needed and so on. Nevertheless, the results can be considered and coincide with the later results.

To receive a well-structured sequence of experiments possible, an experimental matrix, shown in Table 4-1, was made. There all process variables are considered and depending on knowledge from the findings described in the literature the experimental design was established. Therefore, the four main parameters, temperature, catalyst and its concentration as well as substrate, influencing the end result were considered. In Table 4-1 the variables and how often they were changed (numbers) are shown. The other influencing values are constant "C" at the beginning of the experiments but in the course of time they change caused by reactions and temperature. For example, the pressure is linked to the temperature as well as gas-forming or consuming reactions.

Table 4-1: Experimental matrix of experiments; Sub.: Substrate, c: concentration, Temp.: temperature, Pres.: pressure, Cat.: catalyst, Atm.: reaction atmosphere, C: constant; the numbers show how often the dedicated variables were changed

Sub.	c Sub.	Temp.	Pres.	Cat.	c Cat.	Atm.	Impacts
C	C	3x	C	C	2x	C	Temperature
C	C	C	C	2x	C	C	Catalyst
C	C	C	C	2x	3x	C	Catalyst concentration
9x	C	C	C	C	C	C	Substrate

Nevertheless, some additional experiments were done, because of some interesting results of former experiments. The whole experimental schedule can be seen in Table 4-2. Some experiments were repeated to check the correctness of prior results as well as the effect of longer treatment times.

Table 4-2: Experimental schedule; abbreviations of substrates see Table 4-3

#	Sub.	Temp. [°C]	Duration [min]	Catalyst	c Cat. [mol·l ⁻¹]	Observed impact
E1	SPB	170	123	CaOH ₂	0.400	Temperature
E2	SPB	170	132	CaOH ₂	0.400	Temperature
E3	BL	200	360	-	-	Substrate
E4	SPB	200	295	CaOH ₂	0.400	Temperature
E5	SPU	200	295	CaOH ₂	0.400	Temperature & Substrate
E6	SPU	230	320	CaOH ₂	0.400	Temperature & Substrate
E7	SPB	230	315	CaOH ₂	0.400	Temperature
E8	SFU	230	375	CaOH ₂	0.400	Substrate
E9	SFB	230	315	CaOH ₂	0.400	Substrate
E10	BL	230	375	-	-	Substrate
E11	SPB	230	1440	CaOH ₂	0.025	c Catalyst & Temperature
E12	SPB	200	1440	CaOH ₂	0.025	c Catalyst & Temperature
E13	SPB	170	1440	CaOH ₂	0.025	c Catalyst & Temperature
E14	SPB	200	1440	CaOH ₂	0.400	Duration & Temperature
E15	SPB	230	1440	CaOH ₂	0.400	Duration & Temperature
E16	SPB	230	1440	CaOH ₂	0.200	c Catalyst & Temperature
E17	SPB	230	1440	NaOH	2.000	Catalyst
E18	HPB	230	1440	CaOH ₂	0.400	Substrate
E19	HPU	230	1440	CaOH ₂	0.400	Substrate
E20	SPU	230	1440	CaOH ₂	0.400	Substrate
E21	SPB	230	1440	NaOH	0.400	c Catalyst
E22	SPB	200	2880	CaOH ₂	0.400	Duration & Temperature
E23	SPB	230	2880	CaOH ₂	0.400	Duration & Temperature
E24	SPB	170	2880	CaOH ₂	0.400	Duration & Temperature
E25	BL	200	2880	-	-	Substrate & Temperature
E26	BL	200	180	-	-	Substrate flash
E27	BL	170	2880	-	-	Substrate & Temperature
E28	BL	200	2880	-	-	Substrate & Temperature
E29	SPB	230	1440	NaOH	0.025	c Catalyst
E30	PaB	230	1440	CaOH ₂	0.400	Substrate
E31	SFU	230	1440	CaOH ₂	0.400	Substrate
E32	L	200	1440	NaOH	0.500	Substrate
E33	SPU	230	1440	CaOH ₂	0.400	Substrate

4.2 Substrates and chemicals

The tested substrates are intermediates or products that occur in local pulp and paper mills. Basically, they can be differed into four main groups; the pulp fraction (SPB, SPU, HPB, HPU), the fines fraction (SFB, SFU) the black liquor fraction (BL, L) and finally printing paper which was done to give a practical example. In Table 4-3 they are listed including their used abbreviation. All of them were used for hydrothermal treatment.

Table 4-3: Used substrates from the pulp and paper industry

Abbreviation	Description
SPB	Softwood pulp bleached
SPU	Softwood pulp unbleached
HPB	Hardwood pulp bleached
HPU	Hardwood pulp unbleached
SFB	Softwood fines bleached
SFU	Softwood fines unbleached
BL	Black liquor softwood
L	Lignin precipitated from softwood black liquor
PaB	Printing paper bleached

Figure 4-1 shows the used substrates except lignin and printing paper are shown. Hardwood has evidently shorter fibers compared to softwood. Black liquor is a black-brown colored liquid that can be very viscous depending on solids content and treatment. Due to their nature, fines can absorb a lot of water and often form viscous solutions even at low concentrations.

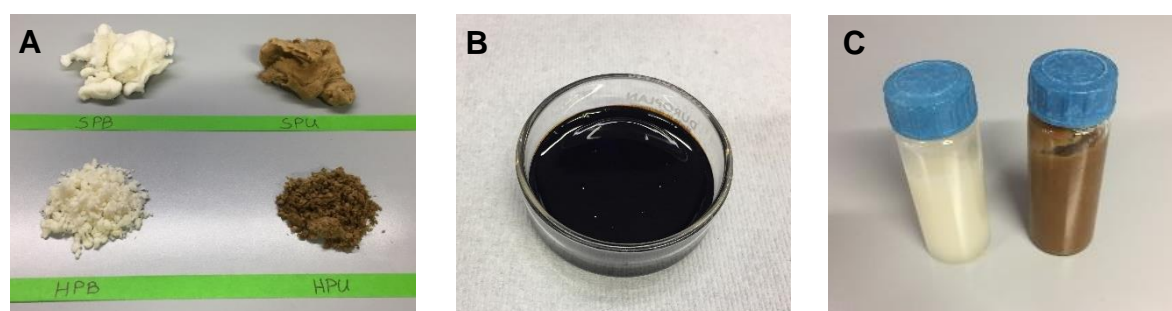


Figure 4-1: Used substrates – A; pulp, B; black liquor, C; fines

Chemicals were used as catalysts, precipitation agents, pH-regulators, standard solutions and as auxiliary substances for devices. The most important are figured below in Table 4-4.

Table 4-4: Used chemicals

Chemical	Formula	Purity	CAS	Use
Calcium hydroxide	Ca(OH) ₂	96.0%	1305-62-0	Cat. solution
Sodium hydroxide	NaOH	98.0%	1310-73-2	Cat. solution/diluent
Sulfuric acid	H ₂ SO ₄	96.0%	7664-93-9	Precipitation agent
Lactic acid	C ₃ H ₆ O ₃	80.0%	50-21-5	HPLC standard
Formic acid	CH ₂ O ₂	99.5%	64-18-6	HPLC standard
Acetic acid	CH ₃ COOH	99.5%	64-19-7	HPLC standard
Propionic acid	C ₃ H ₆ O ₂	99.5%	79-09-4	HPLC standard
Sulfuric acid	H ₂ SO ₄	0.5 M	7664-93-9	HPLC running agent

4.3 Procedure

The experimental procedure is separated in three different parts. The preparation of the feed mixture, the cooking including sampling and the postprocessing.

Preparation of the mixtures

The mixtures were prepared according to the volumes and masses shown in Table 8-2 (appendix). Different masses of substrates were added because of their varying dry substance content.

All substrates, deionized water and chemicals were directly mixed in the reactor. The pulp and fine substances as well as the catalysts were weighted, the volume of deionized water and black liquor was measured using a volumetric flask. The lignin sample was weighted and dissolved in a sodium hydroxide solution at 70°C for 2 hours and afterwards stored in the fridge for one day.

Cooking

The cooking was performed with the setup described in chapter 3. The heat up time depended mainly on the set temperature which is explained in more detail in chapter 3.2. Samples were taken at defined time intervals by the sampling line. If not stated otherwise, the last sample was taken at the set-temperature directly before the cooldown of the reactor.

Postprocessing

After cooldown the reactor was opened, see Figure 4-2_A, and the mixture was transferred into a beaker. With a filter paper and Büchner funnel the remaining solids were separated from the liquid phase under vacuum (Figure 4-2_B). The taken samples were prepared and analyzed with respect to their pH-value, dry substance content, lignin content and acids by the methods described in chapter 5.

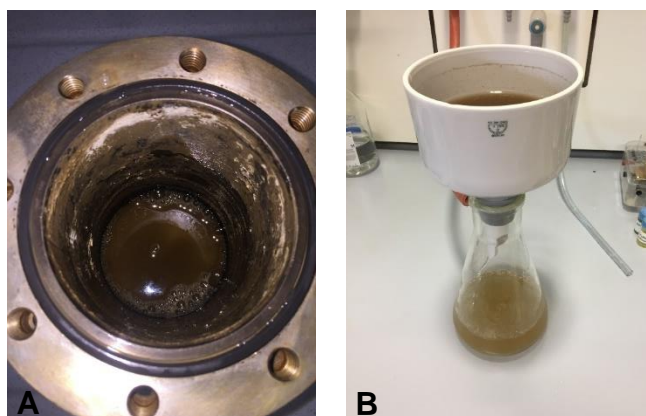


Figure 4-2: A; opened vessel after the experiment (E33), B; separation of the remaining solids by vacuum filtration

5 Analysis

5.1 High-performance liquid chromatography

5.1.1 General

High-performance liquid chromatography (HPLC) is used to separate a homogenous mixture of liquid substances into their individual components. The components are interacting with the stationary phase based on their chemical and physical properties. Depending on the interaction with the stationary phase some components move slower and consequently elute later than others.

In this thesis an Ultimate 3000 HPLC system from Dionex™ was used. Figure 5-1 shows the setup which consists of the modules pump, sampler, detector and column. For the evaluation of the results the data system software Chromeleon™ was used.



Figure 5-1: HPLC system at TU Graz (ICVT)

The separation depends on different parameters and separation methods have to be developed depending on the substance mixture to be analyzed. In this case, the separation and detection of acids was realized by the setup shown in Table 5-1.

Table 5-1: Setup of HPLC analysis

Parameter	Value
Column	REZEX-ROA
Temperature	Room temp.
Time	30 min
Mobile phase	0.005 M H ₂ SO ₄
Flow rate	0.5 ml·min ⁻¹
Pressure	28 bar
Detector	UV - 210 nm

The concentrations are detected by UV measurement. It results in a chromatogram that shows the amount of substances in absorbance peaks at a defined retention time.

By using standard solutions of pure substances, shown in Table 4-4, the retention time as well as the proportion of peak to concentration can be evaluated. The used calibration curves for the analyzed acids are shown in Table 5-2.

Table 5-2: Functions of the calibration curves; y means the concentration [$\text{g}\cdot\text{L}^{-1}$] and x means the height of the respective peak

Substance	Function	r^2
Lactic acid	$y = 0.261 \cdot x$	0.989
Formic acid	$y = 0.185 \cdot x$	0.978
Acetic acid	$y = 0.322 \cdot x$	0.978

As described above the height of the peak was used for the evaluation of the concentrations. It was measured from a baseline up to the highest point at a defined elution time interval for each substance. To ensure comparable results the baseline was drawn manually from one significant point, appearing at every compared experiment, to another. Figure 5-2 shows a chromatogram of the first and final sample taken from a pulp experiment. The baseline (red dotted line) and the heights of acid peaks (green arrows) are sketched. The upper section shows the time interval, where the acids elute.

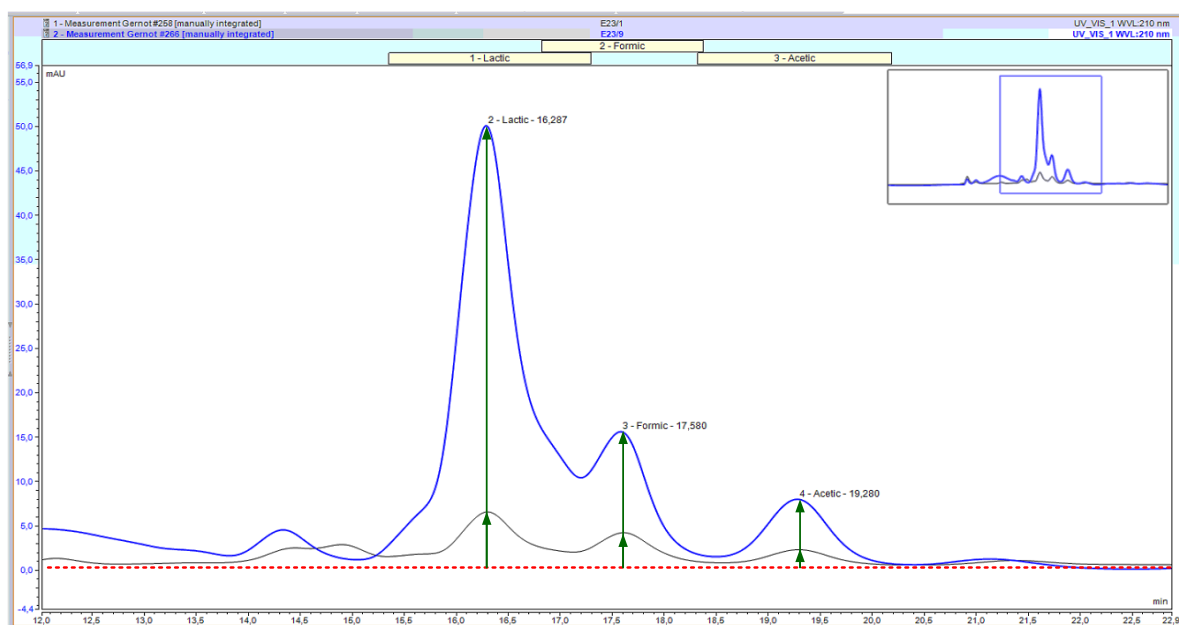


Figure 5-2: Chromatogram of first and final sample of a pulp experiment, the baseline and the peaks are sketched; the red dotted line shows the baseline; the green arrows signify the evaluated acids peaks

5.1.2 Sample preparation

The samples analyzed with the HPLC system were filtered (0.45 μm) and also acidified. The acidification was done because lignin, which is present in the original feed substrates, precipitates at low pH-values. The initial pH of the samples was about 11, hence dissolved lignin may be present in the samples. Since the mobile phase is acidic and lowers the pH, lignin could precipitate and destroy the column as well as the pumping system. [73]

To avoid this scenario, the samples were acidified with sulfuric acid to a $\text{pH} < 2$. By this step the whole lignin precipitates. Depending on the type of feed substance some adjusted pretreatment steps were done:

- Pulp and Fines

The samples were pipetted into test tubes and 98% sulphuric acid was added. Table 8-1 (appendix) shows the applied sample and acid volumes. Both substances were mixed by numerous inversions of the test tubes.

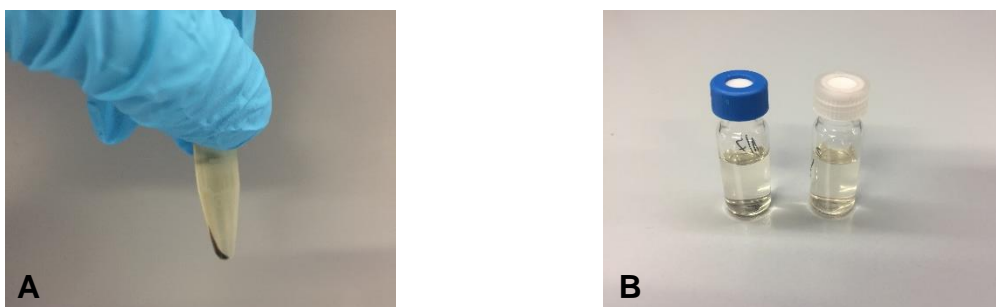


Figure 5-3: A; Test tube showing precipitate after acidification and centrifugation, B; HPLC-vials ready for the analysis

After a certain residence time in the fridge the precipitate was formed and subsequently separated with the centrifuge, see Figure 5-3_A. Finally, the liquid phase was transferred from the test tubes to the HPLC vials, see Figure 5-3_B, per using an injection filter.

- Black Liquor and Lignin

Because of gas-forming reactions during acidification, where among others the toxic gas hydrogen sulfide is formed, the acidification step was done exclusively under the fume hood. For the acidification, centrifuge tubes were used. Because of the gas-forming reaction, the samples are foaming upon acidification and sample losses must be

preserved. The acidification of the black liquor samples immediately leads to lignin precipitation (foaming) and the formation of an interfacial layer. In order to ensure a complete mixing, the sequence shown in Figure 5-4 was used.

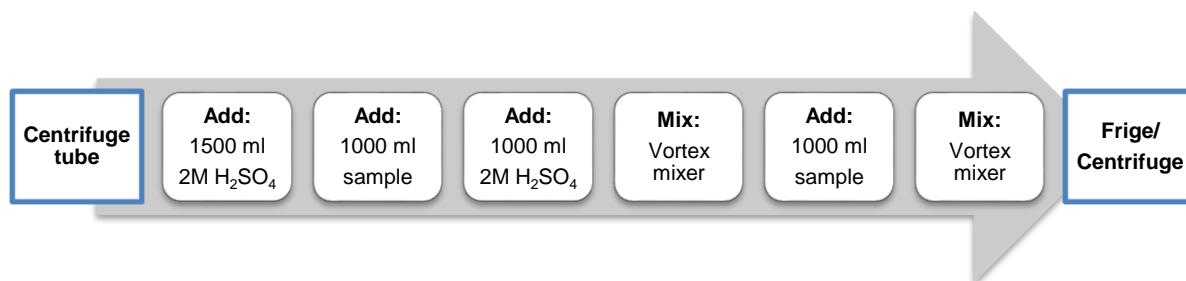


Figure 5-4: Sequence used for the acidification of the samples from black liquor and lignin

To separate the precipitate from the fluid phase, the tubes were centrifuged after a certain residence time in the fridge. In Figure 5-5_B the result of centrifugation after mixing with a vortex device (see Figure 5-5_A) is shown. Subsequently, the liquid phase was transferred from the centrifuge tubes to the HPLC vials using an injection filter.

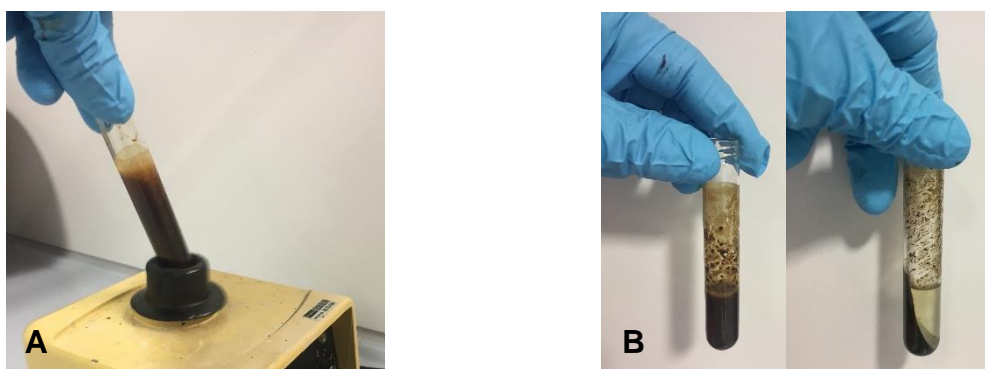


Figure 5-5: A; mixing the tube of acidified BL with a vortex device, B; acidified BL before (left) and after (right) centrifugation

Table 8-1 (appendix) shows the applied sample and acid volumes for the acidification as well as the dilution factor for each experiment.

5.2 UV-VIS spectroscopy analysis

5.2.1 General

The ultraviolet-visible spectroscopy is a visual analysis method that measures the reduction of the electromagnetic radiation by the absorption of the molecules. This reduction can be quantitatively analyzed by the Beer-Lambert law:

$$A = \log \frac{I_0}{I} = \varepsilon * c * d \quad \text{Equation 5-1}$$

The dimensionless absorption A is calculated by the device by measuring the intensity of the light before (I_0) and after (I) it passes the sample solution. The concentration c is proportional to the absorption and can be calculated with the length of the measurement cell d and the absorption coefficient ε . The absorption coefficient is constant for a substance at a certain wavelength.



Figure 5-6: UV/VIS system at TU Graz (ICVT)

In this thesis a Shimadzu UV-1800 Spectrophotometer, see Figure 5-6, was used to analyze the concentration of lignin or rather of lignin phenolic groups. The analysis was done using the parameters shown in Table 5-3.

Table 5-3: Setup of UV/VIS analysis

Parameter	Value
Type of cuvettes	UV-PP
Pathlength of cuvettes	10 mm
Temperature	Room temp.
Wavelength	280 nm

The wavelength around 280 nm refers to the maximum absorbance of the phenolic hydroxyl groups of lignin. Figure 5-7 shows the spectrum of a lignin sample between 220 and 400 nm. At 280 nm wavelength an absorption coefficient of $23.7 \text{ L}\cdot\text{g}^{-1}\cdot\text{cm}^{-1}$ was used. [74,75]

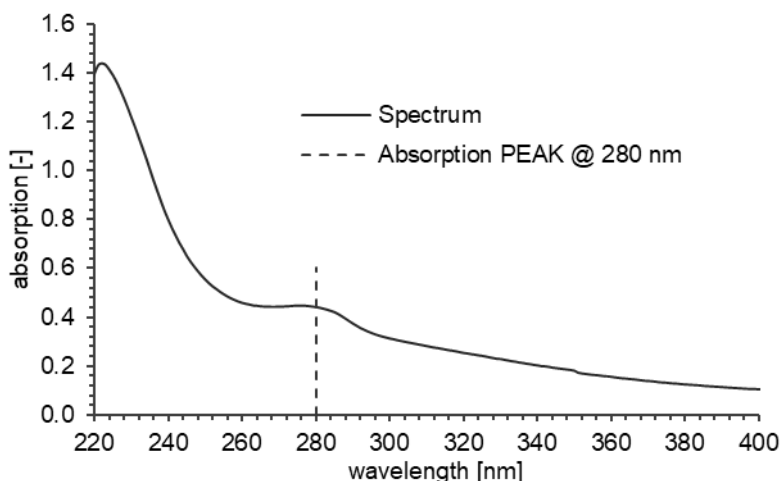


Figure 5-7: UV/VIS spectrum of initial unbleached fines sample (E31) from 220 nm to 400 nm

5.2.2 Sample preparation

The samples were diluted with a 0.1 M NaOH-solution. On the one hand that was done because of the pH-dependency of the absorption coefficient and the lignin dissolution, and on the other hand because of the maximum measured absorbance of 1.5 to ensure a reliable measurement. Since the pH-value of the samples was usually very high, the maximum absorbance limit determined the degree of dilution. The samples were diluted to a factor of 30 for cellulose and up to 8000 for black liquor. In general, the samples were measured in duplicate. Presented data are mean values.

5.3 pH-measurement

The pH-measurement was done using a glass electrode at room temperature. There was no sample preparation necessary. A two-point calibration was performed using buffer solutions at pH-values 7 and 10 as shown in Figure 5-8. In order to measure the buffers and the samples at the same temperature they were taken out of the fridge 24 hours before pH measurement. Because of the stickiness of black liquor and lignin a separate electrode, see Figure 5-8_B, was used.



Figure 5-8: A; calibration of WTW pH522 at pH 7, B; calibration of WTW Multi. P4 at pH 10

5.4 Dry solids content measurement

To measure the dry solids content, the ceramic crucibles were dried at 90°C for 24 hours in an oven. After cooling down to room temperature, the samples were put in the crucibles and the weight was noted. Depending on the type of the sample (liquid or solid) it was dried up to 100 hours at 90°C. After drying, the crucibles were cooled down at room temperature and the final weight was measured. The dry solids content (DS) in percent was calculated by dividing the final weight by the starting weight and multiplying it by 100.

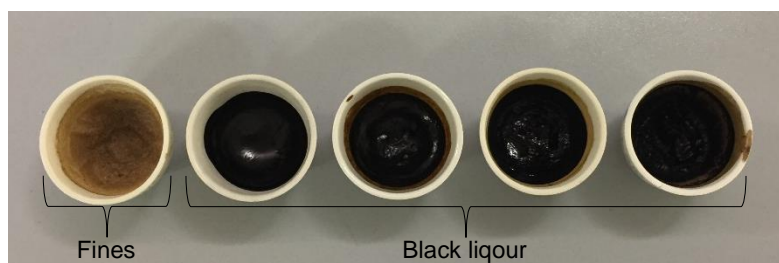


Figure 5-9: Ceramic crucibles after drying of fines and black liquor samples

6 Results and discussion

Data analysis included the calculation of representative numerical values. The acids yield was calculated according to Equation 6-1 by the formed mass of acids divided by the initial dry solids. With the exception of black liquor, lignin and fines, it was assumed that no acids were present in the starting material.

$$\text{Yield of acids [\%]} = \frac{m_{acid} [g]}{m_{initial_s} [g]} * 100 [\%] \quad \text{Equation 6-1}$$

For the calculation of the total conversion, the dry solids mass at the start of the experiment and that of the remaining insoluble solids at the end of the experiment were measured. Equation 6-2 shows the formula that led to the total conversion.

$$\text{Total conversion [\%]} = \frac{m_{initial_s} [g] - m_{final_s} [g]}{m_{initial_s} [g]} * 100 [\%] \quad \text{Equation 6-2}$$

The whole results of pH-measurement, concentrations of acids, lignin content and dry solid mass after conversion are summarized in Table 8-4 (appendix).

The reaction law of the formation of acids was calculated by the curve fitting software TableCurve 2D. The mechanism was simplified by a simple reaction shown in Equation 6-3. "A" represents the initial substrate that was partly converted to "B" which illustrates one of the acids. Therefore, Equation 6-4 describes the reaction law for the formation of acids.



$$r_B = \frac{dc_B}{dt} = k * c_A^n \quad \text{Equation 6-4}$$

Figure 6-1 pictures the first order TableCurve-fit of the formation of lactic acid from the experiment with SPB at 230°C (E23). "a" represents the maximum concentration and "b" the rate constant k. For the temperatures 200°C and 170°C, where the conversion was not finished at the end of the experiment, the final time for maximum concentration (value of 230°) was estimated by the mean of the last three reaction rates of Table 8-5. The values were added to the time course to get comparable kinetic results of the experiments at different temperatures like shown in Figure 6-1.

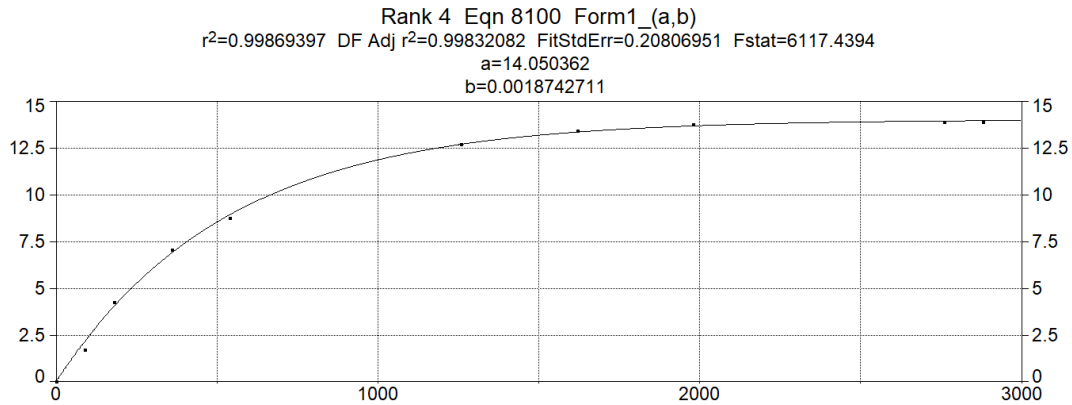


Figure 6-1: Fit of LA (E23) by Table Curve 2D; a: maximum concentration, b: rate constant

Equation 6-5 shows the corresponding function of the formation curve-fit. The decomposition function is described by Equation 6-6.

$$y = a * (1 - e^{-b*x}) \quad \text{Equation 6-5}$$

$$y = a * e^{-b*x} \quad \text{Equation 6-6}$$

To describe the influence of the temperature on the reaction quantitatively, the Arrhenius parameters were evaluated by linearization according Equation 6-7.

$$\ln(k_i) = \frac{E_a}{R} * \frac{1}{T_i} + \ln(A) \quad \text{Equation 6-7}$$

By the evaluated experimental variable k_i and the corresponding temperature T_i the parameters E_a and A were defined by linear fit. Figure 6-2 shows the linear fit of LA, FA and AA for 230°C, 200°C and 170°C.

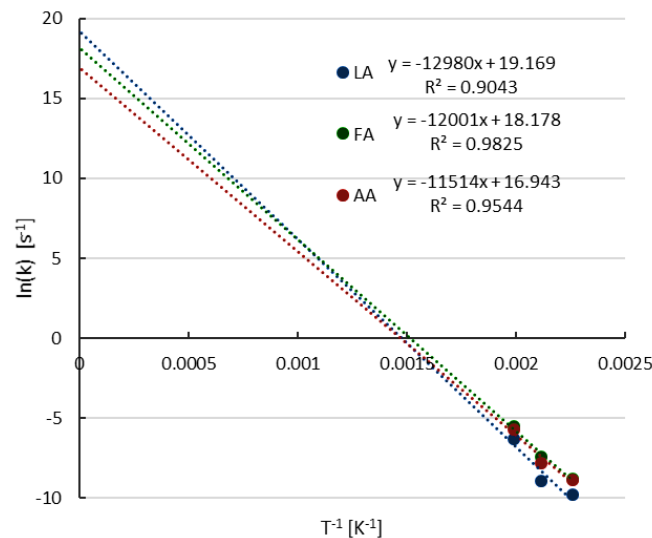


Figure 6-2: Linear fit to calculate the Arrhenius parameters; SPB experiments at 230°C, 200°C and 170°C in a 0.4 M $\text{Ca}(\text{OH})_2$ -solution

6.1 Conversion of pulp

The behavior of pulp, as the main product of a pulp and paper plant, was investigated under different heat treatment conditions. It was used as model substrate for the study of the characteristics of hydrothermal treatment of fines. For that, the temperature, the type of pulp, the catalysts and its concentrations were varied to analyze their influence on acids formation and find the best conditions for the highest yield for the three targeted acids.

6.1.1 Temperature dependency

It is well known that the temperature influences the reaction kinetics massively. It accelerates the observed degradation reactions to a certain degree. Figure 6-3 shows the conversion of bleached softwood pulp to lactic acid at three different temperatures. The reaction was carried out in a solution of 0.4 M calcium hydroxide. As expected, the formation of lactic acid at 230°C is much faster than at 200°C or 170°C. The increase in concentration over time follows the course of an exponential curve. A final yield of about 38% was achieved after 2000 minutes and did not change significantly during the following 1000 minutes of treatment that were observed.

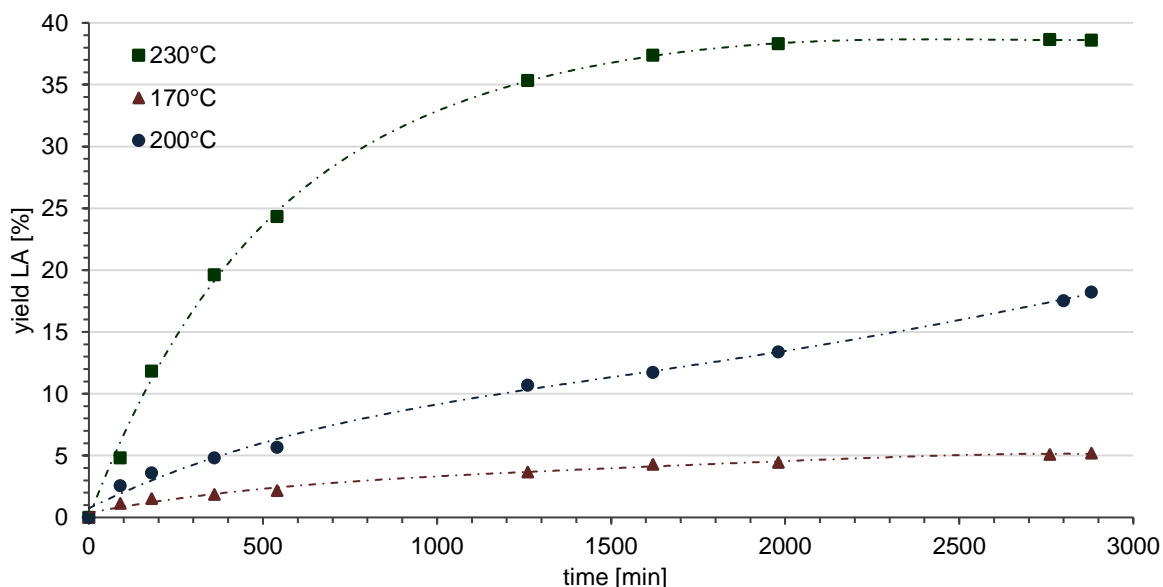


Figure 6-3: Yield of LA for SPB in a 0.4 M $\text{Ca}(\text{OH})_2$ -solution at varying temperature (E22, E23, E24)

The situation is different at lower temperatures. Especially at 200°C, it can be seen very well that the yield increases linearly and does not level off in the observed time

interval. The conversion to lactic acid is therefore not yet completed and would probably get closer and closer to the maximum yield if the experiment was prolonged. The situation at 170°C is a bit different again, since very little happens there, which suggests too little energy to activate the conversion mechanisms for the formation of acids in general. The pH-value can be considered as constant (about pH 12) over the entire duration of the experiments.

As displayed in Figure 6-4, the formation of formic acid and acetic acid shows a similar behavior as lactic acid, but with lower yield. The highest yields were reached at the highest temperature of 230°C. The maximum yield of formic acid was 10% and that of acetic acid 8%. Same as for lactic acid, also for acetic acid and formic acid the maximum yield was reached after 2000 minutes. In contrast to lactic acid the concentration decreased in the further course of the experiment at 230°C, especially for formic acid. This may be due to the decomposition or a side reaction with other substances. Thermal decomposition of acetic acid leads to gases like carbon dioxide or carbon monoxide. [76] After about 1500 min of treatment, the pressure increased by about 3 bar to 34 bar. This observation fits well to the decrease in formic acid concentration indicating gas formation.

The mean reaction rates at defined time are shown in Table 8-5 (appendix).

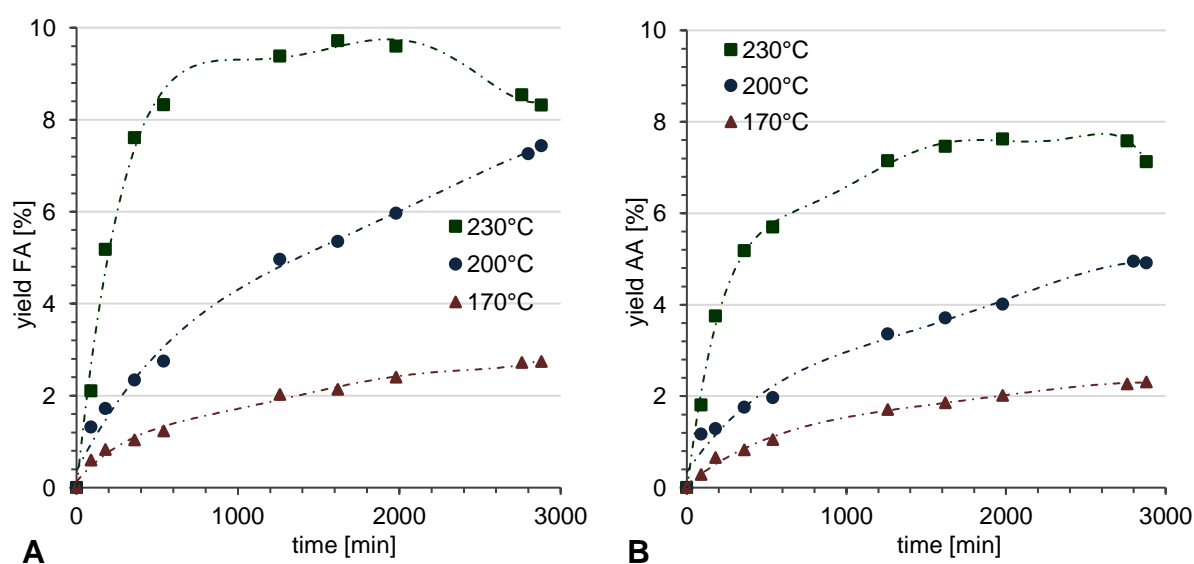


Figure 6-4: Yield of FA (A) and AA (B) for SPB in a 0.4 M $\text{Ca}(\text{OH})_2$ -solution at varying temperature (E22, E23, E24)

The reaction kinetics were calculated by the assumption of simple first order parallel reactions from the pulp to the single analyzed acid. To be able to compare the reaction kinetics at different temperatures based on the rate constant, they must be of the same reaction order. Therefore, the decomposition of the initial pulp and the formation of the acids was calculated by a first order curve-fit (kinetics equations – TableCurve) on the time course of the concentrations. Because the pulp is totally converted only at 230°C and other substances beside the analyzed acids were formed, some simplifications and assumptions had to be made. The calculated kinetics of pulp decomposition concern the direct conversion of pulp mass to the mass of analyzed acids. The effective decomposition is much higher because of the formation of a large number of non-analyzed substances (see lower paragraph). At lower temperature experiments (no total conversion of pulp) the duration to reach the minimum (decomposition) or maximum (formation) concentration values were estimated by the mean reaction rate.

Table 6-1 shows the data where the formation of lactic acid is predominating the kinetic course because of its predomination concentration of minimum 50%. At 230°C the rate constant is significantly higher than that of lower temperatures. In the appendix (Figure 8-9) the corresponding fit at 230°C is shown. The Arrhenius parameters were graphically determined by Figure 8-11 (appendix).

Table 6-1: First order reaction kinetics for the decomposition of SPB to the analyzed acids including Arrhenius parameters; rate constant calculated by TableCurve (Figure 8-9)

T [°C]	Rate constant k [s ⁻¹] x 10 ⁻³	r ²	Pre-exponential factor A [s ⁻¹] x 10 ⁶	Activation energy E _A [J·mol ⁻¹] x 10 ⁵
230	2.391	0.997		
200	0.166	0.992	129.734	1.049
170	0.077	0.994		

Table 6-2 shows the first order reaction kinetics for the formation of the single acids. The maximum concentration values at 100% pulp conversion are 14.05 g·L⁻¹ for lactic acid, 3.48 g·L⁻¹ for formic acid and 2.70 g·L⁻¹ for acetic acid. By that values and the rate constants the fitted c/t-functions are given by Equation 6-5. Table 6-3 illustrates the calculate Arrhenius parameters. The activation energies of the acids are on the similar

level and naturally in the range of that from the decomposition of pulp. The pre-exponential factor, which describes the number of times two molecules collide, is quite different. It has the highest amount for lactic acid which resulted in the largest yield.

Table 6-2: First order reaction kinetics for the formation of analyzed acids from SPB at 230°C, 200°C and 170°C by a 0.4 M Ca(OH)₂-catalyst; rate constant calculated by TableCurve (exemplary see Figure 6-1)

T [°C]	Rate constant k [s ⁻¹] x 10 ⁻³			r^2		
	LA	FA	AA	LA	FA	AA
230	1.874	3.920	3.236	0.999	0.991	0.991
200	0.134	0.590	0.416	0.984	0.977	0.949
170	0.055	0.153	0.142	0.994	0.962	0.973

Table 6-3: Arrhenius parameter of SPB experiments for the formation of acids at 230°C, 200°C and 170°C by a 0.4 M Ca(OH)₂-catalyst; the corresponding linear fit is shown in Figure 6-2

Pre-exponential factor A [s ⁻¹] x 10 ⁶			Activation energy E_A [J·mol ⁻¹] x 10 ⁵		
LA	FA	AA	LA	FA	AA
211.344	78.452	22.816	1.079	0.998	0.957

The sum of analyzed acids resulted in a yield of 55%, 30% and 10% at temperatures of 230°C, 200°C and 170°C respectively (see Figure 6-5). Figure 8-10 (appendix) shows the corresponding chart of the course. The formation of other non-analyzed and soluble substances was calculated and resulted in 44% (230°C), 49% (200°C) and 59% (170°C) of the converted pulp (Table 8-3-appendix). That means, that a huge amount of other reactions to other products occurred.

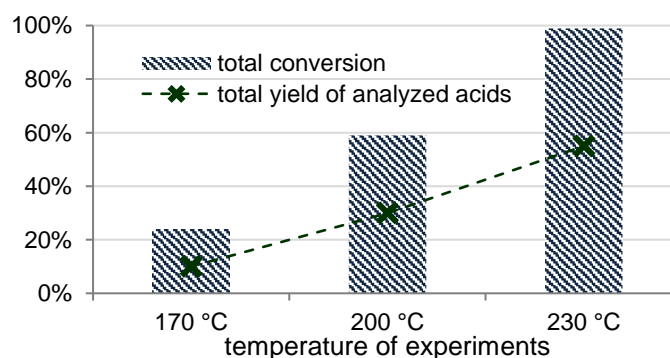


Figure 6-5: Total conversion (decomposition) of SPB and its total yield of acids (LA, FA, AA) at different temperatures after 2880 min (E24, E22, E23)

By the total conversion at different temperatures, the progress of the first reaction step, the hydrolysis from cellulose or its derivatives to sugars or soluble oligomers, can be determined. As shown in Figure 6-5 the total conversion matches well with the above described yields of the sum of analyzed acids formed. It can be said that at 230°C the whole pulp was converted to soluble substances. In contrast to that, the initial mass was converted only partly with about 60% and 25% at 200°C and 170°C, respectively.

Hence, it can be assumed that the hydrolysis to the soluble sugars is one of the limiting reaction steps at low temperatures. At the experiment with shorter duration of 1440 minutes, the total conversion was already close to 100% which implies that the maximum yield is already reached after this time. In Figure 6-6 the dried solid remains of the described experiments are shown.

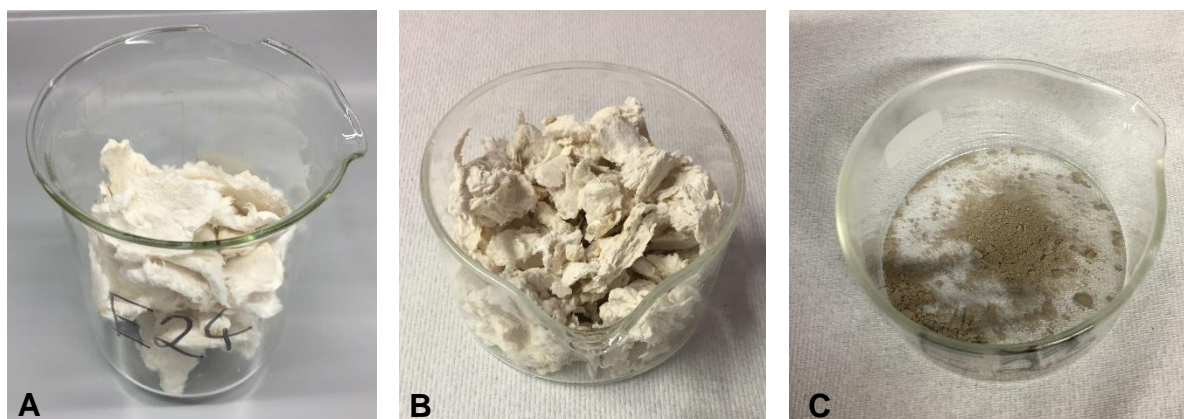


Figure 6-6: Remains after experiments with SPB with a 0.4 M $\text{Ca}(\text{OH})_2$ -solution at 170°C (A), 200°C (B) and 230°C (C); (E22, E23, E24)

Because the total conversion as well as the yields of acids reached the maximum at 230°C, most of the further experiments were performed at this temperature.

6.1.2 Substrate dependency

Softwood and hardwood pulps in bleached and unbleached condition were treated at 230°C in a 0.4 M calcium hydroxide solution, to investigate the different influence of their nature on the formation of acids. Figure 6-7 shows a similar reaction process for the formation of lactic acid (yield between 29% and 34% after 1440 minutes) of each substrate but the bleached samples have a slightly higher yield of about 5%. That can be explained by the remaining lignin content of 2% to 3% of the unbleached samples. [17] The yield refers to the initial dry mass that includes the lignin that is on the one hand harder to convert and on the other hand reacts to different products than cellulosic material. Additionally, the harsh conditions during the bleaching treatment and therefore the creation of more unstable macromolecules in bleached pulp influence the acid formation. [77] Nevertheless, the difference between bleached and unbleached pulps was not significant.

For the formation of formic acid similar reaction kinetics but lower yields of about 9% after 1440 minutes were observed (see appendix Figure 8-6). This is not surprising since both acids have similar reaction mechanisms. [56]

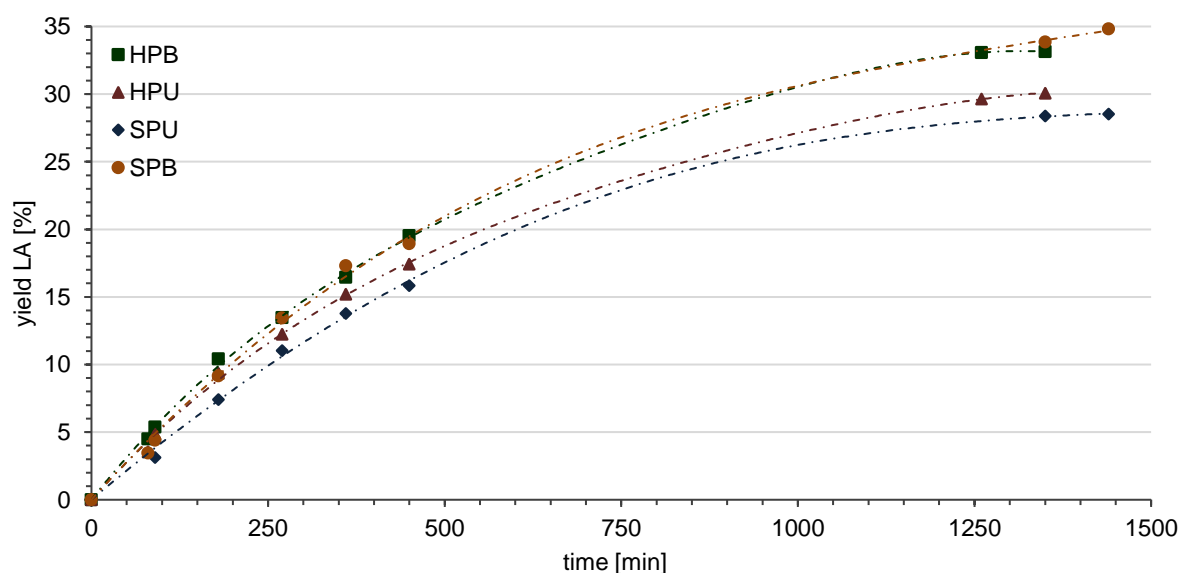


Figure 6-7: Yield of LA for varying pulp types with a 0.4 M $\text{Ca}(\text{OH})_2$ -solution at 230°C (E15, E18, E19, E33)

For the formation of acetic acid, the biggest deviation between hardwood and softwood pulp occurred. As shown in Figure 6-8, hardwood pulp (bleached and unbleached) had

a yield of about 9% which is 3 % higher compared to the softwood pulps. At comparable conditions the same behavior was found in the literature, where hardwood and softwood had similar yields in lactic acid and formic acid but different ones in acetic acid. Also hardwood yields of acetic acid were significantly higher than that of softwood. [4]

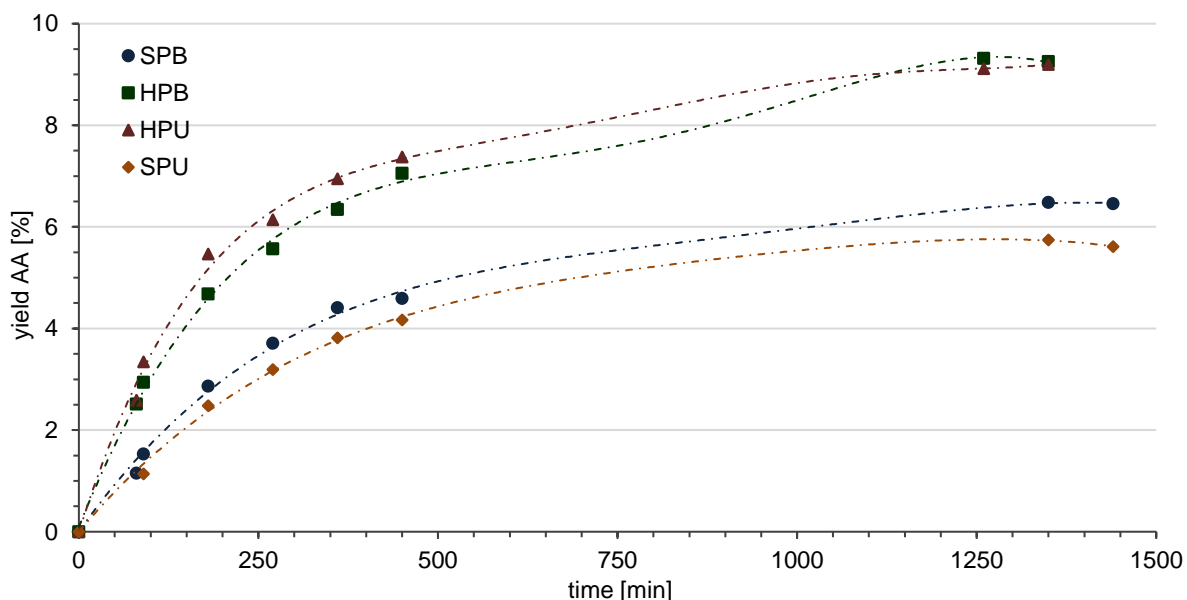


Figure 6-8: Yield of AA for varying pulp types in a 0.4 M $\text{Ca}(\text{OH})_2$ -solution at 230°C (E15, E18, E19, E33)

The results of the analyzed lignin content by measurement of the representative phenolic hydroxylic groups are depicted in Figure 6-9. There are no big differences between the two experiments for unbleached softwood and hardwood pulp. It looks as if the lignin first dissolves and then degrades. The same trend can be observed for the intensity of discoloration of the taken samples. As shown in Figure 6-10 throughout the course of the experiment the color of the samples first becomes darker and then becomes brighter again towards the end. A further reason for the detection of phenolic hydroxylic groups and the coloration could be

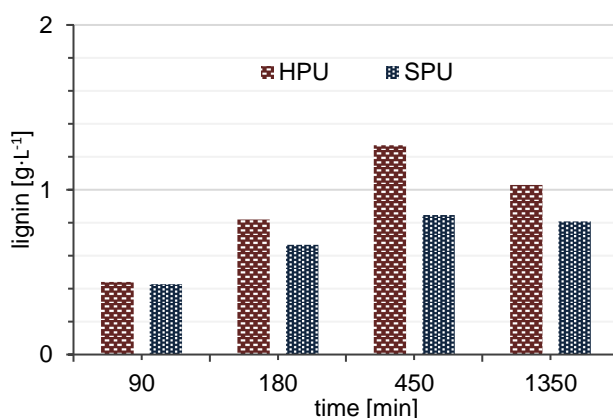


Figure 6-9: Change of detected concentration of lignin phenolic hydroxy groups on the experimental period at 230°C (E19, E33)

extractives, like phenolic, aliphatic and alicyclic compounds from waxes, resin or terpenes that are already present in the pulp at low concentrations. [17,78]

Furfural and HMF for example are partly formed during thermal carbohydrate degradation and also absorb UV light at 280 nm. [79,80] Similar lignin contents and colorations were also observed for bleached pulps.



Figure 6-10: Samples taken from softwood pulp experiment (E23); 230°C, 0.4 M $\text{Ca}(\text{OH})_2$, 2880 min

6.1.3 Influence of different catalysts

The catalyst is a very important parameter to steer the reaction into the desired direction to a product. Because of that, two different catalysts were compared by experiments with bleached softwood pulp at 230°C. One of them was calcium hydroxide and the other one was sodium hydroxide. In fact, both are not the most effective catalysts known from the literature, but they are readily available, easy to trade, cheap, non-toxic and they have no foreign ions.

Because of the different structural formula of both chemicals, it is impossible to have the same amount of metal cations and hydroxide anions in both catalytic-solutions which makes the comparison difficult. To compare the influence of the divalent Ca^{2+} -cation and the monovalent Na^{+} -cation, 0.025 M-solutions of both catalysts were used. The chosen concentration was the solubility limit of calcium hydroxide, so that all the metal ions were dissolved. Because of that, it was not possible to keep a constant pH-value over the duration of the experiments, as shown in Figure 6-11. Nevertheless, the course of the pH-value was quite similar for both catalysts, so they can be compared very well. The experiment started at a pH of 12.3 and dropped relatively fast to about pH 3.7 after 200 minutes due the formation of acids. For the remaining reaction time the pH-value of both experiments stayed constant.

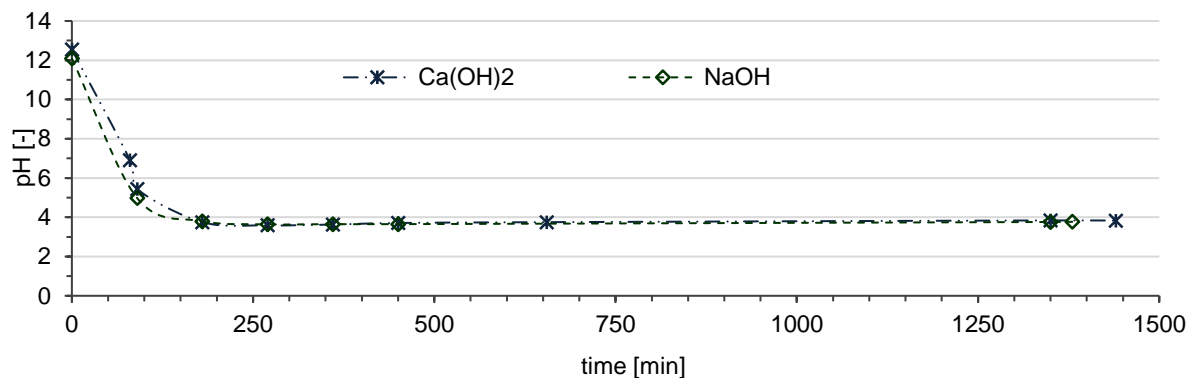


Figure 6-11: Comparison of pH-value with a 0.025 M solution of $\text{Ca}(\text{OH})_2$ and NaOH at 230°C with SPB as feed (E11, E29)

Figure 6-12 shows the yield of the acids, a correlation with the change in the pH-value of Figure 6-11 can be seen. The acids were formed to their maximum concentration in the time range from 250 to 500 minutes, after that a reduction of the acid concentration due to decomposition can be observed. It is well known that the pH-value has a huge influence on the reaction mechanism of biomass, but this will be discussed in more detail in the next chapter. [1]

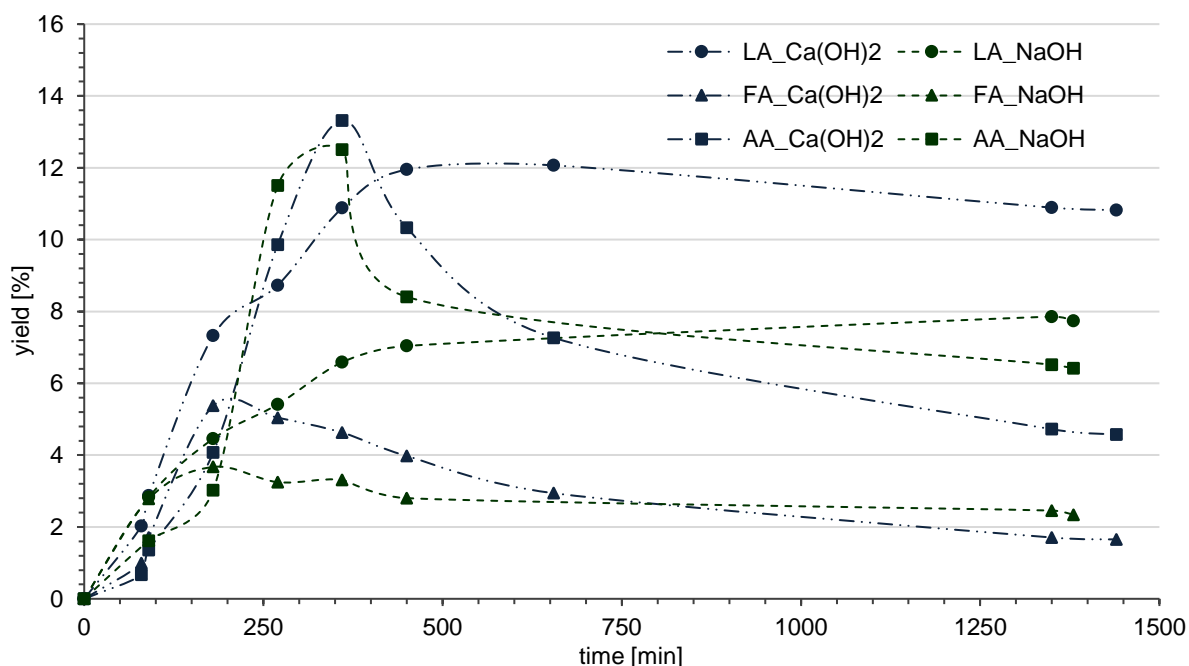


Figure 6-12: Comparison of acid yields of SPB by using a 0.025M catalyst-solution of $\text{Ca}(\text{OH})_2$ and NaOH at 230°C (E11, E29)

The influence of the different catalyst's metal ions had an influence on the acid formation. In all cases, the calcium hydroxide catalyzed experiment had higher maximum yields although the final yield was lower for formic and acetic acid caused by higher

degradation shown in Figure 6-12. Especially the maximum yield of lactic acid was about 5% higher compared to the use of sodium hydroxide as catalyst. A possible explanation for the higher yields with calcium hydroxide is that the divalent Ca^{2+} has a larger radius than the monovalent Na^+ and so its tendency to form complexes with two oxygen atoms is higher. These complexes may be responsible for the fission of $\text{C}_3\text{-C}_4$ bonds. [52]

6.1.4 Influence of catalysts concentration

To examine the influence of the catalyst concentration for both above described catalysts, experiments with three different concentrations were performed.

Calcium hydroxide has a poor solubility in water with 1.7 grams per liter at room temperature. For the experiments, concentrations of 0.025 M, 0.2 M and 0.4 M were used, whereas only at the lowest concentration the calcium hydroxide was almost completely dissolved in the water. The other ones formed a suspension where most of the catalyst stayed in solid form. Because of the different concentrations the pH-value changed significantly over time. As it can be seen in Figure 6-13, at the concentration of 0.4 M the pH-value stayed constant with pH 12.5 throughout the experiment. When 0.2 M of calcium oxide were applied the value stayed constant only during the initial phase, probably until the last solid calcium hydroxide had dissolved due to the formation of acids.

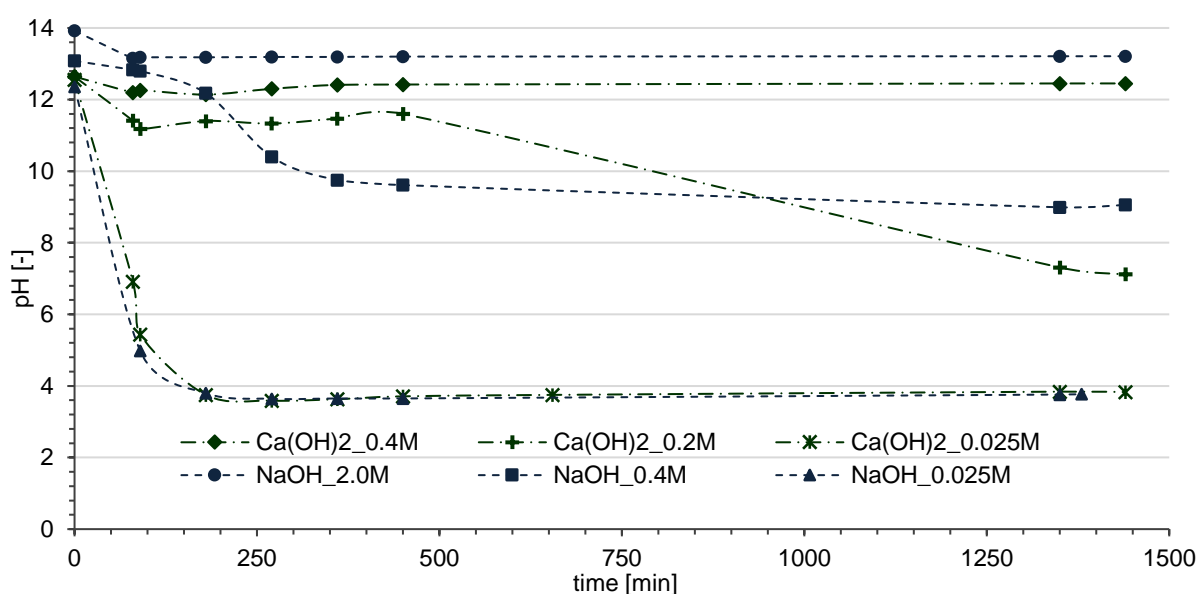


Figure 6-13: Change of pH-value for varying concentrations of $\text{Ca}(\text{OH})_2$ and NaOH at 230°C (E11, E15, E16, E17, E21, E29)

Afterwards the formation of acids regulates the pH-value to about pH 7. In the course of the experiment with 0.025 M the pH decreased rapidly because of the formation of acids and stayed constant at the acidic value of pH 3.8.

In contrast to the calcium hydroxide, the solubility of sodium hydroxide is much higher. Because of that, at the chosen concentrations (0.025 M, 0.4 M and 2.0 M), the solid catalyst was completely dissolved in the reaction solution. Figure 6-13 shows similar behavior to calcium hydroxide at the different concentration. At the medium concentration of 0.4 M the value decreases faster because of the faster formation of acids shown below. The final values were about pH 13.2 (2.0 M), pH 9.1 (0.4 M) and pH 3.8 (0.025 M).

The pH-value for a base concentration of 0.4 M stayed constant for calcium hydroxide and decreased for sodium hydroxide. It can be assumed that the double amount of hydroxide ions from calcium hydroxide is the reason for that, since more of the formed acids can be neutralized. The proportion of hydroxide ions was the same for the two experiments with 0.025 M solutions but the general course of the pH-value over time was quite similar. One reason for that could be the low concentration of catalysts and therefore low concentration of hydroxide ions. Another one could be the pK_a -values of the formed acids that are in the range of the final constant pH-value (about 3.8) and formed an acidic pH buffer. [81]

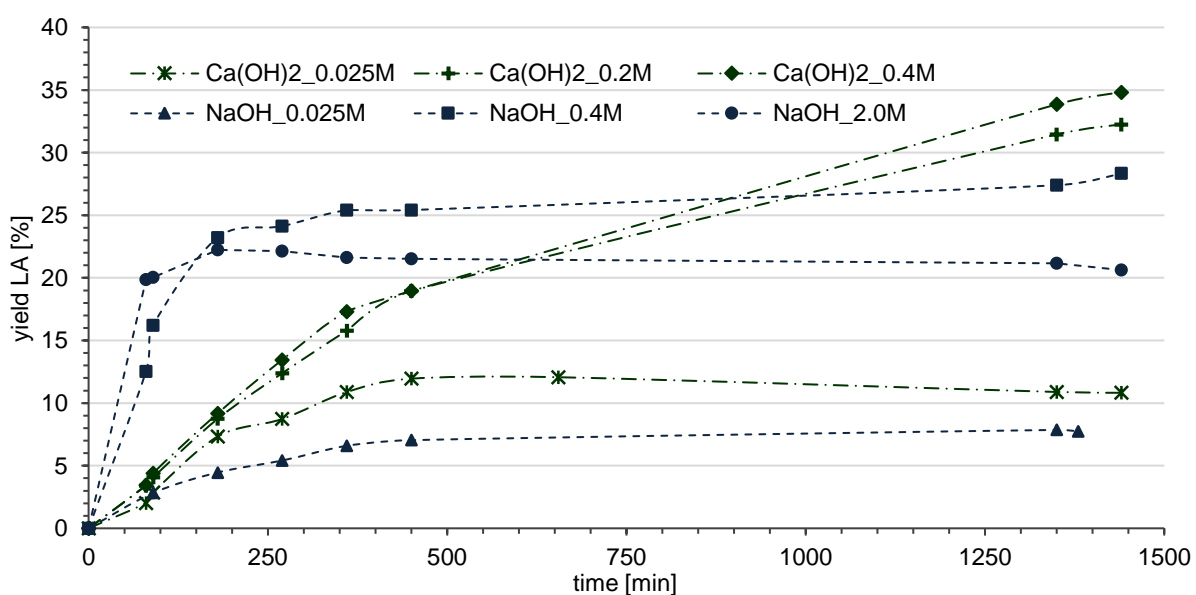


Figure 6-14: Yield of LA for SPB with varying concentration of the Ca(OH)_2 - and NaOH-solution at 230°C (E11, E15, E16, E17, E21, E29)

The influence of the changing pH-value on the formation of acids can be seen in Figure 6-14 and Figure 6-15. For lactic acid and formic acid, the yield increases with increasing concentration of calcium hydroxide. For the formation of lactic acid and formic acid, the time when the pH-value started to decrease differed. This decrease caused a lower yield in lactic acid and a slight decomposition of formic acid. This decomposition can also be observed at lower concentration (0.025 M), shown in Figure 6-15.

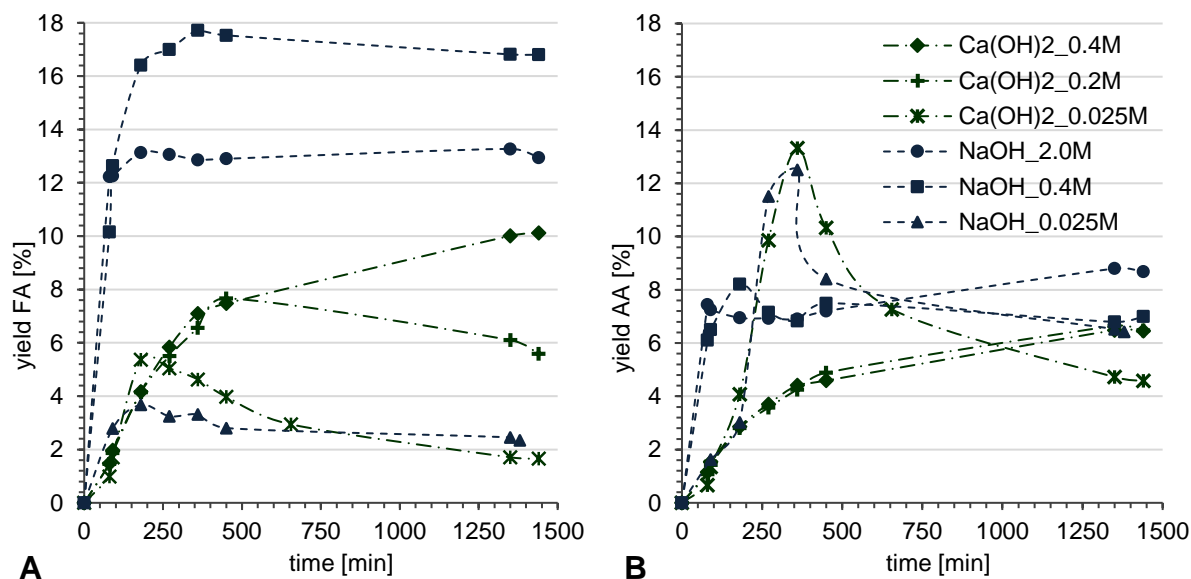


Figure 6-15: Yield of FA (A) and AA (B) for SPB with varying concentration of the Ca(OH)_2 - and NaOH-solution at 230°C (E11, E15, E16, E17, E21, E29)

Sodium hydroxide showed a different behavior regarding the change in acid concentrations. At a catalyst concentration of 0.4 M the yield of lactic acid was considerable higher (28%) than at 2.0 M (20%). The same was observed for formic acid, where the highest yield (17%) of all experiments was achieved with this setup. Compared to the reaction kinetics of pulp degradation catalyzed by calcium hydroxide, it can be seen that the reactions to form the acids are a lot faster at higher concentrations. The maximum yields were reached after 400 minutes at most.

In Figure 6-16, it can be seen that the total pressures at the end of the experiments were different, depending on the concentrations of catalyst. Because the reactor is a closed system and the temperature was constant, gas forming reactions may have occurred to different extends. Comparing lactic acid and formic acid formation there is a connection between the yield and the total pressure at the end of the experiments. The higher the total pressure, the lower the yields. It is well known that in the course

of the formation or degradation of organic substances gases like carbon dioxide are generated. [1,82] Especially the experiments where the final pH-value was acidic showed totally different results. As can be seen in Figure 6-17, char was formed on the vessel's wall only during these experiments.

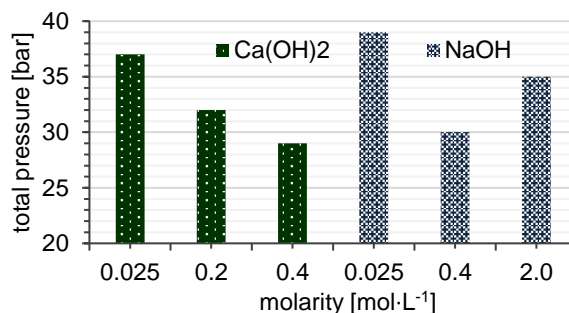


Figure 6-16: Total pressure at the end of experiments with SPB and different catalyst and concentration at 230°C

This is not very surprising because for this experiments the parameters are in the range where hydrochar formation is promoted. The underlying mechanism is a hydrothermal carbonization that converts biomass into a highly carbon rich solid. Furthermore, in the course of this conversion several gases but mainly carbon dioxide are formed. [82] That could be one of the reasons for the high increase of pressure.

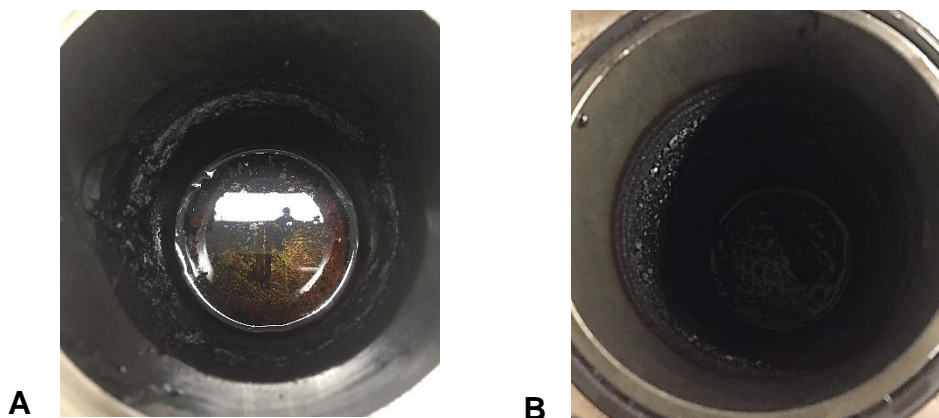


Figure 6-17: Formation of char during experiment E11 (A) and E29 (B)

6.2 Conversion of paper

The experiment using printing paper as substrate for the conversion to carboxylic acids was done to have a tangible example, with which probably everyone had to deal with. Furthermore, large quantities of paper waste accumulate daily and in addition to recycling or combustion, the conversion to acids would be another option. Paper is made of pulp and therefore it is expected that the formation of acids follows the same course as shown in Figure 6-18, but compared to bleached softwood pulp the yields are lower. A lactic acid yield of 26% was achieved which is by about 9% lower than that of pulp.

Many fillers like calcium carbonate and kaolin are additional compounds of printing paper. [83] These inorganic substances are not convertible to acids but are part of the total mass and thus they reduced the yield.

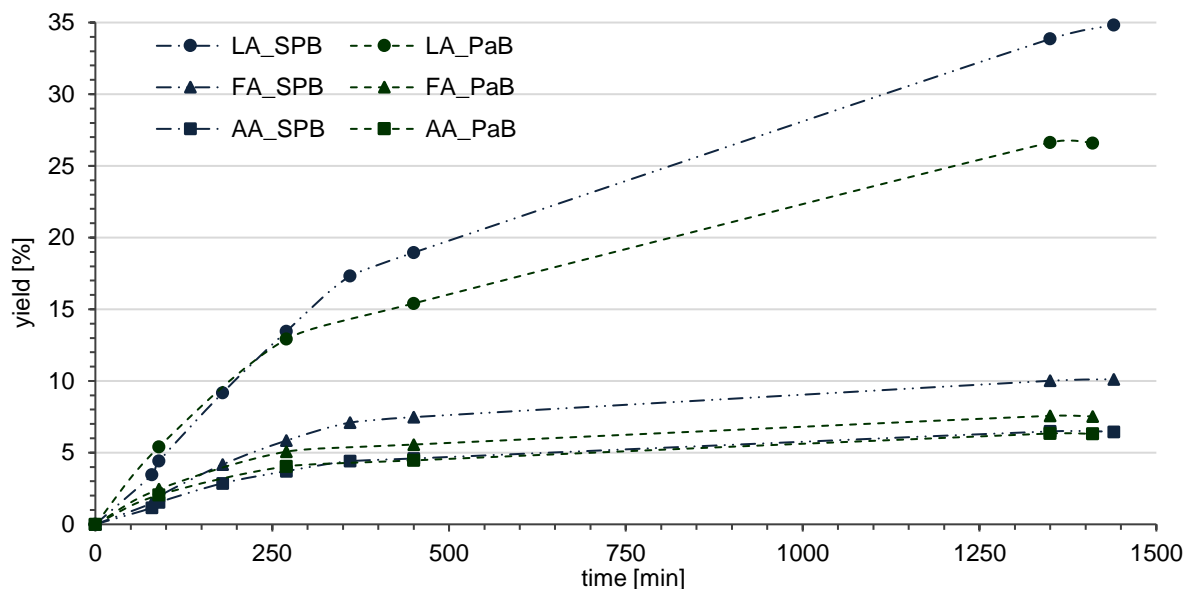


Figure 6-18: Comparison of acid yields of SPB and PaB at 230°C in a 0.4M $\text{Ca}(\text{OH})_2$ -solution. The acids are differentiated by the different markers. (E15, E30)

6.3 Conversion of fines

The highly heterogeneous morphology and chemical composition of chemical pulp fines makes them a hard-to-describe substrate. Depending on the treatment, the properties vary to a certain degree. [25]

In this thesis two different types of fines were investigated. On the one hand secondary bleached pulp fines (SFB) and on the other hand primary unbleached ones (SFU) were heat treated and finally analyzed. The experiments were performed at 230°C in a 0.4 M calcium hydroxide solution. Because the fines were delivered as suspension the dry substance content varied to a certain degree.

Figure 6-19, shows a short time experiment of SFB compared with SPB of the same process. The formation of lactic acid and formic acid is significantly faster for SFB. This can be attributed to the high number of smaller fragments like ray cells or hemicellulosic fragments as well as shorter chained partly soluble carbohydrates that therefore have a higher reactivity. Their higher mass transfer area enhances the reactions to a large degree. The courses of acetic acid are similar, but it needs to be considered that

in contrast to the other acids the initial value of acetic acid was not zero. There already was a concentration of 0.17 g/L in the fines solution. This most likely happened during the heat up to about 80°C for 4 hours to evaporate water in order to achieve a higher solids concentration. However, prior to that evaporation step no acids were detected. Therefore, in Figure 6-19 the course of acetic acid is standardized to the initial value.

The detected chromatograms of both experiments were quite similar as can be reviewed in the appendix (Figure 8-7). That shows that the reaction mechanism with regard to the formed products is similar. The fines may start at a later reaction step and are therefore sooner decomposed to smaller molecules like acids.

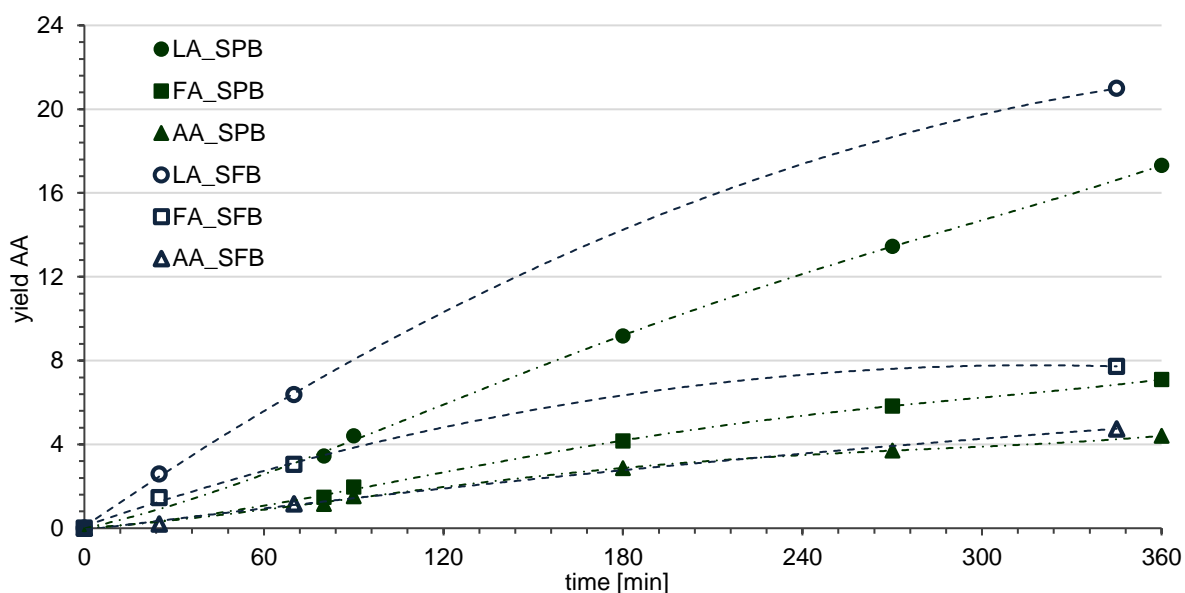


Figure 6-19: Comparison of acid yields of SPB and SFB in a 0.4 M solution of $\text{Ca}(\text{OH})_2$ at 230°C (E9, E15)

Furthermore, it can be seen in Figure 6-19 that the formation of acids was still ongoing at the end of the experiment and so the biomass was not completely converted. Therefore, the duration of the experiment of SFU was extended. Figure 6-20 shows that the formation of acids stopped at about 1500 minutes of treatment time for both SFU and SPU. For the fines experiment, SFU was not treated beforehand and no acids were found in the initial substrate. The chart below shows that during the first 90 minutes all analyzed acids were formed to about the double amount compared to SPU. In the following course this gap stayed either constant or decreased. If one considers the above-mentioned factors and the fact that during this time the heat up from 25°C to 230°C took place one might suspect that the conversion of the fines already begins or

happens to a larger extent at lower temperatures than that of pulp. The fact that the solids content of the SFU mixture is significantly lower than that of SPU and therefore a higher catalyst concentration per solids is present, can be neglected at this high catalyst concentration. Studies have shown that increasing concentrations of catalyst from this point on resulted in no considerable increase of lactic acid formation. [51] One influencing factor could be that chemical transport mechanisms are more hindered at higher solids contents but this was not reviewed in this thesis.

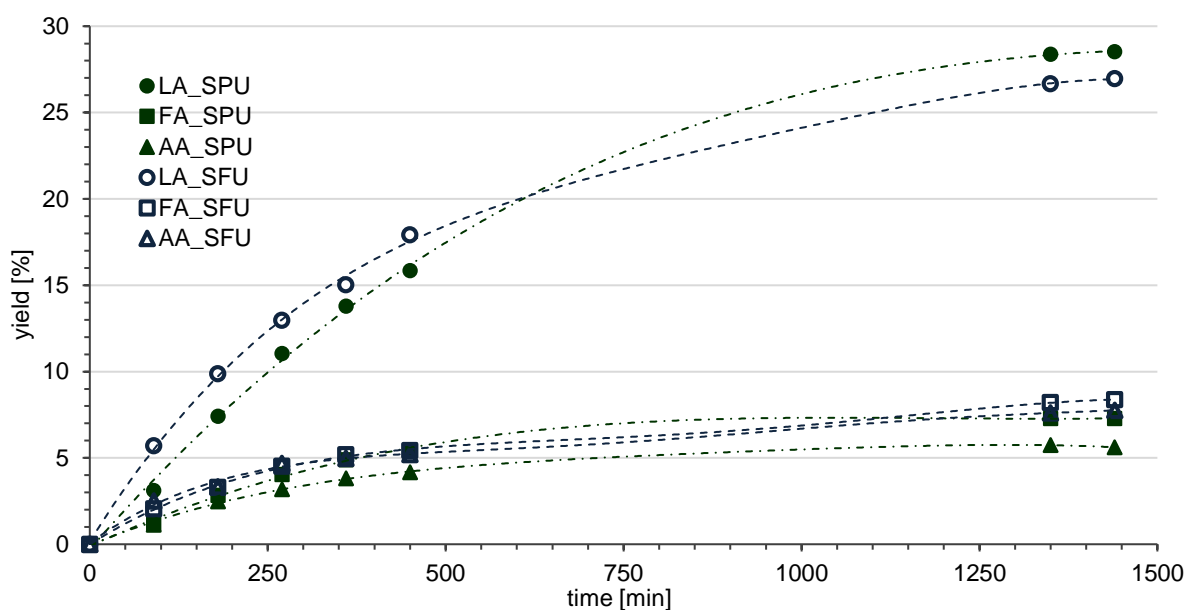


Figure 6-20: Comparison of acid yields of SPU and SFU in a 0.4 M solution of $\text{Ca}(\text{OH})_2$ at 230°C (E31, E33)

6.4 Conversion of lignin

Lignin is one of the main constituents of wood biomass and a valuable attendant of the pulp and paper industry. For the experiment 15w% isolated Kraft lignin was treated at 200°C in a 0.5 M sodium hydroxide solution. As one of the main organic components of black liquor it is used as model substrate therefore. Sodium hydroxide, also present as cooking chemical in black liquor, was used as catalyst to create similar conditions.

To enhance the dissolution of the Kraft lignin it was mixed at 90°C for 2 hours. Afterwards it was stored in the fridge for 24 hours before the start of the experiment. This is of interest because in that solution acids were already found before the actual heat treatment (LA: 1.11 g/L, FA: 1.61 g/L, AA: 1.60 g/L). Probably, some were already present in the isolated Kraft lignin and few were formed during the dissolution procedure.

A further analysis where the lignin was dissolved in the sodium hydroxide solution at room temperature was done. It gave no clear results because no clear separation of the acids during the HPLC-analysis was observed.

During heat treatment, the acids were rapidly formed at the beginning until 180 minutes like shown in Figure 6-21. Afterwards there was no increase of the concentration of lactic acid but a slight one of formic acid and acetic acid up to 540 minutes. Finally, acetic acid reached the highest rise in concentration with $1.67 \text{ g}\cdot\text{L}^{-1}$. The formation of lactic acid and formic acid amounted to $1.32 \text{ g}\cdot\text{L}^{-1}$ and $1.30 \text{ g}\cdot\text{L}^{-1}$, respectively. The rapid formation of acids may be attributed to residual carbohydrates or hemicelluloses which could be present in small amounts in isolated lignin. [80] Afterwards parts of the lignin may have been converted to the acids. It is known from the literature that especially acetic acid is mainly formed from lignin at these conditions. [1] Also, in Figure 6-21 it can be observed that acetic acid had the largest increase. The pressure rose during the experiment from 16 to 18 bar.

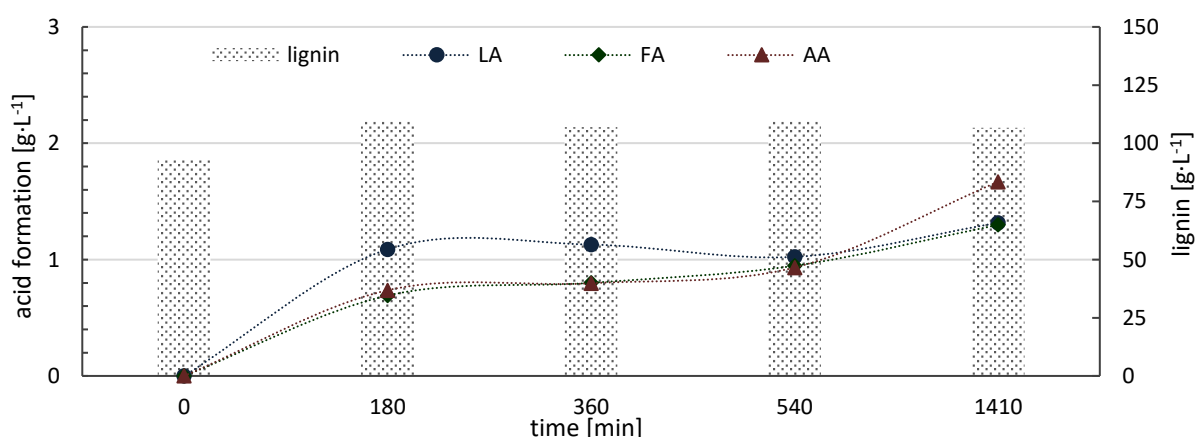


Figure 6-21: Heat treatment of 15%w Kraft lignin at 200°C into a 0.5 M NaOH-solution (E32)

The lignin concentration was analyzed by measurement of the functional phenolic hydroxyl groups using UV/VIS spectroscopy. As it can be seen in Figure 6-21, the concentration increased and stayed quite constant throughout the whole experiment. This might be attributed to cleavage of ether bonds that result in more free phenolic hydroxyl groups at this temperature. [84] Furthermore, the pH-value fell from about pH 12.4 (initial value) to pH 10.7 after 180 minutes and then decreased slowly to the final value of pH 10.2 at the end. Beside the formation of acids, the formation of carboxyl and hydroxyl groups that are reacting acidic could be a reason for that decrease and also

justify the trends seen in Figure 6-21. Vice versa it is also known that the amount of carboxyl and phenolic hydroxyl increases by lowering the pH-value. [85]

6.5 Conversion of black liquor

The heterogenous solution black liquor consists of various organic and inorganic substances. The organic matter mainly consists of modified lignin as well as of degraded polysaccharides. The inorganics consist of cooking chemicals like sodium hydroxide and sodium sulfide.

For the experiments black liquor with a dry solids content of 40.9% was treated at 200°C and 170°C. In Figure 6-22 the course of acid formation and the pressure are shown. The initial solution already contained acids to a considerable amount, formed during the Kraft process. [18] The behavior of additional acid formation was totally different at both temperatures. As shown in Figure 6-22, at 170°C the formation increased faster at the beginning, stagnated thereafter and resumed at about 1500 minutes. It looks like a two-step process, maybe more stable groups, like phenolic molecules, were decomposed later at this temperature. The concentration of lactic acid rose to the highest value of about 11 g·L⁻¹. That was also the final increase at 200°C but before it was twice as much, namely after already 500 minutes. After that, the acid was decomposed to the final value. The other acids show similar behavior but at smaller concentrations at this temperature.

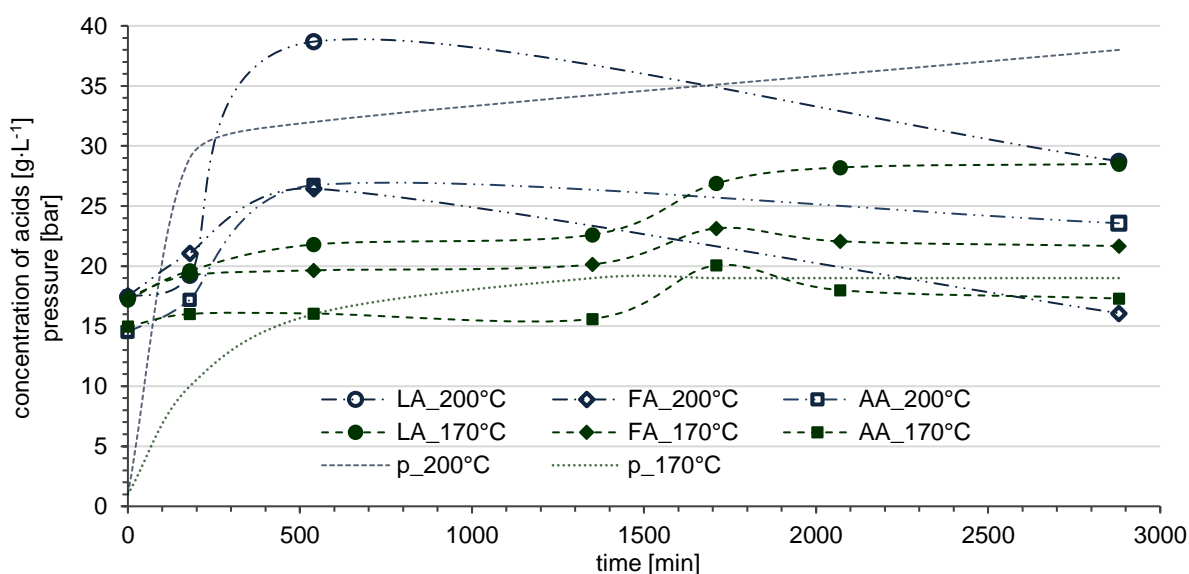


Figure 6-22: Results of the treatment of black liquor at 200°C and 170°C; p denotes the pressure (E27, E28)

Compared to pure lignin the yield of acids is much higher, also considering that the lignin sample had a lower initial dry solids content. That could be because in addition to lignin, there are many other organic substances in black liquor that probably react more likely or faster (hemicellulose) to acids.

If one takes a look at the change of pressure shown in Figure 6-22, it is noticeable that at both experiments it is far above the vapor pressure of water, which is 7.9 bar at 170°C and 15.6 bar at 200°C. At 200°C it increased to 38 bar and at 170°C to 19 bar. Hence, many gas forming reactions occurred. One of them was the reaction to toxic hydrogen sulphide that was detected by the gas warning device.

In Figure 6-23 the change of the lignin content and of the pH-value are shown. The connection of these two parameters has already been discussed in chapter 6.4 and is confirmed by this course especially during the first minutes. Decreasing pH means increasing lignin concentration measured in terms of phenolic

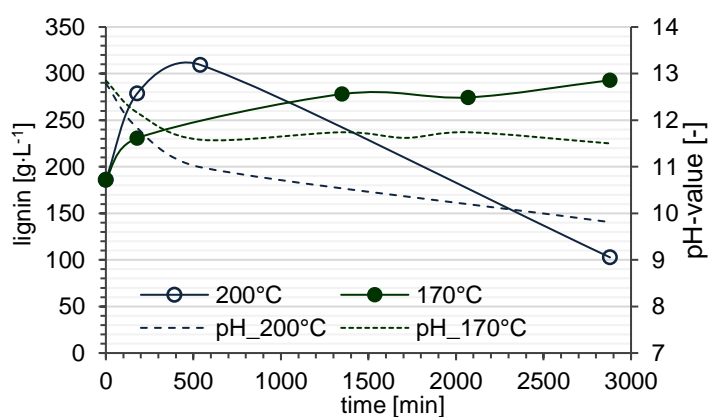


Figure 6-23: Change of lignin concentration and pH-value of black liquor experiments at 170°C and 200°C (E27, E28)

hydroxyl groups. But this is not confirmed by the course of the experiment at 200°C after 540 minutes. That can be justified by the totally different reaction mechanism where lignin is converted to char. That sample, taken at 540 minutes, had significantly different properties compared to the initial samples, it had a much higher viscosity than the other samples. The substrate was already so tough that it completely blocked the sample line. The opposite is known from the literature that says that the viscosity decreases during heat treatment caused by depolymerization of components with larger molar mass to ones with comparably lower molar mass. [86] However, the concentration of NaOH plays a key role in the thermal reactions that take place. It is known that heat treatment of liquors with low levels of NaOH can lead to an increase in viscosity [87] Furthermore, the pH-value was below 11. At about this value the lignin begins to precipitate. [73] Consequently the viscosity of the liquor can increase.

Figure 6-24 shows the highly viscous sample as well as the substances formed until the end of the experiment. Char was formed to a large extent. In some other experiments hydrochar was formed under similar conditions. [88,89] It is known that lignin is a suitable substrate for that formation. Its stable phenolic structure is beneficial for the formation of char, resulting from condensation reactions. [89] It can be formed by homogeneous polymerization of phenolics and water-soluble compounds but the fragments are hard to dissolve at low temperatures. So a solid-solid conversion is preferred at lower temperatures, where non-dissolved lignin is pyrolyzed to form polyaromatic char. [14,89] The observed increase in viscosity due to higher non-dissolved solids would at least affirm this theory.

Finally, it needs to be said that the analysis of the black liquor with HPLC showed a strong noise and no clear separation of acids in the chromatogram. Therefore, the samples were analyzed at least twice to find representative values.

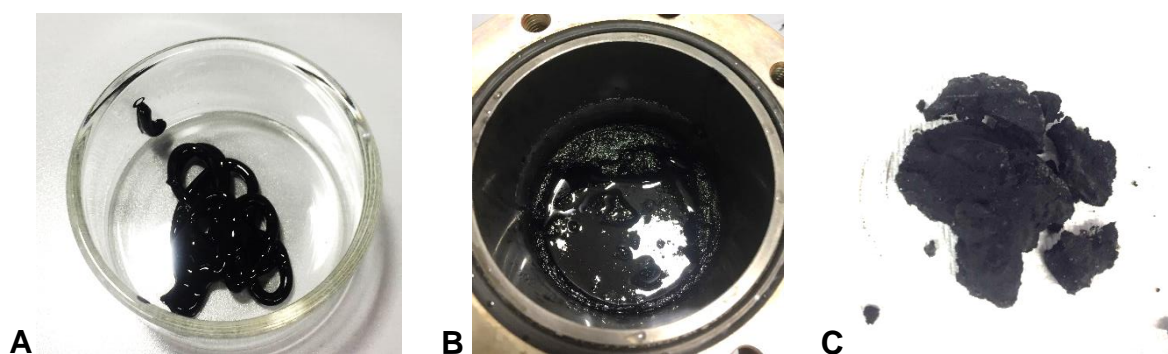


Figure 6-24: Pictures of E28; sample taken after 540 minutes which had a very high viscosity (A), modified black liquor at the end of the experiment (B), formed char (C)

7 Conclusion and outlook

Biorefining means the analogon of the conventional oil refinery, but uses renewable resources for the same purpose. From renewable resources energy, products and fuels shall be produced at the same time. When focusing on products, carboxylic acids are of interest as bulk chemicals for a broad range of end-products and applications. In the future it could be a sustainable and serious alternative to fossil sources. The hydrothermal conversion of lignocellulosic biomass under mild conditions is a suitable method for the generation of carboxylic acids. The treatment leads to degradation of polysaccharides to monosaccharides and consequently to the conversion to acids or other chemicals. In contrast to many other bioconversion methods, hydrothermal conversion is characterized by stable process properties, rapid conversion and no need for special pretreatment.

Because of the high heating value of lignocellulosic material and the related process streams, the combustion and energy production is a logical and widespread form of its conversion. Besides that, the demand for chemicals in general and their origin from non-fossil resources becomes more and more important. A life cycle assessment of lactic acid produced from renewable and fossil sources was performed by scientists. The assessment shows huge environmental savings when bioresources are used. [90] Although this study was carried out for fermentative production, it shows the potential in acids production by renewable sources such as with hydrothermal conversion.

The present thesis develops the basics for the utilization of products from the pulp and paper industry and their ability to produce carboxylic acids by hydrothermal treatment thereof. It deals with the most abundantly available biomass, namely wood, in different conditions as substance source. Therefore, the carbon-rich products and process streams from the Kraft process, pulp, paper, fines, isolated lignin and black liquor were studied regarding their behavior and potential to acid formation in the course of hydrothermal treatment, supported by the catalysts calcium or sodium hydroxide. The first three materials mentioned can be assigned to the group of cellulose-containing substrates, the other two into those of the lignin-based substrates that have different degradation mechanisms caused by the aromatic structure of lignin.

The highest yield of cellulosic conversion was achieved with bleached pulp at a temperature of 230°C catalyzed by 0.4 M calcium hydroxide solution. 38% of dry substance was converted to lactic acid at this temperature. A lower maximum yield of 10% and 8% for formic acid and acetic acid was accomplished, respectively. The total amount of pulp was already converted after 1500 minutes of heat treatment and also the maximum acids formation was reached at this time. In contrast to that with a reaction temperature of 200°C and 170°C, only 60% and 25% of pulp dry mass was degraded. The acids conversion was steady, however with ongoing time it was significantly lower. By comparing hardwood and softwood pulp in bleached and unbleached form a slightly higher yield was observed for lactic and formic acid when bleached pulp was used. Acetic acid was formed to a larger amount from hardwood samples compared to softwood samples. The lignin content analyzed by UV-spectroscopy showed for both, bleached and unbleached samples, an initial increase and later decrease.

The influence of the catalyst and its concentration was analyzed with bleached pulp and yielded very heterogeneous results. At constant concentration of metal ions, the divalent calcium led to higher maximum yields but also to higher degradation than the monovalent sodium. Throughout these experiments the pH-value was not stable and decreased rapidly to pH 3.8, because of the low concentration of alkaline catalyst. This resulted in char formation for both catalysts. By increasing the catalyst concentration, the formation of acids increased, but in contrast to calcium hydroxide, the highest concentration of sodium hydroxide did not result in the highest acid yield. However, the overall highest maximum yield of formic acid was achieved with 17%. Furthermore, the formation of acids was much faster when sodium hydroxide at higher concentrations was used.

The acids formation of fines was compared to that of pulp under identical conditions. For both, bleached and unbleached samples, the acids yield with fines during the first 90 minutes was about twice as high as that of pulp. That shows that the reactivity of fines is higher and they thus degrade faster compared to pulp, most likely due to a lower molecular mass of cellulose monomers and a higher specific surface of the fibers. Nevertheless, the reaction kinetic did not change and results from pulp can be transferred to fines easily.

Lignin was treated as model substrate for black liquor. The treatment at 200°C showed a slight increase of acid concentration in the range of 1.3 - 1.6 g·L⁻¹ whereas acetic acid had the highest concentration. Lignin content and pressure increased and the pH-value decreased. In experiments under similar conditions with black liquor, higher amounts of acids of up to 11 g·L⁻¹ were formed. The acids yield of both is much lower compared to that of cellulosic substrates.

Summing up, high yields of lactic acid were achieved in the course of heat treatment of different pulps as well as for fines at high temperatures. The catalysts and their concentration played an important role regarding the reaction mechanisms. Despite total conversion of the initial substrates, the yields were very different. Especially the pH-value steered the reactions to different substances. Considering lactic acid an alkaline pH-value led to high final concentrations. An acidic pH-value led to the formation of char and gaseous substances.

The much lower acid yields with isolated lignin and black liquor can be attributed to the need of higher activation energy for ring-opening reactions of aromatic groups. Higher temperature or the use of special catalysts would increase the formation of acids. However, the reaction mechanisms at higher temperatures (>200°C) then go in a different direction, like char formation, gasification or pyrolysis.

Further investigations should be done by adjustment of the reaction atmosphere by superposition of gases. Inert ones for instance can enhance the yield of lactic acid. Furthermore, experiments with different catalyst, like can be performed. Also, solid catalysts like tungstated alumina or lanthanum cobaltite, which would be easier to separate, or the addition of metal ions like Pb^{II} or Zn^{II} need to be taken into consideration. However, these should always be chosen in terms of economy, availability and handling.

Besides the formation of acids, the separation is a task no less challenging. Many studies are currently done to find suitable methods. Possible physical separation technologies to isolate carboxylic acids from aqueous solutions are liquid and membrane extraction, ultra-filtration, reverse osmosis, direct distillation or adsorption, to name some. [91] They have different advantages and drawbacks but nevertheless high concentrations of the acid to be isolated are very beneficial for selective separation.

8 Appendix

8.1 Bibliography

1. Jin, F., "Application of Hydrothermal Reactions to Biomass Conversion," Springer Berlin Heidelberg, ISBN 9783642544583, 2014.
2. Deng, W., Zhang, Q., and Wang, Y., "Catalytic transformations of cellulose and cellulose-derived carbohydrates into organic acids," *Catal. Today*, 2014, doi:10.1016/j.cattod.2013.12.041.
3. Deng, W., Zhang, Q., and Wang, Y., Catalytic transformation of cellulose and its derived carbohydrates into chemicals involving C-C bond cleavage, *J. Energy Chem.*, 2015, doi:10.1016/j.jechem.2015.08.016.
4. Hundt, M., "Der AlkaPoIP-Prozess als Ausgangspunkt für eine lignocellulosebasierte Bioraffinerie," Technischen Universität Cottbus-Senftenberg, 2015.
5. Bajpai, P., "Pulp and Paper Industry," ISBN 9780128034088, 2015, doi:10.1016/B978-0-12-803408-8.00006-8.
6. Feedstocks, B., "Biomass Feedstocks," *Biofuels* 45–85, 2009, doi:10.1007/978-1-84882-011-1_2.
7. Pérez, J., Muñoz-Dorado, J., La Rubia, T. De, and Martínez, J., Biodegradation and biological treatments of cellulose, hemicellulose and lignin: An overview, *Int. Microbiol.* 5(2):53–63, 2002, doi:10.1007/s10123-002-0062-3.
8. Saha, B.C., "Hemicellulose bioconversion," *Journal of Industrial Microbiology and Biotechnology*, ISBN 1367-5435 (Print)r1367-5435 (Linking), 2003, doi:10.1007/s10295-003-0049-x.
9. Sorieul, M., Dickson, A., Hill, S.J., and Pearson, H., "Plant fibre: Molecular structure and biomechanical properties, of a complex living material, influencing its deconstruction towards a biobased composite," *Materials (Basel)*, 2016, doi:10.3390/ma9080618.
10. Pastusiak, R., "Charakterisierung von Zellstoffkomponenten: Analytik, Spektroskopie, Reaktionskinetik und Modellierung," 2003.
11. Tekin, K., Karagöz, S., and Bektaş, S., A review of hydrothermal biomass processing, *Renew. Sustain. Energy Rev.*, 2014, doi:10.1016/j.rser.2014.07.216.
12. Hansen, C.M. and Björkman, A., "The Ultrastructure of Wood from a Solubility Parameter Point of View," *Holzforschung*, 1998, doi:10.1515/hfsg.1998.52.4.335.
13. Vanholme, R., Demedts, B., Morreel, K., Ralph, J., and Boerjan, W., "Lignin Biosynthesis and Structure," *PLANT Physiol.*, 2010, doi:10.1104/pp.110.155119.
14. Kang, S., Li, X., Fan, J., and Chang, J., Hydrothermal conversion of lignin: A review, *Renew. Sustain. Energy Rev.*, 2013, doi:10.1016/j.rser.2013.07.013.
15. Biermann, C.J., "Handbook of Pulping and Papermaking," ISBN

- 9780120973620, 1996, doi:10.1016/B978-012097362-0/50008-X.
16. Ragnar, M., Henriksson, G., Lindström, M.E., Wimby, M., Blechschmidt, J., and Heinemann, S., "Pulp," *Ullmann's Encyclopedia of Industrial Chemistry*, American Cancer Society, ISBN 9783527306732: 1–92, 2014, doi:10.1002/14356007.a18_545.pub4.
 17. Sixta, H., "Handbook of Pulp," ISBN 3527309993, 2008, doi:10.1002/9783527619887.
 18. Bajpai, P., "Black Liquor Gasification," ISBN 9780081000090, 2014, doi:10.1016/C2013-0-12854-1.
 19. Bajpai, P., "Brief Description of the Pulp and Paper Making Process," *Biotechnology for Pulp and Paper Processing*, Springer US, Boston, MA, ISBN 978-1-4614-1409-4: 7–14, 2012, doi:10.1007/978-1-4614-1409-4_2.
 20. SCANDINAVIEN PULP PAPER AND BOARD - TESTING COMMITTEE, "SCAN-CM66:05," SCANDINAVIEN PULP, PAPER AND BOARD, 2005.
 21. Fischer, W.J., Mayr, M., Spirk, S., Reishofer, D., Jagiello, L.A., Schmiedt, R., Colson, J., Zankel, A., and Bauer, W., "Pulp fines-characterization, sheet formation, and comparison to microfibrillated cellulose," *Polymers (Basel)*, 2017, doi:10.3390/polym9080366.
 22. Odabas, N., Henniges, U., Potthast, A., and Rosenau, T., "Cellulosic Fines: Properties and Effects," *Progress Material Sci.*, 2016.
 23. Liu, H., Yang, S., and Ni, Y., "Effect of Pulp Fines on the Dye–Fiber Interactions during the Color-Shading Process," *Ind. Eng. Chem. Res.* 49(18):8544–8549, 2010, doi:10.1021/ie101169s.
 24. Olejnik, K., Skalski, B., Stanislawski, A., and Wysocka-Robak, A., "Swelling properties and generation of cellulose fines originating from bleached kraft pulp refined under different operating conditions," *Cellulose* 24(9):3955–3967, 2017, doi:10.1007/s10570-017-1404-9.
 25. Mayr, M., Eckhart, R., Thaller, A., and Bauer, W., "CHARACTERIZATION OF FINES QUALITY AND THEIR INDEPENDENT EFFECT ON SHEET PROPERTIES," Graz University of Technology, 2017.
 26. Taipale, T., Österberg, M., Nykänen, A., Ruokolainen, J., and Laine, J., "Effect of microfibrillated cellulose and fines on the drainage of kraft pulp suspension and paper strength," *Cellulose*, 2010, doi:10.1007/s10570-010-9431-9.
 27. Castillo Martinez, F.A., Balciunas, E.M., Salgado, J.M., Domínguez González, J.M., Converti, A., and Oliveira, R.P. de S., Lactic acid properties, applications and production: A review, *Trends Food Sci. Technol.*, 2013, doi:10.1016/j.tifs.2012.11.007.
 28. PubChem, "PubChem Compound Database," n.d, <https://pubchem.ncbi.nlm.nih.gov/compound/24360>, 2018, doi:CID=445639.
 29. Ameen, S.M. and Caruso, G., "Chemistry of Lactic Acid," 7–17, 2017, doi:10.1007/978-3-319-58146-0_2.
 30. Deng, W., Zhang, Q., and Wang, Y., Catalytic transformations of cellulose and its derived carbohydrates into 5-hydroxymethylfurfural, levulinic acid, and lactic acid, *Sci. China Chem.*, 2015, doi:10.1007/s11426-014-5283-8.

31. Chahal, S.P., "Lactic Acid," *Ullmann's Encyclopedia of Industrial Chemistry*, Wiley-VCH Verlag GmbH & Co. KGaA, Weinheim, Germany, 2000, doi:10.1002/14356007.a15_097.
32. Dusselier, M., Wouwe, P. Van, Dewaele, A., Makshina, E., and Sels, B.F., Lactic acid as a platform chemical in the biobased economy: The role of chemocatalysis, *Energy Environ. Sci.*, 2013, doi:10.1039/c3ee00069a.
33. Hietala, J., Vuori, A., Johnsson, P., Pollari, I., Reutemann, W., and Kieczka, H., "Formic Acid," *Ullmann's Encyclopedia of Industrial Chemistry*, ISBN 9783527306732, 2016, doi:10.1002/14356007.a12_013.pub3.
34. Willmes, A., "Taschenbuch Chemische Substanzen," Harri Deutsch, ISBN 9783808556641, 2007.
35. Berre, C. Le, Serp, P., Kalck, P., and Torrence, G.P., "Acetic Acid," *Ullmann's Encyclopedia of Industrial Chemistry*, Wiley-VCH Verlag GmbH & Co. KGaA, Weinheim, Germany: 1–34, 2014, doi:10.1002/14356007.a01_045.pub3.
36. FU-Berlin, "Reaktionstypen der organischen Chemie," <http://kirste.userpage.fu-berlin.de/chemistry/oc/reac/reaktionstypen.html>, Jan. 2019.
37. Addition, Elimination And Substitution Reactions | Organic Molecules | Siyavula, <https://www.siyavula.com/read/science/grade-12/organic-molecules/04-organic-molecules-06>, Jan. 2019.
38. Cycloaddition Reactions - Chemistry LibreTexts, [https://chem.libretexts.org/Bookshelves/Organic_Chemistry/Supplemental_Modules_\(Organic_Chemistry\)/Reactions/Pericyclic_Reactions/Cycloaddition_Reactions](https://chem.libretexts.org/Bookshelves/Organic_Chemistry/Supplemental_Modules_(Organic_Chemistry)/Reactions/Pericyclic_Reactions/Cycloaddition_Reactions), Jan. 2019.
39. 13.3: Aldol reactions - Chemistry LibreTexts, [https://chem.libretexts.org/Bookshelves/Organic_Chemistry/Book%3A_Organic_Chemistry_with_a_Biological_Emphasis_\(Soderberg\)/13%3A_Reactions_with_stabilized_carbanion_intermediates_/13.3%3A_Aldol_reactions](https://chem.libretexts.org/Bookshelves/Organic_Chemistry/Book%3A_Organic_Chemistry_with_a_Biological_Emphasis_(Soderberg)/13%3A_Reactions_with_stabilized_carbanion_intermediates_/13.3%3A_Aldol_reactions), Jan. 2019.
40. Eliminierungsreaktion, <http://www.chemie.de/lexikon/Eliminierungsreaktion.html>, Jan. 2019.
41. 14.5: Reactions of Alcohols - Chemistry LibreTexts, [https://chem.libretexts.org/Bookshelves/Introductory_Chemistry/Book%3A_The_Basics_of_GOB_Chemistry_\(Ball_et_al.\)/14%3A_Organic_Compounds_of_Oxygen/14.05_Reactions_of_Alcohols](https://chem.libretexts.org/Bookshelves/Introductory_Chemistry/Book%3A_The_Basics_of_GOB_Chemistry_(Ball_et_al.)/14%3A_Organic_Compounds_of_Oxygen/14.05_Reactions_of_Alcohols), Jan. 2019.
42. Wamser, C.C., Rearrangement reaction, 2019, doi:10.1036/1097-8542.757361 OP - AccessScience.
43. Illustrated Glossary of Organic Chemistry - Isomerization, <http://www.chem.ucla.edu/~harding/IGOC/I/isomerization.html>, Jan. 2019.
44. 1,2-Hydride Shift - Chemistry LibreTexts, https://chem.libretexts.org/Ancillary_Materials/Reference/Organic_Chemistry_Glossary/1%2C2-Hydride_Shift, Jan. 2019.
45. Kühl, O., "Allgemeine Chemie - für Biochemiker, Lebenswissenschaftler, Mediziner, Pharmazeuten ... : Für Lebenswissenschaftler, Mediziner, Pharmazeuten ...," Wiley, ISBN 352766968X, 2012.
46. Hofmann, H. and Jander, G., "Qualitative Analyse," Walter de Gruyter, ISBN

- 311083488X, 1972.
47. Saure Hydrolyse - Chemiezauber.de, <https://chemiezauber.de/inhalt/q1/polysaccharide/saure-hydrolyse.html>, Jan. 2019.
 48. Rosatella, A.A., Simeonov, S.P., Frade, R.F.M., and Afonso, C.A.M., 5-Hydroxymethylfurfural (HMF) as a building block platform: Biological properties, synthesis and synthetic applications, *Green Chem.*, 2011, doi:10.1039/c0gc00401d.
 49. Bicker, M., Endres, S., Ott, L., and Vogel, H., "Catalytical conversion of carbohydrates in subcritical water: A new chemical process for lactic acid production," *J. Mol. Catal. A Chem.*, 2005, doi:10.1016/j.molcata.2005.06.017.
 50. Li, J., Ding, D.J., Deng, L., Guo, Q.X., and Fu, Y., "Catalytic air oxidation of biomass-derived carbohydrates to formic acid," *ChemSusChem*, 2012, doi:10.1002/cssc.201100466.
 51. Yan, X., Jin, F., Tohji, K., Kishita, A., and Enomoto, H., "Hydrothermal conversion of carbohydrate biomass to lactic acid," *AIChE J.* 56(10):2727–2733, 2010, doi:10.1002/aic.12193.
 52. Yan, X., Jin, F., Tohji, K., Kishita, A., and Enomoto, H., "Hydrothermal conversion of carbohydrate biomass to lactic acid," *AIChE J.*, 2010, doi:10.1002/aic.12193.
 53. Jin, F. and Enomoto, H., Rapid and highly selective conversion of biomass into value-added products in hydrothermal conditions: Chemistry of acid/base-catalysed and oxidation reactions, *Energy Environ. Sci.*, 2011, doi:10.1039/c004268d.
 54. Chambon, F., Rataboul, F., Pinel, C., Cabiac, A., Guillon, E., and Essayem, N., "Cellulose hydrothermal conversion promoted by heterogeneous Brønsted and Lewis acids: Remarkable efficiency of solid Lewis acids to produce lactic acid," *Appl. Catal. B Environ.*, 2011, doi:10.1016/j.apcatb.2011.04.009.
 55. Wang, Y., Deng, W., Wang, B., Zhang, Q., Wan, X., Tang, Z., Wang, Y., Zhu, C., Cao, Z., Wang, G., and Wan, H., "Chemical synthesis of lactic acid from cellulose catalysed by lead(II) ions in water," *Nat. Commun.*, 2013, doi:10.1038/ncomms3141.
 56. Tang, Z., Deng, W., Wang, Y., Zhu, E., Wan, X., Zhang, Q., and Wang, Y., "Transformation of cellulose and its derived carbohydrates into formic and lactic acids catalyzed by vanadyl cations," *ChemSusChem*, 2014, doi:10.1002/cssc.201400150.
 57. Wang, F.F., Liu, C.L., and Dong, W.S., "Highly efficient production of lactic acid from cellulose using lanthanide triflate catalysts," *Green Chem.*, 2013, doi:10.1039/c3gc40836a.
 58. Sánchez, C., Egüés, I., García, A., Llano-Ponte, R., and Labidi, J., "Lactic acid production by alkaline hydrothermal treatment of corn cobs," *Chem. Eng. J.*, 2012, doi:10.1016/j.cej.2011.12.033.
 59. Jin, F., Yun, J., Li, G., Kishita, A., Tohji, K., and Enomoto, H., "Hydrothermal conversion of carbohydrate biomass into formic acid at mild temperatures," *Green Chem.*, 2008, doi:10.1039/b802076k.

60. Calvo, L. and Vallejo, D., "Formation of organic acids during the hydrolysis and oxidation of several wastes in sub- and supercritical water," *Ind. Eng. Chem. Res.*, 2002, doi:10.1021/ie020441m.
61. Jin, F., Zhou, Z., Moriya, T., Kishida, H., Higashijima, H., and Enomoto, H., "Controlling hydrothermal reaction pathways to improve acetic acid production from carbohydrate biomass," *Environ. Sci. Technol.*, 2005, doi:10.1021/es048867a.
62. Teong, S.P., Yi, G., and Zhang, Y., Hydroxymethylfurfural production from bioresources: Past, present and future, *Green Chem.*, 2014, doi:10.1039/c3gc42018c.
63. Kim, B., Jeong, J., Lee, D., Kim, S., Yoon, H.J., Lee, Y.S., and Cho, J.K., "Direct transformation of cellulose into 5-hydroxymethyl-2-furfural using a combination of metal chlorides in imidazolium ionic liquid," *Green Chem.*, 2011, doi:10.1039/c1gc15152e.
64. Weingarten, R., Conner, W.C., and Huber, G.W., "Production of levulinic acid from cellulose by hydrothermal decomposition combined with aqueous phase dehydration with a solid acid catalyst," *Energy Environ. Sci.*, 2012, doi:10.1039/c2ee21593d.
65. Lin, H., Strull, J., Liu, Y., Karmiol, Z., Plank, K., Miller, G., Guo, Z., and Yang, L., "High yield production of levulinic acid by catalytic partial oxidation of cellulose in aqueous media," *Energy Environ. Sci.*, 2012, doi:10.1039/c2ee23225a.
66. Shen, J. and Wyman, C.E., "Hydrochloric acid-catalyzed levulinic acid formation from cellulose: Data and kinetic model to maximize yields," *AIChE J.*, 2012, doi:10.1002/aic.12556.
67. Araújo, J.D.P., Grande, C.A., and Rodrigues, A.E., "Vanillin production from lignin oxidation in a batch reactor," *Chem. Eng. Res. Des.*, 2010, doi:10.1016/j.cherd.2010.01.021.
68. Suzuki, H., Cao, J., Jin, F., Kishita, A., Enomoto, H., and Moriya, T., "Wet oxidation of lignin model compounds and acetic acid production," *J. Mater. Sci.*, 2006, doi:10.1007/s10853-006-4653-9.
69. Christen, D.S., "Praxiswissen der chemischen Verfahrenstechnik: Handbuch für Chemiker und Verfahreningenieure," ISBN 978-3-540-88974-8, 2005, doi:10.1007/978-3-540-88975-5.
70. Schwister, K. and Leven, V., Verfahrenstechnik für Ingenieure, *Lehr- Und Übungsb.*, 2014, doi:10.3139/9783446440012.
71. Schwister, K. and Leven, V., "08 Aktivierung von Reaktionen und Katalyse," *Verfahrenstechnik für Ingenieure*, ISBN 0780381386, 2014, doi:10.1109/IDAACS.2003.1249543.
72. Schwister, K. and Leven, V., "07 Kinetik chemischer Reaktionen," *Verfahrenstechnik für Ingenieure*, ISBN 978-3-446-43070-9, 2014, doi:10.1016/j.chiabu.2013.02.006.
73. Norgren, M., Edlund, H., Wågberg, L., Lindström, B., and Annergren, G., "Aggregation of kraft lignin derivatives under conditions relevant to the process, part I: Phase behaviour," *Colloids Surfaces A Physicochem. Eng. Asp.*, 2001, doi:10.1016/S0927-7757(01)00753-1.

74. Kannangara, M., Marinova, M., Fradette, L., and Paris, J., "Effect of mixing hydrodynamics on the particle and filtration properties of precipitated lignin," *Chem. Eng. Res. Des.*, 2016, doi:10.1016/j.cherd.2015.11.003.
75. Schiegl, C., Helmreich, B. und Wilderer, P.A., "Quantifizierung von Lignin aus Papierfabriksabwässern mittels Py-GC/MS," *Vom Wasser*, ISBN 00284793, 1997.
76. Bjerre, A.B. and Sørensen, E., Thermal Decomposition of Dilute Aqueous Formic Acid Solutions, *Ind. Eng. Chem. Res.*, 1992, doi:10.1021/ie00006a022.
77. Popescu, C.M., Tibirna, C.M., Raschip, I.E., Popescu, M.C., Ander, P., and Vasile, C., "BULK AND SURFACE CHARACTERIZATION OF UNBLEACHED AND BLEACHED SOFTWOOD KRAFT PULP FIBRES," *Cellul. Chem. Technol.*, 2008.
78. Hillis, W.E., "Formation and properties of some wood extractives," *Phytochemistry* 11(4):1207–1218, 1972, doi:10.1016/S0031-9422(00)90067-0.
79. Zhang, H., Ping, Q., Zhang, J., and Li, N., "Determination of Furfural and Hydroxymethyl furfural by UV Spectroscopy in ethanol-water hydrolysate of Reed," *J. Bioresour. Bioprod.* 2(4):170–174, 2017, doi:10.21967/JBB.V2I4.84.
80. Brodin, I., "CHEMICAL PROPERTIES AND THERMAL BEHAVIOUR OF KRAFT LIGNINS," KTH Royal Institute of Technology, 2009.
81. Harsch, G. and Heimann, R., "Didaktik der Organischen Chemie nach dem PIN-Konzept," Springer Berlin Heidelberg, Berlin, Heidelberg, ISBN 978-3-540-67032-2, 1998, doi:10.1007/978-3-642-59022-1.
82. Kambo, H.S. and Dutta, A., A comparative review of biochar and hydrochar in terms of production, physico-chemical properties and applications, *Renew. Sustain. Energy Rev.*, 2015, doi:10.1016/j.rser.2015.01.050.
83. Füllstoffe - Austropapier, <https://www.austropapier.at/themen/rohstoffe/fuellstoffe/>, Jan. 2019.
84. Nuopponen, M., Vuorinen, T., Jämsä, S., and Viitaniemi, P., "Thermal Modifications in Softwood Studied by FT-IR and UV Resonance Raman Spectroscopies," *J. Wood Chem. Technol.* 24(1):13–26, 2005, doi:10.1081/WCT-120035941.
85. Jablonsky, M., Kocis, J., Haz, A., and J., S., "Characterization and Comparison by UV Spectroscopy of precipitated Lignins and commercial Lignosulfonates," *Cellul. Chem. Technol.*, 2015, doi:Doi 10.1136/Vr.E6519.
86. Dhermander Kumar, T. and Kasana, H., "Liquor heat treatment of wheat straw black liquor to facilitate recovery process in a paper mill," *Int. J. Recent Sci. Res.* 7:7, 2015.
87. Small, J.D. and Fricke, A.L., "Thermal Stability of Kraft Black Liquor Viscosity at Elevated Temperatures," *Ind. Eng. Chem. Prod. Res. Dev.*, 1985, doi:10.1021/i300020a022.
88. Louhelainen, J., Alen, R., Zielinski, J., and Sagfors, P., "Effects of Oxidative and Non-Oxidative Thermal Treatments on the Viscosity and Chemical Composition of Softwood Kraft Black Liquor," *J. Pulp Pap. Sci.*, 2002.
89. Kang, S., Li, X., Fan, J., and Chang, J., "Characterization of hydrochars

- produced by hydrothermal carbonization of lignin, cellulose, d-xylose, and wood meal," *Industrial and Engineering Chemistry Research*, ISBN 0888-5885, 2012, doi:10.1021/ie300565d.
90. Daful, A.G., Haigh, K., Vaskan, P., and Görgens, J.F., "Environmental impact assessment of lignocellulosic lactic acid production: Integrated with existing sugar mills," *Food Bioprod. Process.*, 2016, doi:10.1016/j.fbp.2016.04.005.
 91. Kumar, S. and Babu, B., "Separation of carboxylic acids from waste water via reactive extraction," *Int. Conv. Water*, 2014.

8.2 List of abbreviations

m	Mass	[g]
c	Concentration	[mol·L ⁻¹] [g·L ⁻¹]
V	Volume	[L] [m ³]
n	Amount of substance	[mol]
T	Temperature	[°C]
p	Pressure	[bar]
t	Time	[min]
E _a	Arrhenius activation energy	[J·mol ⁻¹]
R	Universal gas constant	[J·K ⁻¹ ·mol ⁻¹]
LA	Lactic acid	-
FA	Formic acid	-
AA	Acetic acid	-
TI	Temperature indicator	-
PI	Pressure indicator	-
TH	Temperature high	-
E	Energy	-
r	Reaction rate	[g·min ⁻¹]
k	Reaction rate constant	-
A	Pre-exponential factor	-
DP	Degree of polymerization	-
SPB	Softwood pulp bleached	-
SPU	Softwood pulp unbleached	-
HPB	Hardwood pulp bleached	-
HPU	Hardwood pulp unbleached	-
SFB	Softwood fines bleached	-
SFU	Softwood fines unbleached	-
BL	Black liquor softwood	-
L	Lignin precipitated from black liquor	-
PaB	Printing paper bleached	-

8.3 List of figures

Figure 1-1: Simplified scheme of hydrothermal conversion of biomass to carboxylic acids, including the reaction parameters	1
Figure 2-1: Chemical structure of cellulose [10].....	3
Figure 2-2: Pentoses and hexoses that mainly occur in hemicellulose [10].....	4
Figure 2-3: Basic building blocks of lignin (from left to right): p-coumaryl alcohol, coniferyl alcohol, sinapyl alcohol [10]	4
Figure 2-4: Average lignocellulosic composition of (A) hardwood and (B) softwood [9]	5
Figure 2-5: Simplified flow sheet of a pulp and paper making procedure using the Kraft process; circles are representing the taken experimental feed substrates.....	7
Figure 2-6: Types of fines including their main components, adapted [20]	9
Figure 2-7: Structural formula of lactic acid	10
Figure 2-8: Structural formula of formic acid.....	11
Figure 2-9: Structural formula of acetic acid	11
Figure 2-10: Alkaline substitution of bromoethane to ethanol [37]	12
Figure 2-11: Addition reaction of ketone and aldehyde to an aldol, adapted [39]	13
Figure 2-12: Dehydration of ethanol to ethylene, adapted [41]	13
Figure 2-13: Isomerization of one tautomer into another [43]	14
Figure 2-14: Hydrolysis of saccharose to glucose and fructose, adapted [47].....	15
Figure 2-15: Simplified way from polysaccharides to carboxylic acids	15
Figure 2-16: Some possible acids formed by the conversion of cellulose; adapted [2]	16
Figure 2-17: Hydrolysis of cellulose to glucose; adapted [2].....	16
Figure 2-18: Isomerization between glucose and fructose; adapted [2].....	17
Figure 2-19: Scheme of preferred product formation of cellulose at hydrothermal conditions under nitrogen, hydrogen or oxygen superimposed reaction atmospheres [3]	18
Figure 2-20: Supposed pathway to lactic acid [30]	19
Figure 2-21: Scheme of the transformation of glucose to formic acid under O ₂ reaction atmosphere [50].....	21
Figure 2-22: Scheme of the transformation of glucose in water catalyzed by VOSO ₄ under N ₂ and O ₂ reaction atmosphere [56].....	22
Figure 2-23: Conversion of polysaccharides to acetic acid by a two-step process [61]	24
Figure 2-24: Reaction pathway of cellulose to HMF [30]	25
Figure 2-25: Conversion step from HMF to levulinic acid and formic acid as by-product [2].....	25
Figure 2-26: Overall reaction scheme of hydrothermal conversion of lignin at up to 320°C [14]	26
Figure 2-27: Different reaction processes, modified [71]	29
Figure 3-1: Picture of the experimental setup; cycles show the valves for the liquid (green) and gas (blue) sample lines	31
Figure 3-2: Drawing of the vessels – dimensions in mm	32
Figure 3-3: Drawing of covers – dimensions in mm.....	32
Figure 3-4: Cover of the reactor with fittings	33
Figure 3-5: Experimental setup.....	33
Figure 3-6: Scheme of the experimental setup.....	35
Figure 4-1: Used substrates – A; pulp, B; black liquor, C; fines.....	41

Figure 4-2: A; opened vessel after the experiment (E33), B; separation of the remaining solids by vacuum filtration	42
Figure 5-1: HPLC system at TU Graz (ICVT)	43
Figure 5-2: Chromatogram of first and final sample of a pulp experiment, the baseline and the peaks are sketched; the red dotted line shows the baseline; the green arrows significate the evaluated acids peaks	44
Figure 5-3: A; Test tube showing precipitate after acidification and centrifugation, B; HPLC-vials ready for the analysis.....	45
Figure 5-4: Sequence used for the acidification of the samples from black liquor and lignin	46
Figure 5-5: A; mixing the tube of acidified BL with a vortex device, B; acidified BL before (left) and after (right) centrifugation	46
Figure 5-6: UV/VIS system at TU Graz (ICVT)	47
Figure 5-7: UV/VIS spectrum of initial unbleached fines sample (E31) from 220 nm to 400 nm	48
Figure 5-8: A; calibration of WTW pH522 at pH 7, B; calibration of WTW Multi. P4 at pH 10.....	49
Figure 5-9: Ceramic crucibles after drying of fines and black liquor samples	49
Figure 6-1: Fit of LA (E23) by Table Curve 2D; a: maximum concentration, b: rate constant.....	51
Figure 6-2: Linear fit to calculate the Arrhenius parameters; SPB experiments at 230°C, 200°C and 170°C in a 0.4 M Ca(OH) ₂ -solution.....	51
Figure 6-3: Yield of LA for SPB in a 0.4 M Ca(OH) ₂ -solution at varying temperature (E22, E23, E24)	52
Figure 6-4: Yield of FA (A) and AA (B) for SPB in a 0.4 M Ca(OH) ₂ -solution at varying temperature (E22, E23, E24).....	53
Figure 6-5: Total conversion (decomposition) of SPB and its total yield of acids (LA, FA, AA) at different temperatures after 2880 min (E24, E22, E23).....	55
Figure 6-6: Remains after experiments with SPB with a 0.4 M Ca(OH) ₂ -solution at 170°C (A), 200°C (B) and 230°C (C); (E22, E23, E24).....	56
Figure 6-7: Yield of LA for varying pulp types with a 0.4 M Ca(OH) ₂ -solution at 230°C (E15, E18, E19, E33).....	57
Figure 6-8: Yield of AA for varying pulp types in a 0.4 M Ca(OH) ₂ -solution at 230°C (E15, E18, E19, E33).....	58
Figure 6-9: Change of detected concentration of lignin phenolic hydroxy groups on the experimental period at 230°C (E19, E33)	58
Figure 6-10: Samples taken from softwood pulp experiment (E23); 230°C, 0.4 M Ca(OH) ₂ , 2880 min	59
Figure 6-11: Comparison of pH-value with a 0.025 M solution of Ca(OH) ₂ and NaOH at 230°C with SPB as feed (E11, E29)	60
Figure 6-12: Comparison of acid yields of SPB by using a 0.025M catalyst-solution of Ca(OH) ₂ and NaOH at 230°C (E11, E29)	60
Figure 6-13: Change of pH-value for varying concentrations of Ca(OH) ₂ and NaOH at 230°C (E11, E15, E16, E17, E21, E29)	61
Figure 6-14: Yield of LA for SPB with varying concentration of the Ca(OH) ₂ - and NaOH-solution at 230°C (E11, E15, E16, E17, E21, E29).....	62
Figure 6-15: Yield of FA (A) and AA (B) for SPB with varying concentration of the Ca(OH) ₂ - and NaOH-solution at 230°C (E11, E15, E16, E17, E21, E29).....	63
Figure 6-16: Total pressure at the end of experiments with SPB and different catalyst and concentration at 230°C	64
Figure 6-17: Formation of char during experiment E11 (A) and E29 (B)	64

Figure 6-18: Comparison of acid yields of SPB and PaB at 230°C in a 0.4M Ca(OH) ₂ -solution. The acids are differentiated by the different markers. (E15, E30)	65
Figure 6-19: Comparison of acid yields of SPB and SFB in a 0.4 M solution of Ca(OH) ₂ at 230°C (E9, E15).....	66
Figure 6-20: Comparison of acid yields of SPU and SFU in a 0.4 M solution of Ca(OH) ₂ at 230°C (E31, E33).....	67
Figure 6-21: Heat treatment of 15%w Kraft lignin at 200°C into a 0.5 M NaOH-solution (E32)	68
Figure 6-22: Results of the treatment of black liquor at 200°C and 170°C; p denotes the pressure (E27, E28)	69
Figure 6-23: Change of lignin concentration and pH-value of black liquor experiments at 170°C and 200°C (E27, E28)	70
Figure 6-24: Pictures of E28; sample taken after 540 minutes which had a very high viscosity (A), modified black liquor at the end of the experiment (B), formed char (C)	71
Figure 8-1: Datasheet of O-ring gasket	88
Figure 8-2: Material properties of O-ring gasket	88
Figure 8-3: Datasheet of dosing valves	89
Figure 8-4: Flow curve of dosing valves	90
Figure 8-5: Calculation of the maximum allowed pressure of the reactor	90
Figure 8-6: Yield of FA for varying pulp types with a 0.4 M Ca(OH) ₂ -solution at 230°C (E15, E18, E19, E33).....	92
Figure 8-7: Comparison of chromatograms of SPB (E15) and SFB (E9) at similar time. The initial solids content was very different.....	92
Figure 8-8: Samples taken at E33; At sample 6, 7 and B the catalyst is accumulated in the area below	93
Figure 8-9: Fit of the conversion of pulp at 230°C (E23) to analyzed acids by Table Curve 2D; a: minimum concentration, c: rate constant	93
Figure 8-10: Yield of the sum of formed acids for SPB with a 0.4 M Ca(OH) ₂ -solution at varying temperature (E22, E23, E24)	93
Figure 8-11: Graphical fit to calculate the Arrhenius parameters for the decomposition of SPB to the analyzed acids.....	94

8.4 List of tables

Table 2-1: Experiments for hydrothermal conversions of different raw materials to lactic acid in H ₂ O	21
Table 2-2: Experiments for hydrothermal conversions of different raw materials to formic acid	23
Table 2-3: Experiments for hydrothermal conversions of different raw materials to acetic acid.....	24
Table 2-4: Overview of the different forms of rate laws, reaction orders and the associated dimension of the reaction rate constant, adapted [70]	28
Table 3-1: Equipment limits of the experimental setup	37
Table 4-1: Experimental matrix of experiments; Sub.: Substrate, c: concentration, Temp.: temperature, Pres.: pressure, Cat.: catalyst, Atm.: reaction atmosphere, C: constant; the numbers show how often the dedicated variables were changed	39
Table 4-2: Experimental schedule; abbreviations of substrates see Table 4-3.....	40
Table 4-3: Used substrates from the pulp and paper industry	41
Table 4-4: Used chemicals	41
Table 5-1: Setup of HPLC analysis.....	43
Table 5-2: Functions of the calibration curves; y means the concentration [g·L ⁻¹] and x means the height of the respective peak	44
Table 5-3: Setup of UV/VIS analysis	47
Table 6-1: First order reaction kinetics for the decomposition of SPB to the analyzed acids including Arrhenius parameters; rate constant calculated by TableCurve (Figure 8-9)	54
Table 6-2: First order reaction kinetics for the formation of analyzed acids from SPB at 230°C, 200°C and 170°C by a 0.4 M Ca(OH) ₂ -catalyst; rate constant calculated by TableCurve (exemplary see Figure 6-1)	55
Table 6-3: Arrhenius parameter of SPB experiments for the formation of acids at 230°C, 200°C and 170°C by a 0.4 M Ca(OH) ₂ -catalyst; the corresponding linear fit is shown in Figure 6-2	55
Table 8-1: Dilutions of samples for precipitation; not listed experiments were not diluted.....	91
Table 8-2: Dosing of experiments; the compounds in the columns marked grey were mixed together, forming the feed mixture.	91
Table 8-3: Calculated formation of non-analyzed substances	94
Table 8-4: Experiments setup and results	95
Table 8-5: Calculation of mean reaction rate of E22, E23 and E24; the calculation was done by the quotient of the difference of concentrations to time - $r = \Delta c \Delta t$	107

8.5 Supplementary data

8.5.1 Experimental setup



DATENBLATT

FFKM 78 – Qualität für Präzision O-Ringe

09/2015

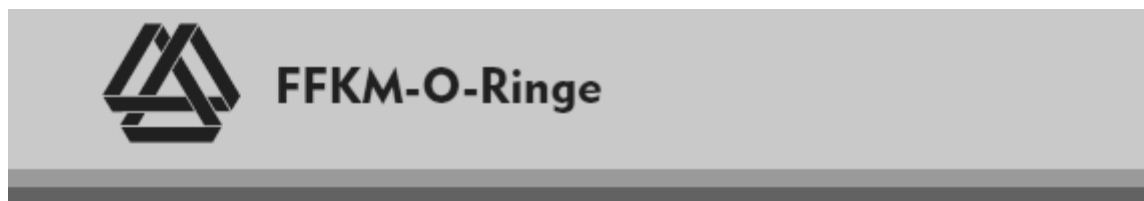
Hennlich Nr.	HZ-169-FFKM		
Farbe	schwarz		
Einsatztemperatur	von -25°C bis +270 °C (kurzzeitig +300°C)		
Gummitechnologische Werte			
<i>Eigenschaften</i>	<i>Einheit</i>	<i>Wert</i>	<i>Prüfmethode</i>
Härte	Shore A	78±5	ASTM D 2240
Spezifisches Gewicht	g/cm ³	1,98±0,04	ASTM D1817
Zugfestigkeit	MPa	18	ASTM D 412
Bruchdehnung	%	145	ASTM D 412
Druckverformungsrest (70 h / 200° C)	%	18,5	ASTM D 395 B/1
TR-10	°C	-4	ASTM D 1329

Beschreibung:

Perfluorelastomere sind zurzeit die chemisch beständigsten Elastomere, welche die elastischen Eigenschaften von Kautschuk mit der hervorragenden chemischen Resistenz und Hitzebeständigkeit von PTFE verbinden. Als Hochleistungselastomer verfügt FFKM neben hervorragender Temperaturbeständigkeit und chemischer Resistenz über relativ hohe Reinheit und verbleibende Dichtwirkung. Zur Anwendung kommt es in Bereichen, in denen andere Elastomerwerkstoffe ihre Grenzen erreichen und höchste Zuverlässigkeit gefragt ist.

Diese Daten sind Richtwerte. Form, Herstellung und konkrete Beanspruchung können zu Veränderung führen.

Figure 8-1: Datasheet of O-ring gasket



Perfluorelastomere (FFKM)

sind Terpolymere bestehend aus Tetrafluorethylen (TFE), Perfluormethylvinylether (PMVE) und einem Vernetzungsmonomer (Cure Site Monomer = CSM).

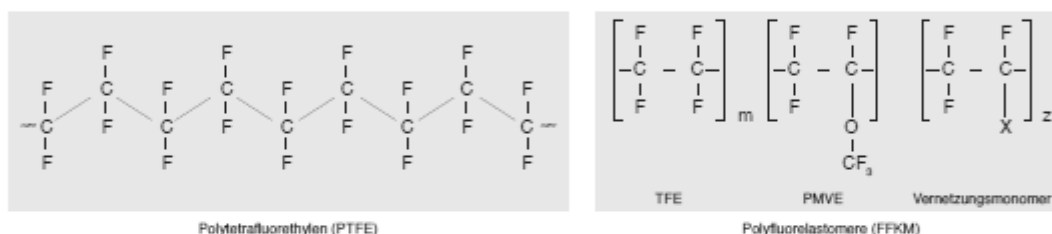
Tetrafluorethylen (TFE) sorgt als Basismonomer für die chemische Beständigkeit, während die elastischen Eigenschaften durch die Vernetzung mit PMVE sowie mit dem perfluorierten Vernetzungsmonomeren (CSM) erzielt werden.

In Perfluorelastomeren wurden sämtliche Wasserstoffatome der Monomere durch Fluoratome ersetzt, welche die Kohlenstoffpolymerkette gegen äußere Einflüsse schützen.

Fluorierte Elastomere sind stabiler als Kohlenwasserstoff-Elastomere (wie z.B. NBR oder EPDM). Aufgrund der höheren Bindungen zwischen Fluor und Kohlenstoff im Vergleich zu Wasserstoff und Kohlenstoff.

Die Molekularstruktur von Perfluorelastomeren ähnelt somit der von Polytetrafluorethylen-Harz (PTFE) und steht für hervorragende Wärmestabilität und Chemikalienbeständigkeit. Gleichzeitig besitzen Perfluorelastomere aber auch die Elastizität (das Rückstellvermögen) und die Dichteigenschaft eines Elastomers.

Aufbau eines PTFE- und eines FFKM-Werkstoffes:



Polyfluorelastomere bieten Ihnen eine Vielzahl von Vorteilen:

- Zuverlässigkeit
- lang anhaltende Dichtungskraft
- niedrige Durchlässigkeit
- Hochtemperaturstabilität (bis zu 330 °C)
- umfangreiche chemische Beständigkeit
- Flexibilität bei der Anwendung
- niedriger Druckverformungsrest
- ausgezeichnetes Vakuumverhalten
- lange Lebensdauer
- Kosteneffektivität

FFKM ist vielseitig

Eine Standardisierung ist ohne Verwechslungsrisiko zwischen ähnlich aussehenden Teilen möglich. Ihr Lagerungsbedarf wird niedrig gehalten und der Einkauf vereinfacht. Bei manchen Anwendungen (Transport von Chemikalien) besteht die Möglichkeit, dass eine einzige Dichtung verschiedenen aggressiven Chemikalien ausgesetzt wird und natürlich auch Dampf und heißem Wasser während des Reinigungsvorgang. Dann kann ein Universal-O-Ring unerlässlich sein.

Die folgenden Chemikalien stellen einige der aggressiven Medien dar, in denen die hervorragenden Eigenschaften von FFKM voll zum Tragen kommen:

- | | | |
|-------------------------------|-------------------------------|---------------------------------------|
| • organische Säuren | • Öle | • Ethylen/Propylenoxid |
| • anorganische Säuren | • Heterozyklische Werkstoffe | • Plasma |
| • Alkohole, Glykole, Glycerin | • Halogenierte Werkstoffe | • Amine, organische Basen |
| • Aldehyd, Ketone | • starke Oxidationsmittel* | • Heißwasser, Dampf |
| • Ester, Anhydride | • Alkalis, anorganische Basen | • Kohlenwasserstoffe (Hydrocarbonate) |
| • Ather, Epoxide | • HF (Fluorwasserstoffsäure) | aliphatisch, aromatisch |

* Starke Oxidationsmittel (z.B. Salpetersäure) greifen Kohlenstoffe, das normalerweise als verstärkender Füllstoff in Gummierwerkstoffen verwendet wird an. Bei Einsätzen in starken Oxidationsmitteln empfehlen wir kohlenstofffreie Spezialfüllstoffe, die die hervorragende Funktionstfähigkeit der FFKM-Qualitäten optimieren.

Allgemeine Sicherheitshinweise

FFKM ist auf keinen Fall für den Einsatz in medizinischen oder zahnärztlichen Implantaten geeignet. FFKM ist nicht entflammbar, jedoch werden im Falle einer thermischen Zersetzung hochgiftige und korrodierende Gase, HF (Fluorwasserstoffsäure) und COF_2 (Karbonylfluorid) freigesetzt.

FFKM darf nie in der Nähe von geschmolzenen oder gasförmigen Alkalimetallen (Kalzium, Lithium, Magnesium, Kalium, Natrium, etc.) verwendet werden, da eine explosive Reaktion erfolgen könnte. Dies gilt übrigens für alle Polymere.

Figure 8-2: Material properties of O-ring gasket



Milli-Mite® 1300 Serie

Dosierventil



Anwendungen

- Feines Dosieren in medizinischen und biochemischen Gasanalysen
- Für Chromatographen, Massenspektrometer und anderen Instrumenten
- Dosieren von Gas- und Flüssigkeitsmischungen

Technical Data

KÖRPER*	316 Edelstahl, Messing
MAXIMALER BETRIEBSDRUCK @ 70°F (21°C)	Messing 3000 psig (207 bar)
	316 Edelstahl 5000 psig (345 bar)
TEMPERATURBEREICH	Messing -65 bis 400°F (-54° bis 204°C)
	316 Edelstahl -65° bis 450°F (-54° bis 232°C)
BOHRUNG	.047" (1.19 mm)
CV FAKTOR	1" Spindelspitze = .010 Cv 3" Spindelspitze = .024 Cv

* Einsatz anderer Materialien, wenden Sie sich an Ihre HOKE Vertretung

Eigenschaften & Merkmale

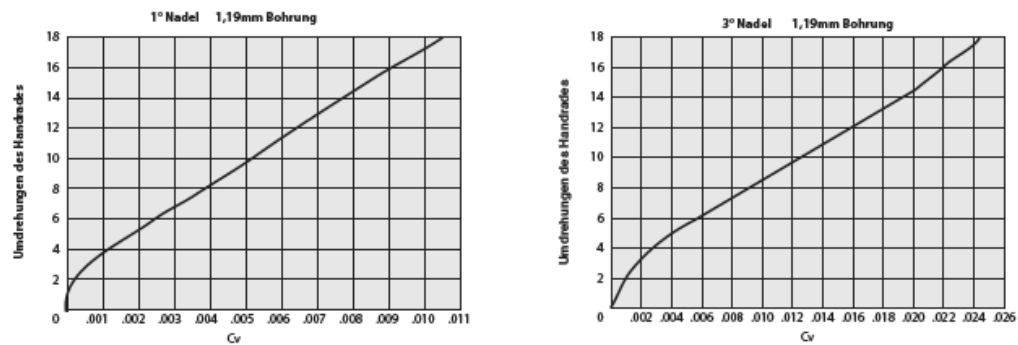
- Genaues Dosieren (kleine Sitzbohrung) bei einem Gesamtweg der Nadel von 18 Umdrehungen des Handrades
- 1° und 3° Nadelspitze gewährleisten eine ausgezeichnete Dosiergenauigkeit
- Schalttafeleinbau bei allen Ventilen standardmäßig
- Präzision des Ventilsitzes und enge Toleranzen des Spindelgewindes minimieren die Hysterese des Ventils
- Mikrometerhandrad erlaubt eine sichtbare Kontrolle und präzises Einstellen des Ventils
- Dyna-Pak® Packung unterhalb dem Spindelgewinde, verhindert Verschmutzung durch das Medium und Auswaschen der Spindelschmierung
- Für Fernsteuerung sind elekt. Antriebe auf Anfrage erhältlich

Dosierventile

Figure 8-3: Datasheet of dosing valves

Milli-Mite® 1300 Serie

Durchflusskurve



Bestellangaben

VENTILFORM	ABMESSUNGEN		BESTELLNUMMER			
	A EINGANG	B AUSGANG	316 EDELSTAHLVENTIL		MESSINGVENTIL	
			1°Nadel Cv=0.010	3°Nadel Cv=0.024	1°Nadel Cv=0.010	3°Nadel Cv=0.024
GERADE	1/4" NPT Innen	1/4" NPT Innen	—	1315F2Y	—	—
	1/4" NPT Außen	1/4" Gyrolok*	—	—	1335H2B	1315H2B
	1/8" NPT Außen	1/8" NPT Außen	—	—	1335M2B	1315M2B
	1/4" NPT Außen	1/4" NPT Außen	1335M4Y	1315M4Y	1335M4B	1315M4B
	1/4" Gyrolok*	1/4" Gyrolok*	1335G2Y	1315G2Y	1335G2B	1315G2B
	1/4" Gyrolok*	1/4" Gyrolok*	1335G4Y	1315G4Y	1335G4B	1315G4B
	3mm Gyrolok*	3mm Gyrolok*	1335G3YMM	1315G3YMM	—	—
6mm Gyrolok*	6mm Gyrolok*	1335G6YMM	1315G6YMM	—	—	
ECK	1/4" NPT Innen	1/4" NPT Innen	—	—	1345F2B	1325F2B
	1/4" NPT Außen	1/4" Gyrolok*	1345H2Y	1325H2Y	1345H2B	1325H2B
	1/4" Gyrolok*	1/4" Gyrolok*	1345G2Y	1325G2Y	1345G2B	1325G2B
	1/4" Gyrolok*	1/4" Gyrolok*	1345G4Y	1325G4Y	1345G4B	1325G4B
	3mm Gyrolok*	3mm Gyrolok*	1345G3YMM	1325G3YMM	—	—
	6mm Gyrolok*	6mm Gyrolok*	1345G6YMM	1325G6YMM	1345G6MM	1325G6MM
	1/8" NPT Innen	1/8" NPT Innen	—	—	1345F2B	—

Figure 8-4: Flow curve of dosing valves

Calculation pressure vessel			
σ _a	Allowed tensile stress (Rp0,2)	108 N/mm ²	for 1.4307 @ 250°C
D _o	Outside diameter of the vessel	107 mm	
D _i	Inside diameter of the vessel	87 mm	
c	Safety factor	1,2	
D _m	Mean diameter	97 mm	$p_{max} = \frac{2 * s_{min} * \frac{\sigma_a}{c}}{d_m}$
s _{min}	Minimum wall thickness	10 mm	
p _{max}	Maximum allowed pressure	18,56 N/mm ²	
		18556701,03 Pa	
		185,57 bar	
Calculation screws			
σ _a	Tensile stress area	58 mm ²	M10, nominal grade 8.8
D _i	Inside diameter of the vessel	87 mm	
n	Number of screws	8	
c	Safety factor	1,2	
			$F_a = \frac{\sigma_a}{c} * A_\sigma$
σ _a	Allowed tensile stress (Rp0,2)	510 N/mm ²	
F _a	Allowed force per screw	24650 N	
A _p	Projected area where pressuer acts	5944,6787 mm ²	
		0,0059 m ²	$p_{max} = \frac{F_a * n}{A_p}$
p _{max}	Maximum allowed pressure	33172524,54 Pa	
		331,73 bar	

Figure 8-5: Calculation of the maximum allowed pressure of the reactor

8.5.2 Analysis

Table 8-1: Dilutions of samples for precipitation; not listed experiments were not diluted

Experiment	Amount of H ₂ SO ₄ -solution [mL]	Overall amount [mL]	Dilution factor
E6, E7	0.030	3.0	1.010
E3	1.500	3.0	1.500
E10	0.150	3.0	1.050
E8, E9	0.012	1.2	1.010
E11, E12	0.015	1.5	1.010
E14, E15, E16, E18, E19, E20, E21, E22, E24, E29, E30, E31, E33	0.010	1.5	1.007
E17, E23	0.100	1.5	1.067
E26, E27, E28, E32	2.500	4.5	1.556

8.5.3 Procedure

Table 8-2: Dosing of experiments; the compounds in the columns marked grey were mixed together, forming the feed mixture.

#	Sub.	Ratio of dry sub. [%w]	Sub. added [g]	Water added [ml]	Cat.	Cat. concentration [mol·l ⁻¹]	Cat. added [g]	Experiments
1	SPB	2.0	36.96	500	Ca(OH) ₂	0.400	15.94	E1, E2
2	SPB	2.1	46.57	600	Ca(OH) ₂	0.400	19.18	E4
3	SPU	1.7	28.20	600	Ca(OH) ₂	0.400	18.69	E5
4	SPU	4.0	66.35	600	Ca(OH) ₂	0.400	19.43	E6
5	SPB	4.0	87.23	590	Ca(OH) ₂	0.400	19.77	E7
6	SFU	3.7	598.80	0	Ca(OH) ₂	0.400	17.47	E8
7	SFB	1.4	499.00	0	Ca(OH) ₂	0.400	14.91	E9
8	SPB	4.0	88.71	600	Ca(OH) ₂	0.025	1.26	E11, E12, E13
9	SPB	4.0	88.71	600	Ca(OH) ₂	0.400	20.11	E14, E15, E22, E23, E24
10	SPB	4.0	88.71	600	Ca(OH) ₂	0.200	10.05	E16
11	SPB	4.0	88.71	600	NaOH	2.000	54.27	E17
12	HPB	4.0	97.76	600	Ca(OH) ₂	0.400	20.38	E18
13	HPU	4.0	80.11	600	Ca(OH) ₂	0.400	19.85	E19
14	SPU	4.0	66.35	600	Ca(OH) ₂	0.400	19.43	E20, E33
15	SPB	4.0	88.71	600	NaOH	0.400	10.85	E21
16	SPB	4.0	88.71	600	NaOH	0.025	0.68	E29
17	SFU	0.86	548.90	0	Ca(OH) ₂	0.400	16.50	E31
18	PB	4.0	23.95	600	Ca(OH) ₂	0.400	18.15	E30
19	L	15.0	89.82	600	NaOH	0.500	12.24	E32

8.5.4 Results

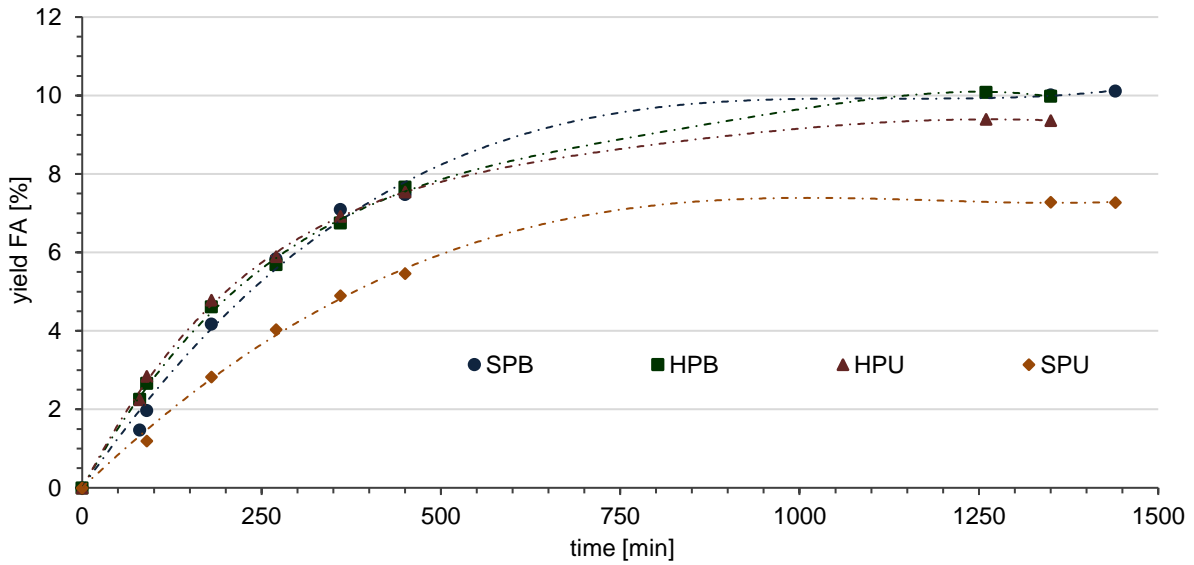


Figure 8-6: Yield of FA for varying pulp types with a 0.4 M Ca(OH)₂-solution at 230°C (E15, E18, E19, E33)

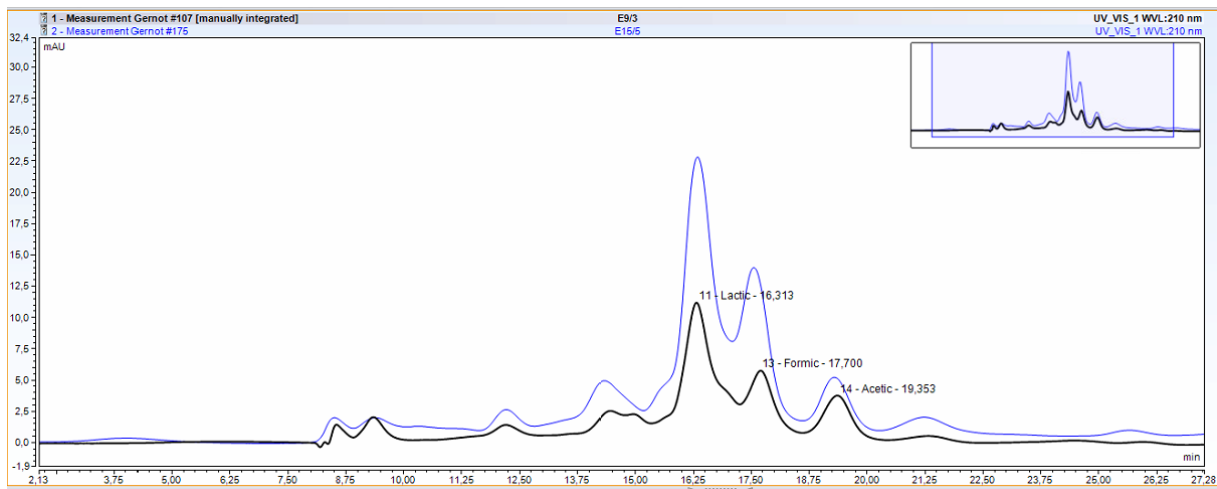


Figure 8-7: Comparison of chromatograms of SPB (E15) and SFB (E9) at similar time. The initial solids content was very different.

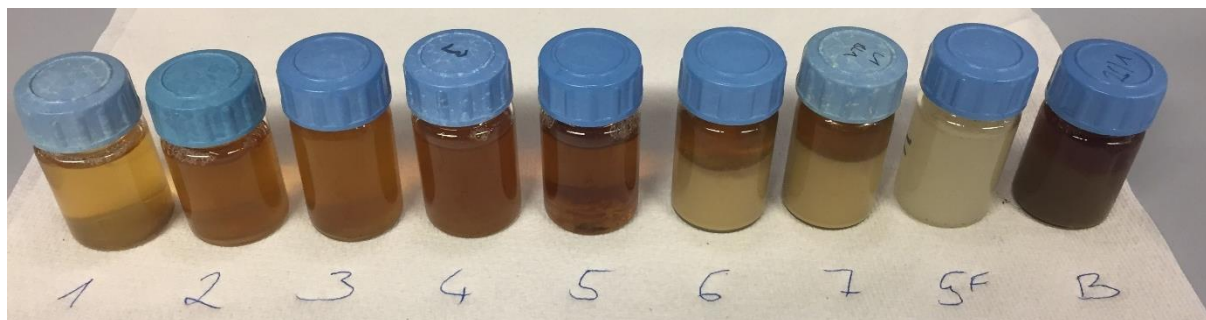


Figure 8-8: Samples taken at E33; At sample 6, 7 and B the catalyst is accumulated in the area below

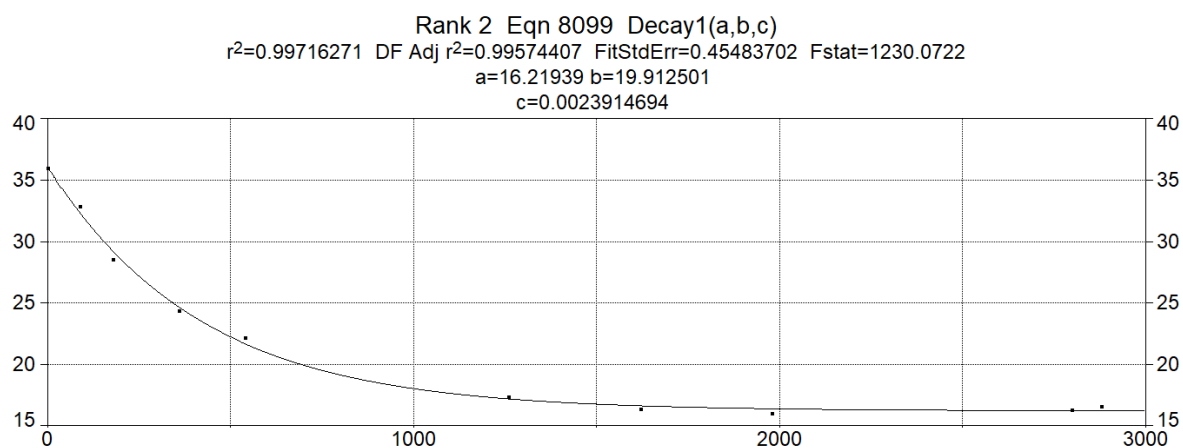


Figure 8-9: Fit of the conversion of pulp at 230°C (E23) to analyzed acids by Table Curve 2D;
a: minimum concentration, c: rate constant

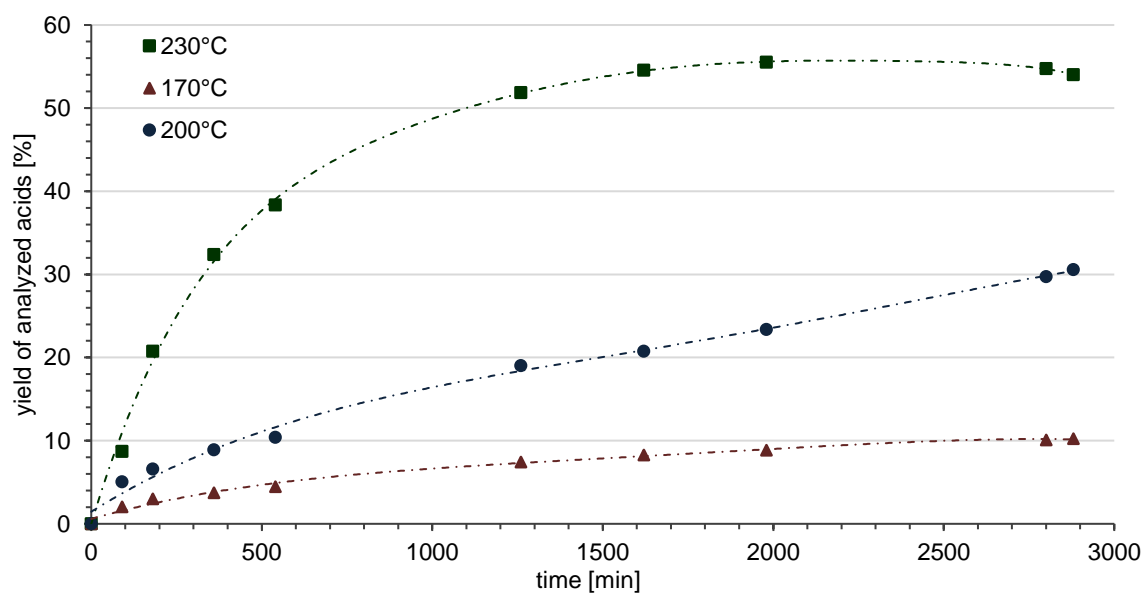


Figure 8-10: Yield of the sum of formed acids for SPB with a 0.4 M $\text{Ca}(\text{OH})_2$ -solution at varying temperature (E22, E23, E24)

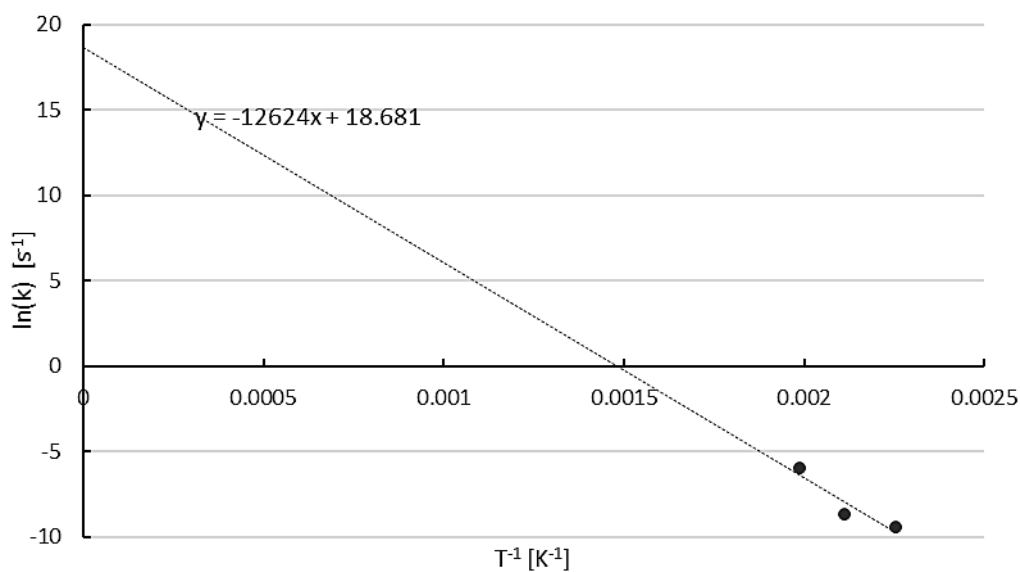


Figure 8-11: Graphical fit to calculate the Arrhenius parameters for the decomposition of SPB to the analyzed acids

Table 8-3: Calculated formation of non-analyzed substances

	E23_230°C	E22_200°C	E24_170°C
Initial pulp [g·L ⁻¹]	36.02	36.02	36.02
Total acids [g·L ⁻¹]	20.00	11.01	3.69
Total conversion	100%	60%	25%
Degraded pulp [g·L ⁻¹]	36.02	21.61	9.01
Other substances [g·L ⁻¹]	16.02	10.61	5.31
Other substances	44%	49%	59%

Table 8-4: Experiments setup and results

Nr.	Properties				Mixture				Parameters			Analysis								Note	
	Sub.	DS [%]	Cat.	c [M]	Liq-uid [mL]	#	Sub. [w%]	m _{Sub} dry [g]	Time [min]	Temp. [°C]	p [bar]	pH	LA [g·L ⁻¹]	m _{LA} /m _{Sub} [%]	FA [g·L ⁻¹]	g _{FA} /g _{Sub} [%]	AA [g·L ⁻¹]	g _{AA} /g _{Sub} [%]	Lignin [g·L ⁻¹]		m Sub. [g]
E1	1	SPB	26.7	Ca(OH) ₂	0.400	528	1	2	9.98	0	75	0	12.64	0.00	0.00	0.00	0.00	0.00	0.00	-	-
E1	2	SPB	26.7	Ca(OH) ₂	0.400	528	1	2	9.98	28	121	1	12.42	0.00	0.00	0.00	0.00	0.00	0.00	-	-
E1	3	SPB	26.7	Ca(OH) ₂	0.400	528	1	2	9.98	55	154	5	12.21	0.04	0.22	0.03	0.16	0.00	0.00	-	-
E1	4	SPB	26.7	Ca(OH) ₂	0.400	528	1	2	9.98	70	170	7	12.09	0.07	0.36	0.04	0.22	0.00	0.00	-	-
E1	5	SPB	26.7	Ca(OH) ₂	0.400	528	1	2	9.98	78	170	8	12.01	0.07	0.37	0.04	0.19	0.00	0.00	-	-
E1	6	SPB	26.7	Ca(OH) ₂	0.400	528	1	2	9.98	92	170	8	11.94	0.12	0.62	0.06	0.34	0.00	0.00	-	-
E1	7	SPB	26.7	Ca(OH) ₂	0.400	528	1	2	9.98	108	170	8	11.94	0.15	0.81	0.08	0.43	0.00	0.00	-	-
E1	8	SPB	26.7	Ca(OH) ₂	0.400	528	1	2	9.98	123	170	8	11.91	0.17	0.90	0.09	0.49	0.00	0.00	-	-
E2	1	SPB	26.7	Ca(OH) ₂	0.400	528	1	2	9.98	0	75	0	12.67	0.00	0.00	0.00	0.00	0.00	0.00	-	-
E2	2	SPB	26.7	Ca(OH) ₂	0.400	528	1	2	9.98	28	128	2	12.47	0.00	0.00	0.00	0.00	0.00	0.00	-	-
E2	3	SPB	26.7	Ca(OH) ₂	0.400	528	1	2	9.98	55	158	5	12.24	0.02	0.11	0.01	0.07	0.00	0.00	-	-
E2	4	SPB	26.7	Ca(OH) ₂	0.400	528	1	2	9.98	71	170	7	12.08	0.06	0.32	0.04	0.19	0.00	0.00	-	-
E2	5	SPB	26.7	Ca(OH) ₂	0.400	528	1	2	9.98	88	170	8	11.97	0.11	0.58	0.06	0.31	0.00	0.00	-	-
E2	6	SPB	26.7	Ca(OH) ₂	0.400	528	1	2	9.98	104	170	8	11.95	0.12	0.62	0.06	0.32	0.00	0.00	-	-
E2	7	SPB	26.7	Ca(OH) ₂	0.400	528	1	2	9.98	117	170	8	11.95	0.14	0.72	0.07	0.35	0.00	0.00	-	-
E2	8	SPB	26.7	Ca(OH) ₂	0.400	528	1	2	9.98	132	170	8	11.95	0.15	0.81	0.08	0.41	0.00	0.00	-	-
E3	1	BL	16.2	-	-	600	-	-	-	0	20.5	0	12.76	7.26	-	7.02	-	6.39	-	-	-
E3	2	BL	16.2	-	-	600	-	-	-	60	200	15	12.60	7.92	-	7.43	-	6.41	-	-	-
E3	3	BL	16.2	-	-	600	-	-	-	90	200	15	12.43	7.87	-	7.38	-	6.45	-	-	-
E3	4	BL	16.2	-	-	600	-	-	-	120	200	15	12.27	7.76	-	7.40	-	6.70	-	-	-
E3	5	BL	16.2	-	-	600	-	-	-	150	200	15	12.17	8.23	-	7.66	-	6.73	-	-	-
E3	6	BL	16.2	-	-	600	-	-	-	180	200	15	12.14	8.65	-	7.94	-	7.04	-	-	-
E3	7	BL	16.2	-	-	600	-	-	-	240	200	15	12.09	8.29	-	7.72	-	6.88	-	-	-
E3	8	BL	16.2	-	-	600	-	-	-	300	200	15	12.04	8.35	-	7.93	-	7.10	-	-	-
E3	9	BL	16.2	-	-	600	-	-	-	330	200	15	12.00	8.76	-	8.15	-	7.65	-	-	-

Nr.	Properties				Mixture				Parameters			Analysis								Note	
	Sub.	DS [%]	Cat.	c [M]	Liq-uid [mL]	#	Sub. [w%]	m _{Sub} dry [g]	Time [min]	Temp. [°C]	p [bar]	pH	LA [g·L ⁻¹]	m _{LA} /m _{Sub} [%]	FA [g·L ⁻¹]	g _{FA} /g _{Sub} [%]	AA [g·L ⁻¹]	g _{AA} /g _{Sub} [%]	Lignin [g·L ⁻¹]		m Sub. [g]
E3	10	BL	16.2	-	-	600	-	-	-	360	200	15	11.94	8.71	-	8.29	-	7.67	-	-	-
E4	1	SPB	26.7	Ca(OH) ₂	0.400	635	2	2.1	12.57	0	25	0	12.44	0.00	0.00	0.00	0.00	0.00	0.00	-	-
E4	2	SPB	26.7	Ca(OH) ₂	0.400	635	2	2.1	12.57	55	200	16	10.85	0.30	1.50	0.12	0.60	0.10	0.52	-	-
E4	3	SPB	26.7	Ca(OH) ₂	0.400	635	2	2.1	12.57	85	200	16	11.66	0.54	2.70	0.21	1.05	0.19	0.98	-	-
E4	4	SPB	26.7	Ca(OH) ₂	0.400	635	2	2.1	12.57	115	200	16	11.54	0.64	3.24	0.26	1.30	0.25	1.25	-	-
E4	5	SPB	26.7	Ca(OH) ₂	0.400	635	2	2.1	12.57	145	200	16	11.53	0.70	3.52	0.28	1.43	0.27	1.37	-	-
E4	6	SPB	26.7	Ca(OH) ₂	0.400	635	2	2.1	12.57	175	200	16	11.51	0.76	3.86	0.31	1.59	0.30	1.53	-	-
E4	7	SPB	26.7	Ca(OH) ₂	0.400	635	2	2.1	12.57	205	200	16	11.51	0.78	3.94	0.33	1.69	0.32	1.61	-	-
E4	8	SPB	26.7	Ca(OH) ₂	0.400	635	2	2.1	12.57	235	200	16	11.57	0.86	4.36	0.36	1.79	0.33	1.69	-	-
E4	9	SPB	26.7	Ca(OH) ₂	0.400	635	2	2.1	12.57	265	200	16	11.53	0.87	4.41	0.36	1.84	0.35	1.76	-	-
E4	10	SPB	26.7	Ca(OH) ₂	0.400	635	2	2.1	12.57	295	200	16	11.51	0.94	4.73	0.39	1.96	0.36	1.84	-	-
E5	1	SPU	36.6	Ca(OH) ₂	0.400	618	3	1.7	10.18	0	19.8	0	12.51	0.00	0.00	0.00	0.00	0.00	0.00	-	-
E5	2	SPU	36.6	Ca(OH) ₂	0.400	618	3	1.7	10.18	55	200	16	11.43	0.08	0.49	0.03	0.19	0.00	0.00	-	-
E5	3	SPU	36.6	Ca(OH) ₂	0.400	618	3	1.7	10.18	85	200	16	11.90	0.26	1.58	0.09	0.57	0.09	0.55	-	-
E5	4	SPU	36.6	Ca(OH) ₂	0.400	618	3	1.7	10.18	115	200	16	11.86	0.37	2.23	0.13	0.77	0.13	0.78	-	-
E5	5	SPU	36.6	Ca(OH) ₂	0.400	618	3	1.7	10.18	145	200	16	12.05	0.44	2.64	0.15	0.92	0.15	0.94	-	-
E5	6	SPU	36.6	Ca(OH) ₂	0.400	618	3	1.7	10.18	175	200	16	12.09	0.50	3.04	0.18	1.08	0.18	1.11	-	-
E5	7	SPU	36.6	Ca(OH) ₂	0.400	618	3	1.7	10.18	205	200	16	12.07	0.61	3.69	0.21	1.27	0.21	1.27	-	-
E5	8	SPU	36.6	Ca(OH) ₂	0.400	618	3	1.7	10.18	235	200	16	12.12	0.63	3.80	0.23	1.37	0.25	1.50	-	-
E5	9	SPU	36.6	Ca(OH) ₂	0.400	618	3	1.7	10.18	265	200	16	12.12	0.68	4.12	0.25	1.50	0.25	1.54	-	-
E5	10	SPU	36.6	Ca(OH) ₂	0.400	618	3	1.7	10.18	295	200	16	11.88	0.73	4.45	0.27	1.63	0.28	1.68	-	-
E6	1	SPU	36.6	Ca(OH) ₂	0.400	642	4	4	23.95	0	21.2	0	12.49	0.00	0.00	0.00	0.00	0.00	0.00	-	-
E6	2	SPU	36.6	Ca(OH) ₂	0.400	642	4	4	23.95	80	230	29	11.36	0.68	1.81	0.26	0.69	0.25	0.66	-	-
E6	3	SPU	36.6	Ca(OH) ₂	0.400	642	4	4	23.95	110	230	30	11.24	1.23	3.30	0.47	1.26	0.45	1.19	-	-
E6	4	SPU	36.6	Ca(OH) ₂	0.400	642	4	4	23.95	140	230	29	11.35	1.56	4.17	0.59	1.58	0.52	1.39	-	-
E6	5	SPU	36.6	Ca(OH) ₂	0.400	642	4	4	23.95	170	230	29	11.23	1.86	4.99	0.71	1.89	0.59	1.58	-	-

Nr.	Properties				Mixture				Parameters			Analysis								Note	
	Sub.	DS [%]	Cat.	c [M]	Liq-uid [mL]	#	Sub. [w%]	m _{Sub} dry [g]	Time [min]	Temp. [°C]	p [bar]	pH	LA [g·L ⁻¹]	m _{LA} /m _{Sub} [%]	FA [g·L ⁻¹]	g _{FA} /g _{Sub} [%]	AA [g·L ⁻¹]	g _{AA} /g _{Sub} [%]	Lignin [g·L ⁻¹]		m Sub. [g]
E6	6	SPU	36.6	Ca(OH) ₂	0.400	642	4	4	23.95	200	230	29	11.24	2.05	5.49	0.78	2.08	0.63	1.70	-	-
E6	7	SPU	36.6	Ca(OH) ₂	0.400	642	4	4	23.95	230	230	29	12.02	2.33	6.25	0.88	2.36	0.71	1.91	-	-
E6	8	SPU	36.6	Ca(OH) ₂	0.400	642	4	4	23.95	260	230	29	11.88	2.67	7.15	1.00	2.68	0.81	2.16	-	-
E6	9	SPU	36.6	Ca(OH) ₂	0.400	642	4	4	23.95	290	230	29	11.76	2.82	7.54	1.03	2.76	0.78	2.09	-	-
E6	10	SPU	36.6	Ca(OH) ₂	0.400	642	4	4	23.95	320	230	29	11.72	3.12	8.37	1.16	3.10	0.92	2.46	-	-
E7	1	SPB	26.7	Ca(OH) ₂	0.400	655	5	4	23.55	25	100	1	12.09	0.14	0.39	0.08	0.22	0.00	0.00	-	-
E7	2	SPB	26.7	Ca(OH) ₂	0.400	655	5	4	23.55	75	230	29	10.87	1.22	3.39	0.55	1.54	0.45	1.24	-	-
E7	3	SPB	26.7	Ca(OH) ₂	0.400	655	5	4	23.55	105	230	29	10.56	2.12	5.89	0.94	2.62	0.76	2.11	-	-
E7	4	SPB	26.7	Ca(OH) ₂	0.400	655	5	4	23.55	135	230	29	10.72	2.73	7.59	1.19	3.30	0.93	2.58	-	-
E7	5	SPB	26.7	Ca(OH) ₂	0.400	655	5	4	23.55	165	230	29	10.78	3.25	9.04	1.38	3.84	1.04	2.89	-	-
E7	6	SPB	26.7	Ca(OH) ₂	0.400	655	5	4	23.55	195	230	29	10.93	3.72	10.36	1.56	4.35	1.18	3.28	-	-
E7	7	SPB	26.7	Ca(OH) ₂	0.400	655	5	4	23.55	225	230	29	11.03	4.11	11.43	1.67	4.65	1.14	3.18	-	-
E7	8	SPB	26.7	Ca(OH) ₂	0.400	655	5	4	23.55	255	230	29	11.14	4.54	12.63	1.81	5.04	1.23	3.43	-	-
E7	9	SPB	26.7	Ca(OH) ₂	0.400	655	5	4	23.55	285	230	29	11.23	4.97	13.83	1.95	5.43	1.32	3.68	-	-
E7	10	SPB	26.7	Ca(OH) ₂	0.400	655	5	4	23.55	315	230	29	11.41	5.63	15.65	2.19	6.10	1.55	4.31	-	-
E8	0	SFU	3.7	Ca(OH) ₂	0.400	578	6	3.7	22.22	0	25	1	12.15	0.00	0.00	0.00	0.00	0.00	0.00	-	-
E8	1	SFU	3.7	Ca(OH) ₂	0.400	578	6	3.7	22.22	25	100	1	12.15	0.54	1.40	0.36	0.93	0.32	0.83	-	-
E8	2	SFU	3.7	Ca(OH) ₂	0.400	578	6	3.7	22.22	75	230	29	9.51	1.54	4.01	0.58	1.51	0.41	1.07	-	-
E8	3	SFU	3.7	Ca(OH) ₂	0.400	578	6	3.7	22.22	105	230	29	11.64	2.45	6.38	0.89	2.30	0.71	1.84	-	-
E8	4	SFU	3.7	Ca(OH) ₂	0.400	578	6	3.7	22.22	135	230	29	11.40	3.14	8.17	1.10	2.87	0.87	2.25	-	-
E8	5	SFU	3.7	Ca(OH) ₂	0.400	578	6	3.7	22.22	165	230	29	12.33	3.70	9.61	1.25	3.25	0.93	2.43	-	-
E8	6	SFU	3.7	Ca(OH) ₂	0.400	578	6	3.7	22.22	195	230	29	12.32	4.31	11.20	1.45	3.77	1.10	2.87	-	-
E8	7	SFU	3.7	Ca(OH) ₂	0.400	578	6	3.7	22.22	225	230	29	12.26	4.82	12.52	1.62	4.21	1.28	3.32	-	-
E8	8	SFU	3.7	Ca(OH) ₂	0.400	578	6	3.7	22.22	255	230	29	12.11	5.32	13.84	1.76	4.59	1.40	3.63	-	-
E8	9	SFU	3.7	Ca(OH) ₂	0.400	578	6	3.7	22.22	285	230	29	11.92	5.82	15.14	1.89	4.92	1.48	3.84	-	-
E8	10	SFU	3.7	Ca(OH) ₂	0.400	578	6	3.7	22.22	315	230	29	11.48	6.28	16.34	2.01	5.23	1.56	4.06	-	-

Nr.	Properties				Mixture				Parameters			Analysis								Note	
	Sub.	DS [%]	Cat.	c [M]	Liq-uid [mL]	#	Sub. [w%]	m _{Sub} dry [g]	Time [min]	Temp. [°C]	p [bar]	pH	LA [g·L ⁻¹]	m _{LA} /m _{Sub} [%]	FA [g·L ⁻¹]	g _{FA} /g _{Sub} [%]	AA [g·L ⁻¹]	g _{AA} /g _{Sub} [%]	Lignin [g·L ⁻¹]		m Sub. [g]
E8	11	SFU	3.7	Ca(OH) ₂	0.400	578	6	3.7	22.22	345	230	29	11.87	6.73	17.51	2.13	5.53	1.66	4.32	-	-
E8	12	SFU	3.7	Ca(OH) ₂	0.400	578	6	3.7	22.22	375	230	29	11.86	7.11	18.48	2.20	5.73	1.72	4.47	-	-
E9	0	SFB	1.4	Ca(OH) ₂	0.400	493	7	1.4	6.99	0	25	1	12.42	0.00	0.00	0.00	0.00	0.59	4.17	-	-
E9	1	SFB	1.4	Ca(OH) ₂	0.400	493	7	1.4	6.99	25	100	1	12.42	0.37	2.58	0.21	1.45	0.62	4.38	-	-
E9	2	SFB	1.4	Ca(OH) ₂	0.400	493	7	1.4	6.99	70	230	29	11.80	0.90	6.38	0.43	3.04	0.76	5.34	-	-
E9	3	SFB	1.4	Ca(OH) ₂	0.400	493	7	1.4	6.99	345	230	29	12.38	2.98	20.99	1.09	7.72	1.27	8.92	-	-
E10	1	BL	16.2	-	-	650	-	-	-	0	22	0	13.07	7.29	-	7.32	-	6.15	-	-	-
E10	2	BL	16.2	-	-	650	-	-	-	75	230	29	12.57	8.44	-	7.91	-	6.48	-	-	-
E10	3	BL	16.2	-	-	650	-	-	-	135	230	31	12.04	8.94	-	8.02	-	7.01	-	-	-
E10	4	BL	16.2	-	-	650	-	-	-	195	230	31	11.82	9.61	-	8.38	-	7.33	-	-	-
E10	5	BL	16.2	-	-	650	-	-	-	255	230	31	11.73	14.89	-	11.48	-	10.93	-	-	-
E10	6	BL	16.2	-	-	650	-	-	-	315	230	31	11.65	18.39	-	13.22	-	13.12	-	-	-
E10	7	BL	16.2	-	-	650	-	-	-	375	230	31	11.58	20.79	-	14.31	-	14.51	-	-	-
E11	0	SPB	26.7	Ca(OH) ₂	0.025	665	8	4	23.95	0	25	1	12.55	0.00	0.00	0.00	0.00	0.00	0.00	-	-
E11	1	SPB	26.7	Ca(OH) ₂	0.025	665	8	4	23.95	80	230	29	6.91	0.73	2.03	0.36	0.99	0.24	0.67	-	-
E11	2	SPB	26.7	Ca(OH) ₂	0.025	665	8	4	23.95	90	230	30	5.44	1.03	2.87	0.61	1.71	0.49	1.35	-	-
E11	3	SPB	26.7	Ca(OH) ₂	0.025	665	8	4	23.95	180	230	34	3.75	2.64	7.33	1.94	5.37	1.47	4.07	-	-
E11	4	SPB	26.7	Ca(OH) ₂	0.025	665	8	4	23.95	270	230	36	3.59	3.14	8.73	1.82	5.04	3.55	9.86	-	-
E11	5	SPB	26.7	Ca(OH) ₂	0.025	665	8	4	23.95	360	230	38	3.63	3.92	10.88	1.67	4.63	4.80	13.32	-	-
E11	6	SPB	26.7	Ca(OH) ₂	0.025	665	8	4	23.95	450	230	38	3.71	4.30	11.95	1.43	3.98	3.72	10.33	-	-
E11	7	SPB	26.7	Ca(OH) ₂	0.025	665	8	4	23.95	655	230	37	3.75	4.35	12.07	1.06	2.94	2.62	7.27	-	-
E11	8	SPB	26.7	Ca(OH) ₂	0.025	665	8	4	23.95	1350	230	37	3.84	3.92	10.89	0.61	1.71	1.70	4.72	-	-
E11	9	SPB	26.7	Ca(OH) ₂	0.025	665	8	4	23.95	1440	230	37	3.83	3.90	10.82	0.60	1.65	1.65	4.58	-	0.21
E12	0	SPB	26.7	Ca(OH) ₂	0.025	665	8	4	23.95	0	25	1	12.55	0.00	0.00	0.00	0.00	0.00	0.00	-	-
E12	1	SPB	26.7	Ca(OH) ₂	0.025	665	8	4	23.95	55	200	16	11.50	0.64	1.79	0.31	0.87	0.34	0.96	-	-
E12	2	SPB	26.7	Ca(OH) ₂	0.025	665	8	4	23.95	90	200	17	9.67	1.01	2.80	0.46	1.27	0.46	1.27	-	-

Nr.	Properties				Mixture				Parameters			Analysis								Note		
	Sub.	DS [%]	Cat.	c [M]	Liq-uid [mL]	#	Sub. [w%]	m _{Sub} dry [g]	Time [min]	Temp. [°C]	p [bar]	pH	LA [g·L ⁻¹]	m _{LA} /m _{Sub} [%]	FA [g·L ⁻¹]	g _{FA} /g _{Sub} [%]	AA [g·L ⁻¹]	g _{AA} /g _{Sub} [%]	Lignin [g·L ⁻¹]		m Sub. [g]	
E12	3	SPB	26.7	Ca(OH) ₂	0.025	665	8	4	23.95	180	200	17	6.04	1.03	2.85	0.56	1.56	0.37	1.03	-	-	
E12	4	SPB	26.7	Ca(OH) ₂	0.025	665	8	4	23.95	270	200	17	5.24	1.34	3.72	0.93	2.59	0.64	1.77	-	-	
E12	5	SPB	26.7	Ca(OH) ₂	0.025	665	8	4	23.95	360	200	17	4.67	1.62	4.51	1.32	3.67	0.87	2.41	-	-	
E12	6	SPB	26.7	Ca(OH) ₂	0.025	665	8	4	23.95	450	200	18	4.33	1.82	5.06	1.62	4.49	1.06	2.95	-	-	
E12	7	SPB	26.7	Ca(OH) ₂	0.025	665	8	4	23.95	1350	200	21	3.74	2.36	6.55	1.82	5.06	1.44	4.00	-	-	
E12	8	SPB	26.7	Ca(OH) ₂	0.025	665	8	4	23.95	1440	200	20	3.71	2.35	6.52	1.80	4.99	1.40	3.89	-	5.96	
E12	B	SPB	26.7	Ca(OH) ₂	0.025	665	8	4	23.95	1700	25	1	3.76	3.62	10.06	3.69	10.23	1.98	5.50	-	-	
E12	G	SPB	26.7	Ca(OH) ₂	0.025	665	8	4	23.95	1700	25	1	3.42	0.00	0.00	2.63	7.31	0.83	2.31	-	-	
E13	0	SPB	26.7	Ca(OH) ₂	0.025	665	8	4	23.95	0	25	1	12.55	0.00	0.00	0.00	0.00	0.00	0.00	-	-	
E13	1	SPB	26.7	Ca(OH) ₂	0.025	665	8	4	23.95	43	170	8	12.06	0.49	1.36	0.33	0.90	0.00	0.00	-	-	
E13	2	SPB	26.7	Ca(OH) ₂	0.025	665	8	4	23.95	90	170	8	11.72	0.72	2.00	0.46	1.27	0.28	0.79	-	-	
E13	3	SPB	26.7	Ca(OH) ₂	0.025	665	8	4	23.95	180	170	8	11.61	0.51	1.42	0.20	0.55	0.14	0.40	-	-	
E13	4	SPB	26.7	Ca(OH) ₂	0.025	665	8	4	23.95	270	170	8	11.24	0.67	1.87	0.32	0.88	0.35	0.97	-	-	
E13	5	SPB	26.7	Ca(OH) ₂	0.025	665	8	4	23.95	360	170	8	10.30	0.71	1.98	0.32	0.89	0.30	0.84	-	-	
E13	6	SPB	26.7	Ca(OH) ₂	0.025	665	8	4	23.95	450	170	8	8.43	0.71	1.98	0.32	0.89	0.31	0.85	-	-	
E13	7	SPB	26.7	Ca(OH) ₂	0.025	665	8	4	23.95	1350	170	8	6.24	0.95	2.63	0.59	1.63	0.53	1.47	-	-	
E13	8	SPB	26.7	Ca(OH) ₂	0.025	665	8	4	23.95	1440	170	8	6.05	0.98	2.72	0.62	1.73	0.57	1.57	-	20.46	Charred remnants on reactor wall
E14	0	SPB	26.7	Ca(OH) ₂	0.400	665	9	4	23.95	0	25	1	12.65	0.00	0.00	0.00	0.00	0.00	0.00	-	-	
E14	1	SPB	26.7	Ca(OH) ₂	0.400	665	9	4	23.95	55	200	16	12.08	0.52	1.44	0.25	0.69	0.20	0.56	-	-	
E14	2	SPB	26.7	Ca(OH) ₂	0.400	665	9	4	23.95	90	200	16	11.99	1.00	2.77	0.45	1.24	0.36	0.99	-	-	
E14	3	SPB	26.7	Ca(OH) ₂	0.400	665	9	4	23.95	180	200	16	12.07	1.48	4.12	0.71	1.98	0.59	1.64	-	-	
E14	4	SPB	26.7	Ca(OH) ₂	0.400	665	9	4	23.95	270	200	16	11.46	1.66	4.62	0.81	2.25	0.66	1.85	-	-	
E14	5	SPB	26.7	Ca(OH) ₂	0.400	665	9	4	23.95	360	200	16	11.58	1.89	5.24	0.93	2.59	0.72	2.01	-	-	
E14	6	SPB	26.7	Ca(OH) ₂	0.400	665	9	4	23.95	450	200	16	11.65	2.10	5.84	1.06	2.93	0.79	2.20	-	-	
E14	7	SPB	26.7	Ca(OH) ₂	0.400	665	9	4	23.95	1350	200	16	11.65	3.88	10.77	1.83	5.09	1.22	3.38	-	-	

Nr.	Properties				Mixture				Parameters			Analysis									Note
	Sub.	DS [%]	Cat.	c [M]	Liq-uid [mL]	#	Sub. [w%]	m _{Sub} dry [g]	Time [min]	Temp. [°C]	p [bar]	pH	LA [g·L ⁻¹]	m _{LA} /m _{Sub} [%]	FA [g·L ⁻¹]	g _{FA} /g _{Sub} [%]	AA [g·L ⁻¹]	g _{AA} /g _{Sub} [%]	Lignin [g·L ⁻¹]	m Sub. [g]	
E14	8	SPB	26.7	Ca(OH) ₂	0.400	665	9	4	23.95	1440	200	16	11.50	4.01	11.14	1.88	5.22	1.25	3.48	-	15.35
E15	0	SPB	26.7	Ca(OH) ₂	0.400	665	9	4	23.95	0	25	1	12.64	0.00	0.00	0.00	0.00	0.00	0.00	-	-
E15	1	SPB	26.7	Ca(OH) ₂	0.400	665	9	4	23.95	80	230	29	12.20	1.24	3.46	0.53	1.47	0.42	1.15	0.53	-
E15	2	SPB	26.7	Ca(OH) ₂	0.400	665	9	4	23.95	90	230	29	12.26	1.59	4.41	0.71	1.97	0.55	1.53	-	-
E15	3	SPB	26.7	Ca(OH) ₂	0.400	665	9	4	23.95	180	230	29	12.14	3.31	9.18	1.50	4.17	1.03	2.86	0.90	-
E15	4	SPB	26.7	Ca(OH) ₂	0.400	665	9	4	23.95	270	230	29	12.30	4.85	13.45	2.10	5.84	1.34	3.71	-	-
E15	5	SPB	26.7	Ca(OH) ₂	0.400	665	9	4	23.95	360	230	29	12.41	6.24	17.31	2.56	7.10	1.59	4.41	1.10	-
E15	6	SPB	26.7	Ca(OH) ₂	0.400	665	9	4	23.95	450	230	29	12.42	6.83	18.95	2.69	7.48	1.65	4.59	-	-
E15	7	SPB	26.7	Ca(OH) ₂	0.400	665	9	4	23.95	1350	230	29	12.45	12.20	33.86	3.61	10.01	2.33	6.48	0.92	-
E15	8	SPB	26.7	Ca(OH) ₂	0.400	665	9	4	23.95	1440	230	29	12.45	12.54	34.82	3.64	10.12	2.32	6.45	-	2.05
E15	G	SPB	26.7	Ca(OH) ₂	0.400	665	9	4	23.95	1440	230	29	11.99	0.00	0.00	0.00	0.00	0.00	0.00	-	-
E16	0	SPB	26.7	Ca(OH) ₂	0.200	665	10	4	23.95	0	25	1	12.64	0.00	0.00	0.00	0.00	0.00	0.00	-	-
E16	1	SPB	26.7	Ca(OH) ₂	0.200	665	10	4	23.95	80	230	29	11.41	1.22	3.40	0.53	1.46	0.39	1.08	-	-
E16	2	SPB	26.7	Ca(OH) ₂	0.200	665	10	4	23.95	90	230	29	11.18	1.46	4.06	0.67	1.87	0.52	1.43	-	-
E16	3	SPB	26.7	Ca(OH) ₂	0.200	665	10	4	23.95	180	230	29	11.40	3.15	8.74	1.49	4.15	1.01	2.81	-	-
E16	4	SPB	26.7	Ca(OH) ₂	0.200	665	10	4	23.95	270	230	29	11.33	4.46	12.38	1.98	5.50	1.29	3.57	-	-
E16	5	SPB	26.7	Ca(OH) ₂	0.200	665	10	4	23.95	360	230	29	11.47	5.68	15.78	2.37	6.57	1.53	4.26	-	-
E16	6	SPB	26.7	Ca(OH) ₂	0.200	665	10	4	23.95	450	230	29	11.60	6.82	18.94	2.76	7.67	1.76	4.89	-	-
E16	7	SPB	26.7	Ca(OH) ₂	0.200	665	10	4	23.95	1350	230	31	7.31	11.33	31.46	2.20	6.10	2.39	6.64	-	-
E16	8	SPB	26.7	Ca(OH) ₂	0.200	665	10	4	23.95	1440	230	32	7.12	11.62	32.25	2.01	5.59	2.33	6.47	-	1.04
E17	0	SPB	26.7	NaOH	2.000	665	11	4	23.95	0	25	1	13.92	0.00	0.00	0.00	0.00	0.00	0.00	-	-
E17	1	SPB	26.7	NaOH	2.000	665	11	4	23.95	80	230	28	13.15	7.15	19.85	4.41	12.23	2.68	7.44	-	-
E17	2	SPB	26.7	NaOH	2.000	665	11	4	23.95	90	230	29	13.18	7.21	20.03	4.42	12.26	2.61	7.25	-	-
E17	3	SPB	26.7	NaOH	2.000	665	11	4	23.95	180	230	31	13.18	8.01	22.24	4.73	13.13	2.50	6.95	-	-
E17	4	SPB	26.7	NaOH	2.000	665	11	4	23.95	270	230	31	13.19	7.97	22.12	4.71	13.06	2.50	6.93	-	-
E17	5	SPB	26.7	NaOH	2.000	665	11	4	23.95	360	230	31	13.19	7.79	21.61	4.63	12.86	2.48	6.90	-	-

Nr.	Properties				Mixture				Parameters			Analysis								Note	
	Sub.	DS [%]	Cat.	c [M]	Liq-uid [mL]	#	Sub. [w%]	m _{Sub} dry [g]	Time [min]	Temp. [°C]	p [bar]	pH	LA [g·L ⁻¹]	m _{LA} /m _{Sub} [%]	FA [g·L ⁻¹]	g _{FA} /g _{Sub} [%]	AA [g·L ⁻¹]	g _{AA} /g _{Sub} [%]	Lignin [g·L ⁻¹]		m Sub. [g]
E17	6	SPB	26.7	NaOH	2.000	665	11	4	23.95	450	230	31	13.20	7.75	21.52	4.65	12.90	2.59	7.20	-	-
E17	7	SPB	26.7	NaOH	2.000	665	11	4	23.95	1350	230	34	13.21	7.62	21.15	4.78	13.27	3.17	8.80	-	-
E17	8	SPB	26.7	NaOH	2.000	665	11	4	23.95	1440	230	35	13.21	7.43	20.63	4.66	12.94	3.13	8.68	-	0.39
E18	0	HPB	26.7	Ca(OH) ₂	0.400	674	12	4	23.95	0	25	1	12.64	0.00	0.00	0.00	0.00	0.00	0.00	-	-
E18	1	HPB	26.7	Ca(OH) ₂	0.400	674	12	4	23.95	80	230	29	11.55	1.60	4.51	0.80	2.25	0.89	2.51	-	-
E18	2	HPB	26.7	Ca(OH) ₂	0.400	674	12	4	23.95	90	230	30	11.68	1.91	5.38	0.95	2.66	1.04	2.94	-	-
E18	3	HPB	26.7	Ca(OH) ₂	0.400	674	12	4	23.95	180	230	30	11.67	3.70	10.41	1.64	4.61	1.66	4.68	-	-
E18	4	HPB	26.7	Ca(OH) ₂	0.400	674	12	4	23.95	270	230	30	11.66	4.79	13.49	2.02	5.69	1.98	5.57	-	-
E18	5	HPB	26.7	Ca(OH) ₂	0.400	674	12	4	23.95	360	230	30	11.64	5.85	16.47	2.40	6.75	2.25	6.34	-	-
E18	6	HPB	26.7	Ca(OH) ₂	0.400	674	12	4	23.95	450	230	30	11.55	6.95	19.55	2.73	7.67	2.51	7.05	-	-
E18	7	HPB	26.7	Ca(OH) ₂	0.400	674	12	4	23.95	1260	230	30	12.22	11.75	33.07	3.58	10.08	3.31	9.32	-	-
E18	8	HPB	26.7	Ca(OH) ₂	0.400	674	12	4	23.95	1350	230	30	12.18	11.78	33.14	3.55	9.98	3.29	9.25	-	1.32
E19	0	HPU	29.9	Ca(OH) ₂	0.400	656	13	4	23.95	0	25	1	12.64	0.00	0.00	0.00	0.00	0.00	0.00	-	-
E19	1	HPU	29.9	Ca(OH) ₂	0.400	656	13	4	23.95	80	230	29	10.83	1.30	3.56	0.82	2.25	0.94	2.59	0.44	-
E19	2	HPU	29.9	Ca(OH) ₂	0.400	656	13	4	23.95	90	230	29	10.97	1.78	4.87	1.04	2.84	1.22	3.34	-	-
E19	3	HPU	29.9	Ca(OH) ₂	0.400	656	13	4	23.95	180	230	29	10.82	3.42	9.37	1.75	4.78	1.99	5.46	0.82	-
E19	4	HPU	29.9	Ca(OH) ₂	0.400	656	13	4	23.95	270	230	29	10.94	4.47	12.26	2.15	5.90	2.24	6.14	-	-
E19	5	HPU	29.9	Ca(OH) ₂	0.400	656	13	4	23.95	360	230	29	10.91	5.55	15.20	2.53	6.93	2.54	6.95	-	-
E19	6	HPU	29.9	Ca(OH) ₂	0.400	656	13	4	23.95	450	230	29	11.45	6.36	17.43	2.75	7.54	2.69	7.37	1.27	-
E19	7	HPU	29.9	Ca(OH) ₂	0.400	656	13	4	23.95	1260	230	29	12.37	10.82	29.66	3.43	9.39	3.33	9.12	-	-
E19	8	HPU	29.9	Ca(OH) ₂	0.400	656	13	4	23.95	1350	230	29	12.41	10.98	30.08	3.42	9.37	3.36	9.20	1.03	1.91
E20	0	SPU	36.1	Ca(OH) ₂	0.400	642	14	4	23.95	0	25	1	12.64	0.00	0.00	0.00	0.00	0.00	0.00	-	-
E20	1	SPU	36.1	Ca(OH) ₂	0.400	642	14	4	23.95	80	230	29	11.36	1.45	3.88	0.66	1.77	0.66	1.77	0.43	-
E20	2	SPU	36.1	Ca(OH) ₂	0.400	642	14	4	23.95	90	230	29	11.22	1.71	4.58	0.77	2.07	0.77	2.05	-	-
E20	3	SPU	36.1	Ca(OH) ₂	0.400	642	14	4	23.95	180	230	29	8.32	3.88	10.40	1.58	4.23	1.25	3.37	0.82	-
E20	4	SPU	36.1	Ca(OH) ₂	0.400	642	14	4	23.95	270	230	29	11.94	6.78	18.20	2.73	7.32	2.08	5.57	-	-

Nr.	Properties				Mixture				Parameters			Analysis								Note	
	Sub.	DS [%]	Cat.	c [M]	Liq-uid [mL]	#	Sub. [w%]	m _{Sub} dry [g]	Time [min]	Temp. [°C]	p [bar]	pH	LA [g·L ⁻¹]	m _{LA} /m _{Sub} [%]	FA [g·L ⁻¹]	g _{FA} /g _{Sub} [%]	AA [g·L ⁻¹]	g _{AA} /g _{Sub} [%]	Lignin [g·L ⁻¹]		m Sub. [g]
E20	5	SPU	36.1	Ca(OH) ₂	0.400	642	14	4	23.95	360	230	29	11.76	9.71	26.05	3.48	9.35	2.64	7.09	-	-
E20	6	SPU	36.1	Ca(OH) ₂	0.400	642	14	4	23.95	450	230	29	11.97	10.87	29.17	3.72	9.98	2.80	7.52	1.58	-
E20	7	SPU	36.1	Ca(OH) ₂	0.400	642	14	4	23.95	1260	230	29	12.42	13.77	36.95	3.80	10.18	2.82	7.58	-	-
E20	8	SPU	36.1	Ca(OH) ₂	0.400	642	14	4	23.95	1350	230	29	12.43	13.61	36.51	3.76	10.08	2.76	7.41	1.32	2.72
E21	0	SPB	26.7	NaOH	0.400	665	15	4	23.95	0	25	1	13.08	0.00	0.00	0.00	0.00	0.00	0.00	-	-
E21	1	SPB	26.7	NaOH	0.400	665	15	4	23.95	80	230	29	12.83	4.51	12.52	3.66	10.15	2.20	6.11	-	-
E21	2	SPB	26.7	NaOH	0.400	665	15	4	23.95	90	230	30	12.80	5.83	16.20	4.55	12.64	2.34	6.51	-	-
E21	3	SPB	26.7	NaOH	0.400	665	15	4	23.95	180	230	30	12.18	8.36	23.21	5.91	16.41	2.96	8.21	-	-
E21	4	SPB	26.7	NaOH	0.400	665	15	4	23.95	270	230	30	10.40	8.69	24.13	6.12	17.00	2.58	7.16	-	-
E21	5	SPB	26.7	NaOH	0.400	665	15	4	23.95	360	230	30	9.75	9.15	25.40	6.38	17.72	2.46	6.83	-	-
E21	6	SPB	26.7	NaOH	0.400	665	15	4	23.95	450	230	30	9.61	9.16	25.42	6.31	17.53	2.70	7.50	-	-
E21	7	SPB	26.7	NaOH	0.400	665	15	4	23.95	1350	230	30	8.99	9.87	27.40	6.06	16.82	2.45	6.79	-	-
E21	8	SPB	26.7	NaOH	0.400	665	15	4	23.95	1440	230	30	9.06	10.21	28.34	6.05	16.80	2.52	6.99	-	0.37
E21	G	SPB	26.7	NaOH	0.400	665	15	4	23.95	1440	230	30	6.52	0.00	0.00	0.00	0.00	0.00	0.00	-	-
E22	0	SPB	26.7	Ca(OH) ₂	0.400	665	9	4	23.95	0	25	1	12.64	0.00	0.00	0.00	0.00	0.00	0.00	-	-
E22	1	SPB	26.7	Ca(OH) ₂	0.400	665	9	4	23.95	90	200	17	11.69	0.91	2.54	0.47	1.31	0.42	1.17	-	-
E22	2	SPB	26.7	Ca(OH) ₂	0.400	665	9	4	23.95	180	200	17	11.55	1.29	3.59	0.62	1.72	0.46	1.29	-	-
E22	3	SPB	26.7	Ca(OH) ₂	0.400	665	9	4	23.95	360	200	17	11.50	1.73	4.81	0.84	2.34	0.63	1.76	-	-
E22	4	SPB	26.7	Ca(OH) ₂	0.400	665	9	4	23.95	540	200	17	11.50	2.04	5.67	0.99	2.75	0.71	1.97	-	-
E22	5	SPB	26.7	Ca(OH) ₂	0.400	665	9	4	23.95	1260	200	17	11.74	3.85	10.68	1.79	4.96	1.21	3.36	-	-
E22	6	SPB	26.7	Ca(OH) ₂	0.400	665	9	4	23.95	1620	200	17	11.87	4.22	11.70	1.93	5.35	1.34	3.71	-	-
E22	7	SPB	26.7	Ca(OH) ₂	0.400	665	9	4	23.95	1980	200	17	11.77	4.82	13.38	2.15	5.96	1.45	4.01	-	-
E22	8	SPB	26.7	Ca(OH) ₂	0.400	665	9	4	23.95	2800	200	17	12.02	6.31	17.52	2.62	7.26	1.78	4.95	-	-
E22	9	SPB	26.7	Ca(OH) ₂	0.400	665	9	4	23.95	2880	200	17	11.97	6.56	18.20	2.68	7.43	1.77	4.91	-	9.82
E23	0	SPB	26.7	Ca(OH) ₂	0.400	665	9	4	23.95	0	25	1	12.64	0.00	0.00	0.00	0.00	0.00	0.00	-	-
E23	1	SPB	26.7	Ca(OH) ₂	0.400	665	9	4	23.95	90	230	29	11.60	1.73	4.79	0.76	2.10	0.65	1.81	-	-
E23	2	SPB	26.7	Ca(OH) ₂	0.400	665	9	4	23.95	180	230	30	12.34	4.26	11.82	1.87	5.18	1.35	3.75	-	-

Nr.	Properties				Mixture			Parameters			Analysis								Note				
	Sub.	DS [%]	Cat.	c [M]	Liq-uid [mL]	#	Sub. [w%]	m _{Sub} dry [g]	Time [min]	Temp. [°C]	p [bar]	pH	LA [g·L ⁻¹]	m _{LA} /m _{Sub} [%]	FA [g·L ⁻¹]	g _{FA} /g _{Sub} [%]	AA [g·L ⁻¹]	g _{AA} /g _{Sub} [%]		Lignin [g·L ⁻¹]	m Sub. [g]		
E23	3	SPB	26.7	Ca(OH) ₂	0.400	665	9	4	23.95	360	230	30	12.45	7.06	19.60	2.74	7.61	1.87	5.18	-	-		
E23	4	SPB	26.7	Ca(OH) ₂	0.400	665	9	4	23.95	540	230	30	12.54	8.76	24.32	3.00	8.33	2.05	5.70	-	-		
E23	5	SPB	26.7	Ca(OH) ₂	0.400	665	9	4	23.95	1260	230	32	12.52	12.73	35.33	3.38	9.38	2.57	7.15	-	-		
E23	6	SPB	26.7	Ca(OH) ₂	0.400	665	9	4	23.95	1620	230	31	12.52	13.46	37.36	3.50	9.72	2.69	7.46	-	-		
E23	7	SPB	26.7	Ca(OH) ₂	0.400	665	9	4	23.95	1980	230	31	12.47	13.80	38.30	3.46	9.60	2.75	7.62	-	-		
E23	8	SPB	26.7	Ca(OH) ₂	0.400	665	9	4	23.95	2760	230	34	12.58	13.92	38.63	3.08	8.54	2.73	7.58	-	-		
E23	9	SPB	26.7	Ca(OH) ₂	0.400	665	9	4	23.95	2880	230	31	12.58	13.90	38.58	3.00	8.32	2.57	7.13	-	0.25		
E24	0	SPB	26.7	Ca(OH) ₂	0.400	665	9	4	23.95	0	25	1	12.64	0.00	0.00	0.00	0.00	0.00	0.00	-	-		
E24	1	SPB	26.7	Ca(OH) ₂	0.400	665	9	4	23.95	90	170	8	12.02	0.41	1.13	0.22	0.60	0.10	0.29	-	-		
E24	2	SPB	26.7	Ca(OH) ₂	0.400	665	9	4	23.95	180	170	8	11.79	0.54	1.51	0.30	0.83	0.24	0.66	-	-		
E24	3	SPB	26.7	Ca(OH) ₂	0.400	665	9	4	23.95	360	170	8	11.89	0.67	1.85	0.37	1.04	0.30	0.83	-	-		
E24	4	SPB	26.7	Ca(OH) ₂	0.400	665	9	4	23.95	540	170	8	12.01	0.78	2.17	0.44	1.23	0.38	1.05	-	-		
E24	5	SPB	26.7	Ca(OH) ₂	0.400	665	9	4	23.95	1260	170	8	12.27	1.32	3.67	0.73	2.03	0.62	1.71	-	-		
E24	6	SPB	26.7	Ca(OH) ₂	0.400	665	9	4	23.95	1620	170	8	12.26	1.54	4.28	0.77	2.14	0.67	1.85	-	-		
E24	7	SPB	26.7	Ca(OH) ₂	0.400	665	9	4	23.95	1980	170	8	12.39	1.60	4.45	0.86	2.40	0.73	2.02	-	-		
E24	8	SPB	26.7	Ca(OH) ₂	0.400	665	9	4	23.95	2760	170	8	12.45	1.83	5.09	0.98	2.72	0.82	2.27	-	-		
E24	9	SPB	26.7	Ca(OH) ₂	0.400	665	9	4	23.95	2880	170	8	12.42	1.87	5.20	0.99	2.74	0.83	2.31	-	18.2		
E25	0	BL	40.88	-	-	600	-	-	-	0	25	4	12.86	17.20	-	17.41	-	14.98	-	218.82	-	Reactor was leaking, high viscosity of sample 3, 4, and 5	
E25	4	BL	40.88	-	-	600	-	-	-	180	200	24	11.74	24.36	-	22.63	-	18.27	-	-	-		
E25	2	BL	40.88	-	-	600	-	-	-	540	200	24	10.86	27.29	-	23.41	-	18.99	-	308.99	-		
E25	3	BL	40.88	-	-	600	-	-	-	1350	200	24	-	38.94	-	26.60	-	23.55	-	-	-		
E25	4	BL	40.88	-	-	600	-	-	-	1740	200	24	-	41.13	-	26.54	-	24.90	-	200.32	-		
E25	5	BL	40.88	-	-	600	-	-	-	2070	200	24	10.78	40.78	-	26.81	-	25.66	-	-	-		
E25	6	BL	40.88	-	-	600	-	-	-	2880	200	24	10.76	39.40	-	25.79	-	26.06	-	207.59	-		
E25	7	BL	40.88	-	-	600	-	-	-	2940	25	4	10.78	33.84	-	22.27	-	22.37	-	-	-		
E26	0	BL	40.88	-	-	600	-	-	-	0	25	1	12.82	17.20	-	17.41	-	14.98	-	-	-		
E26	1	BL	40.88	-	-	600	-	-	-	60	200	19	11.71	22.79	-	20.34	-	16.54	-	241.52	-		

Nr.	Properties				Mixture				Parameters			Analysis								Note		
	Sub.	DS [%]	Cat.	c [M]	Liquid [mL]	#	Sub. [w%]	m _{Sub} dry [g]	Time [min]	Temp. [°C]	p [bar]	pH	LA [g·L ⁻¹]	m _{LA} /m _{Sub} [%]	FA [g·L ⁻¹]	g _{FA} /g _{Sub} [%]	AA [g·L ⁻¹]	g _{AA} /g _{Sub} [%]	Lignin [g·L ⁻¹]		m Sub. [g]	
E26	2	BL	40.88	-	-	600	-	-	-	120	200	27	11.64	26.86	-	22.46	-	18.48	-	280.51	-	
E26	3	BL	40.88	-	-	600	-	-	-	180	200	27	11.58	29.09	-	23.88	-	20.75	-	-	-	
E26	4	BL	40.88	-	-	600	-	-	-	240	25	1	11.59	31.72	-	25.15	-	20.31	-	295.89	-	
E26	G	BL	40.88	-	-	600	-	-	-	180	200	15	10.98	26.54	-	17.53	-	15.07	-	-	-	Flash from 27 to 15 bar
E27	0	BL	40.88	-	-	600	-	-	-	0	25	1	12.85	17.20	-	17.41	-	14.98	-	183.25	-	
E27	1	BL	40.88	-	-	600	-	-	-	180	170	10	12.16	19.62	-	19.22	-	16.01	-	230.72	-	
E27	2	BL	40.88	-	-	600	-	-	-	540	170	16	11.58	21.80	-	19.65	-	16.05	-	-	-	
E27	3	BL	40.88	-	-	600	-	-	-	1350	170	19	11.74	22.61	-	20.14	-	15.60	-	277.97	-	
E27	4	BL	40.88	-	-	600	-	-	-	1710	170	19	11.62	26.89	-	23.14	-	20.06	-	-	-	
E27	5	BL	40.88	-	-	600	-	-	-	2070	170	19	11.74	28.21	-	22.06	-	18.00	-	274.43	-	
E27	6	BL	40.88	-	-	600	-	-	-	2880	170	19	11.50	28.50	-	21.67	-	17.31	-	292.88	-	
E27	B	BL	40.88	-	-	600	-	-	-	2940	25	1	11.48	35.74	-	25.60	-	21.42	-	-	-	
E28	0	BL	40.88	-	-	600	-	-	-	0	25	1	12.79	17.43	-	17.52	-	14.51	-	186.08	-	
E28	1	BL	40.88	-	-	600	-	-	-	180	200	29	11.83	19.23	-	21.08	-	17.19	-	278.8	-	
E28	2	BL	40.88	-	-	600	-	-	-	540	200	32	10.99	38.69	-	26.45	-	26.73	-	309.34	-	Blockage of sample line after sampling, high viscosity of sample
E28	3	BL	40.88	-	-	600	-	-	-	2880	25	38	9.81	28.73	-	16.07	-	23.57	-	102.69	-	Formation of char
E28	B	BL	40.88	-	-	600	-	-	-	2880	25	1	9.84	30.87	-	16.85	-	25.28	-	51.14	-	Filtrate of 3
E29	0	SPB	26.7	NaOH	0.025	665	16	4	23.95	0	25	1	12.36	0.00	0.00	0.00	0.00	0.00	0.00	-	-	
E29	1	SPB	26.7	NaOH	0.025	665	16	4	23.95	90	230	28	4.98	1.02	2.82	1.00	2.78	0.58	1.62	-	-	
E29	2	SPB	26.7	NaOH	0.025	665	16	4	23.95	180	230	32	3.80	1.61	4.46	1.32	3.67	1.09	3.02	-	-	
E29	3	SPB	26.7	NaOH	0.025	665	16	4	23.95	270	230	37	3.64	1.95	5.41	1.17	3.25	4.14	11.50	-	-	
E29	4	SPB	26.7	NaOH	0.025	665	16	4	23.95	360	230	39	3.65	2.37	6.59	1.19	3.31	4.50	12.50	-	-	

Nr.	Properties				Mixture				Parameters			Analysis								Note	
	Sub.	DS [%]	Cat.	c [M]	Liq-uid [mL]	#	Sub. [w%]	m _{Sub} dry [g]	Time [min]	Temp. [°C]	p [bar]	pH	LA [g·L ⁻¹]	m _{LA} /m _{Sub} [%]	FA [g·L ⁻¹]	g _{FA} /g _{Sub} [%]	AA [g·L ⁻¹]	g _{AA} /g _{Sub} [%]	Lignin [g·L ⁻¹]		m Sub. [g]
E33	1	SPU	36.1	Ca(OH) ₂	0.400	642	14	4	23.95	90	230	30	11.89	1.16	3.12	0.45	1.19	0.42	1.14	0.43	-
E33	2	SPU	36.1	Ca(OH) ₂	0.400	642	14	4	23.95	180	230	30	11.63	2.77	7.42	1.05	2.83	0.92	2.48	0.67	-
E33	3	SPU	36.1	Ca(OH) ₂	0.400	642	14	4	23.95	270	230	30	11.74	4.12	11.04	1.50	4.03	1.19	3.19	-	-
E33	4	SPU	36.1	Ca(OH) ₂	0.400	642	14	4	23.95	360	230	30	11.50	5.14	13.78	1.83	4.90	1.42	3.82	-	-
E33	5	SPU	36.1	Ca(OH) ₂	0.400	642	14	4	23.95	450	230	30	11.59	5.91	15.84	2.04	5.46	1.55	4.17	0.85	-
E33	6	SPU	36.1	Ca(OH) ₂	0.400	642	14	4	23.95	1350	230	30	12.27	10.58	28.39	2.71	7.28	2.14	5.74	0.81	-
E33	7	SPU	36.1	Ca(OH) ₂	0.400	642	14	4	23.95	1440	230	30	12.28	10.64	28.53	2.71	7.28	2.09	5.61	-	2.1
E33	B	SPU	36.1	Ca(OH) ₂	0.400	642	14	4	23.95	1440	25	1	12.21	14.62	39.21	3.71	9.96	2.94	7.89	-	-

Table 8-5: Calculation of mean reaction rate of E22, E23 and E24; the calculation was done by the quotient of the difference of concentrations to time - $r = \frac{\Delta c}{\Delta t}$

E22 200°C						
Time [min]	C _{LA} [g·L ⁻¹]	C _{F_A} [g·L ⁻¹]	C _{AA} [g·L ⁻¹]	r _{LA} [g·L ⁻¹ ·min ⁻¹]	r _{F_A} [g·L ⁻¹ ·min ⁻¹]	r _{AA} [g·L ⁻¹ ·min ⁻¹]
0	0.00	0.00	0.00	0.00000	0.00000	0.00000
90	0.91	0.47	0.42	0.01016	0.00526	0.00468
180	1.29	0.62	0.46	0.00421	0.00161	0.00047
360	1.73	0.84	0.63	0.00244	0.00125	0.00094
540	2.04	0.99	0.71	0.00172	0.00082	0.00043
1260	3.85	1.79	1.21	0.00251	0.00111	0.00069
1620	4.22	1.93	1.34	0.00102	0.00039	0.00035
1980	4.82	2.15	1.45	0.00168	0.00061	0.00031
2800	6.31	2.62	1.78	0.00182	0.00057	0.00041
2880	6.56	2.68	1.77	0.00309	0.00077	-0.00016

E23 230°C						
Time [min]	C _{LA} [g·L ⁻¹]	C _{F_A} [g·L ⁻¹]	C _{AA} [g·L ⁻¹]	r _{LA} [g·L ⁻¹ ·min ⁻¹]	r _{F_A} [g·L ⁻¹ ·min ⁻¹]	r _{AA} [g·L ⁻¹ ·min ⁻¹]
0	0.00	0.00	0.00	0.00000	0.00000	0.00000
90	1.73	0.76	0.65	0.01917	0.00841	0.00723
180	4.26	1.87	1.35	0.02811	0.01232	0.00780
360	7.06	2.74	1.87	0.01558	0.00486	0.00285
540	8.76	3.00	2.05	0.00943	0.00143	0.00105
1260	12.73	3.38	2.57	0.00551	0.00053	0.00072
1620	13.46	3.50	2.69	0.00203	0.00033	0.00031
1980	13.80	3.46	2.75	0.00095	-0.00012	0.00016
2800	13.92	3.08	2.73	0.00015	-0.00047	-0.00002
2880	13.90	3.00	2.57	-0.00024	-0.00098	-0.00205

E24 170°C						
Time [min]	C _{LA} [g·L ⁻¹]	C _{F_A} [g·L ⁻¹]	C _{AA} [g·L ⁻¹]	r _{LA} [g·L ⁻¹ ·min ⁻¹]	r _{F_A} [g·L ⁻¹ ·min ⁻¹]	r _{AA} [g·L ⁻¹ ·min ⁻¹]
0	0.00	0.00	0.00	0.00000	0.00000	0.00000
90	0.41	0.22	0.10	0.00453	0.00240	0.00115
180	0.54	0.30	0.24	0.00152	0.00093	0.00148
360	0.67	0.37	0.30	0.00069	0.00041	0.00034
540	0.78	0.44	0.38	0.00063	0.00038	0.00045
1260	1.32	0.73	0.62	0.00075	0.00040	0.00033
1620	1.54	0.77	0.67	0.00061	0.00011	0.00014
1980	1.60	0.86	0.73	0.00017	0.00026	0.00016
2800	1.83	0.98	0.82	0.00028	0.00014	0.00011
2880	1.87	0.99	0.83	0.00046	0.00009	0.00020